



Universidad de Valladolid

**PROGRAMA DE DOCTORADO EN CONSERVACIÓN Y
USO SOTENIBLE DE SISTEMAS FORESTALES**

TESIS DOCTORAL:

**The snowpack over the Iberian Peninsula:
climatology and sensitivity to climate
variability**

**El manto de nieve en la península ibérica:
climatología y sensibilidad a la
variabilidad climática**

Presentada por Esteban Alonso González para
optar al grado de
Doctor/a por la Universidad de Valladolid

Dirigida por:
Dr. Juan Ignacio López Moreno
Dr. Antonio Ceballos Barbancho

Índice

Agradecimientos:.....	1
Resumen.....	1
Abstract.....	5
Capítulo 1: Introducción.....	11
1.1 La importancia del manto de nieve.....	11
1.2 Información disponible del manto de nieve.....	13
1.2 Alternativas a las observaciones.....	17
1.2.1 Uso de información por satélite en el estudio del manto de nieve.....	17
1.2.2 Uso de simulaciones numéricas del manto de nieve para generar información del espesor de nieve y del SWE.....	20
1.3 El manto de nieve en la península ibérica.....	23
1.4 Impactos de la variabilidad climática en el manto de nieve de la península ibérica.....	27
1.5 Objetivos.....	28
Referencias:.....	30
Capítulo 2: Rejillas de datos diarias de espesor de nieve y equivalente en agua de nieve de la Península Ibérica desde 1980 hasta 2014.....	43
Daily gridded datasets of snow depth and snow water equivalent for the Iberian Peninsula from 1980 to 2014.....	45
1 Introduction.....	46
2. Data and methods.....	48
2.1 Meteorological driving data.....	49
2.2 Snow energy and mass balance model.....	50
2.3 Validation procedure.....	53
3 Results.....	55
3.1 Validation.....	55
3.2 Gridded snow dataset: applications and limitations.....	58
4. Data availability.....	62
5. Conclusions.....	62
References.....	64
Capítulo 3: Climatología de nieve de las montañas de la Península Ibérica mediante imágenes por satélite y simulaciones con mejoras de escala dinámicas.....	73
Snow climatology for the mountains in the Iberian Peninsula using satellite imagery and simulations with dynamically downscaled reanalysis data.....	75

1 Introduction.....	76
2 Study area.....	78
3 Data and methods.....	80
3.1 Remote sensing.....	80
3.2 SD and SWE simulation.....	81
4 Results and discussion.....	83
4.1 Probability of snow cover from MODIS.....	83
4.2 Simulated snow SD and SWE.....	88
4.3 Intra-range variability from simulated snow data.....	93
4.4 Implications of the presented results.....	94
5 Conclusions.....	95
References.....	96
Capítulo 4: Impacto de la Oscilación del Atlántico Norte en el manto de nieve de las montañas de la Península Ibérica.....	109
Impact of North Atlantic Oscillation on the Snowpack in Iberian Peninsula Mountains.....	111
1. Introduction.....	112
2. Study Area.....	113
3. Methods.....	115
3.1. NAO Index and Temperature and Precipitation Patterns.....	115
3.2. Snowpack Database and Statistical Analysis.....	115
4. Results and Discussion.....	116
4.1. Relationship between the DJFM-NAO and Temperature and Precipitation.....	116
4.2. Relationship between the Winter NAO and Temperature and Precipitation.....	117
4.3. NAO Spatial Influence on Peak SWE and Snow Season Duration.....	119
5. Conclusions.....	124
References.....	126
Capítulo 5: Sensibilidad del manto de nieve a la variabilidad de la temperatura, precipitación y radiación solar en un gradiente altitudinal en la Península Ibérica.....	135
Snowpack sensitivity to temperature, precipitation, and solar radiation variability over an elevational gradient in the Iberian mountains.....	137
1 Introducción.....	138
2 Study Area.....	140
3 Data and methods.....	141
4 Results.....	144
4.1 Selection of representative areas.....	144

4.2 Sensitivity of the snowpack duration and peak SWE to precipitation, short wave radiation, and temperature change.....	146
4.3 Effect of temperature variability on the snowmelt rate.....	150
5 Discussion.....	152
6 Conclusions.....	155
References.....	157
Capítulo 6: Conclusiones.....	167
Conclusions.....	171

Agradecimientos:

Este trabajo no hubiera sido posible sin el apoyo de muchas personas, que de una manera u otra han contribuido a que esté ahora mismo escribiendo estas líneas. Primero, me gustaría agradecer el apoyo recibido por mis dos directores de tesis Nacho y Antonio. En todo momento he tenido la sensación de estar arropado por vuestra experiencia. Siempre habéis estado disponibles para mí, y habéis estado implicados al máximo en este proyecto. Nacho, las charlas sobre monte mientras hacíamos ciencia, y de ciencia mientras hacíamos monte, han sido una de las mayores fuentes de inspiración de estos cuatro años. Espero sigamos así mucho tiempo más, gracias.

A mis compañeros IPErinos, especialmente al superpoblado despacho 3, hacéis que la gente se sienta en casa desde el primer día. Siempre se puede contar con vosotros para arreglar una línea de código, o la tarde de un viernes. Muchas gracias Chavi, Jesús, Fergus, Mocho, Makki, Ivan, Paco, Natalia, Clara, Dani, Ana, Elena solo por nombrarlos a algunos entre la mucha gente con la que he coincidido por el IPE en estos años. También me gustaría daros las gracias a vosotros Guille y Emilian que, a pesar de vuestra corta estancia en el IPE, hemos compartido mucho fuera del IPE, una buena parte del tiempo atados a la misma cuerda.

A mis compañeros de mi estancia en el NCAR, especialmente a Sip, Luuk, Bao y Kris. Fue un poco frustrante aparecer en Colorado, el paraíso de la nieve polvo, en uno de los inviernos con menos nieve que se recuerdan. Pero a cambio, hicimos multitud de viajes juntos que se quedarán en mí memoria. Espero podamos seguir en contacto como hasta ahora, a pesar de los miles de kilómetros que nos separan.

Buena parte de estos años los hemos pasado juntos como “extranjeros” en Zaragoza. Barbara, Feni y Lorenzo, muchas gracias por todas las mañanas, tardes y noches que hemos pasado juntos. Veremos si en la próxima ciudad en la que coincidimos, seguimos discutiendo sobre donde son peores las bravas.

Por supuesto, tengo que agradecer el apoyo de mi familia, ya que de alguna manera también es en parte suyo este trabajo. Los tirones de orejas y las palmadas en la espalda son al final los que me han traído hasta aquí. A mis padres y mi hermana, muchas gracias.

Itsaso, te mereces mucho más que estas líneas. Has conseguido convertir en llevadera la experiencia de escribir una tesis en medio de un confinamiento obligado de varias semanas. Tú me has dado la energía para culminar este trabajo, aportando como solo tú sabes. Este trabajo es en gran medida gracias a ti.

Y por último, me gustaría dedicar este trabajo a sus máximas protagonistas, las montañas. Quien pudiera imaginar que sería de todos, y especialmente de mí, sin vosotras. A vosotras os dedico este trabajo.

Resumen

En la presente tesis doctoral se estudian las características del manto de nieve a escala regional en las principales cadenas montañosas de la península ibérica. A pesar del importante papel que juega el manto de nieve en la península ibérica, no existen hasta hoy trabajos que aborden su estudio desde una perspectiva climatológica para el conjunto de su territorio. La principal razón de esta ausencia ha sido la falta de datos meteorológicos y del manto de nieve suficientes para obtener una visión global y relativa a todas las bandas altitudinales, problema que afecta a la gran mayoría de las cadenas montañosas del mundo.

El presente trabajo aborda la problemática de la falta de datos de campo mediante el uso de modelos de base física y de la teledetección por satélite. Se han utilizado las salidas del modelo numérico mesoatmosférico *Weather Research and Forecast* (WRF), como forzamiento meteorológico del modelo de balance de masa y energía del manto de nieve *Flexible Snow Model* (FSM). La simulación atmosférica cubre el periodo 1979-2014 con una resolución espacial de 0.088° (~10 km). Previamente al acoplamiento de WRF con FSM, se han proyectado las variables de superficie de WRF a diferentes bandas altitudinales mediante el uso de gradientes de temperatura y un conjunto de fórmulas radiativas y psicrométricas. De esta manera se ha construido una base de datos semidistribuida de espesor (SD) y equivalente en agua de nieve (SWE) a resolución diaria de toda la península ibérica que cubre el rango altitudinal de 500 a 2900 m s.n.m a intervalos de 100 m. Para la validación se han utilizado imágenes de covertura de nieve procedentes del sensor MODIS y las series de observaciones existentes sobre la península ibérica procedentes de telenivómetros. Los resultados obtenidos en la comparación con MODIS indican un error de 6,07% y un $R^2 = 0,76$ en los valores de probabilidad de nieve y unos valores de índice kappa generalmente por encima de 0,6 en comparación con las observaciones para la mayoría de los percentiles de acumulación comparados. Estos resultados prueban la consistencia temporal y espacial de la base de datos en comparación con las observaciones. De esta manera, la base de datos generada es capaz de reproducir la variabilidad interanual e intranual del manto de nieve, siendo potencialmente útil para una gran cantidad de estudios hidroclimatológicos, gestión del territorio, turismo de invierno, ecología o riesgos asociados a la nieve entre otros.

Gracias a la nueva base de datos generada, ha sido posible estudiar los diferentes comportamientos que presenta el manto de nieve sobre las cinco principales cordilleras de la península ibérica

(Cordillera Cantábrica, Sistema Central, Sistema Ibérico, Pirineos y Sierra Nevada.). De esta manera se ha realizado la primera climatología del manto de nieve de la península ibérica. Primero, se calculó el máximo de acumulación medio, la duración media de cada temporada y el coeficiente de variación interanual de los máximos de acumulación para cada celda y cada elevación de toda la base de datos. Posteriormente se utilizó la técnica de agrupamiento *k-means* para encontrar zonas En cada cordillera con un comportamiento climático similar. También se estudió como varían los valores de probabilidad de nieve y coeficiente de variación en función de la altura para cada cordillera, así como la variabilidad existente dentro de cada zona de montaña. Los resultados mostraron cómo los diferentes comportamientos del manto de nieve encontrados se distribuyen de manera desigual a lo largo del rango altitudinal de cada cordillera. Los valores de nieve encontrados por encima de 1000 m s.n.m. comienzan mostrando un carácter efímero o prácticamente inexistente, incrementándose progresivamente en altitud hasta encontrar en las cotas más elevadas mantos de nieve de gran duración y espesor (alcanzándose los 200 días de presencia de nieve y más de 3 metros de espesor). Los índices de nieve calculados sugieren que, en términos de bandas altitudinales, la Cordillera Cantábrica y los Pirineos presentan los mantos de nieve de mayor magnitud y duración, seguidos del Sistema Central e Ibérico. Sierra Nevada mostró las temporadas más cortas y mantos de nieve menos profundos a iguales altitudes que las anteriores cordilleras, y una mayor variabilidad interanual.

La precipitación y temperatura de invierno de la península ibérica se ven altamente afectadas por los patrones sinópticos asociados a la Oscilación del Atlántico Norte (NAO) y por lo tanto han de tener necesariamente influencia en la variabilidad interanual del manto de nieve. Hemos estudiado la influencia que tiene la NAO en la duración y la magnitud del manto de nieve en la península ibérica así como los patrones espaciales de esta relación. Para ello se calcularon, a partir de la base de datos anteriormente descrita las series de máxima acumulación y duración anual, correlacionando estas con el valor medio de la NAO de los meses de Diciembre, Enero, Febrero y Marzo (DJFM-NAO). Los resultados muestran valores muy altos de correlación negativa en todas las principales cordilleras de la península ibérica. Esto es particularmente evidente en las vertientes sur de las cordilleras que están más expuestas a las advecciones de componente suroeste y oeste, que son frecuentes durante las fases negativas del índice DJFM-NAO. Dicha diferencia entre vertientes quedó corroborada al aplicar un test estadístico no paramétrico (test Wilcoxon-Mann-Whitney) entre los valores de correlación de los índices del manto de nieve y la DJFM-NAO de ambas vertientes. Únicamente en Sierra Nevada no se encontraron diferencias entre distintas

vertientes. Además se han detectado distintos niveles de correlación según longitud geográfica y la elevación, siendo en general las correlaciones más elevadas en cotas altas y en las zonas occidentales de las cordilleras. Estos resultados abren la puerta a una potencial predicción a medio plazo de la magnitud y duración del manto de nieve a alta resolución espacial, a la vez que demuestran la importancia de la existencia de series largas a la hora de detectar tendencias temporales y espaciales de la duración y magnitud del manto de nieve.

Para finalizar, se ha estudiado la respuesta del manto de nieve a la variabilidad climática en diferentes bandas altitudinales. Se realizaron simulaciones del manto de nieve mediante FSM con perturbaciones progresivas en el forzamiento meteorológico simulado mediante WRF. Las perturbaciones fueron de 0-4 °C de temperatura en incrementos de 0.5 °C, 0-40 Wm⁻² de radiación de onda corta con incrementos de 5 Wm⁻² y ± 20% con incrementos de 5%, realizando simulaciones dentro de esos rangos de perturbación en todas las posibles combinaciones. De las nuevas series de SWE generadas se calcularon las series de máximo anual de SWE, duración de la temporada de nieve y tasa de fusión media anual, para calcular y promediar los cambios porcentuales de los índices. Los resultados han mostrado diferentes sensibilidades a la variabilidad climática, pero siempre con importantes pérdidas de magnitud y duración del manto de nieve asociadas a un calentamiento térmico e incremento de la radiación solar, a todas las alturas y zonas de estudio, e incluso en las situaciones de mayor incremento de precipitación. Los valores de sensibilidad de las tasas de fusión fueron mayoritariamente negativos, sugiriendo periodos de fusión más largos y menos intensos, con obvias repercusiones en la hidrología de las zonas influenciadas por la fusión de nieve.

Abstract

In the following doctoral thesis, the characteristics of the snow cover on a regional scale over the main mountain ranges of the Iberian Peninsula are studied. Despite the important role played by the snow cover in the Iberian Peninsula, there are no studies that address its study from a climatological perspective in the whole of its territory. As in the vast majority of mountain ranges of the world, the generalized lack of snow information over Iberia, has prevented the proper study of the snowpack at a regional scale.

Here we address the problem of the lack of observational data by using physical based models and satellite remote sensing. The outputs of the numerical mesoatmospheric model Weather Research and Forecast (WRF) have been used as meteorological forcing of the mass and energy balance model the Flexible Snow Model (FSM). The atmospheric simulation covers the period 1979-2014 with a spatial resolution of 0.088° (~ 10 km at the main Iberian latitude). Prior to the coupling of WRF with FSM, the surface variables of WRF have been projected at different elevational bands using temperature lapse-rates and an array of radiative and psychrometric formulas. Thus, a semi-distributed database of snow depth (SD) and snow water equivalent (SWE) at daily resolution has been built for the whole Iberian Peninsula covering the elevational range from 500 to 2900 m asl at 100 m intervals. The validation was done using snow cover area images from the MODIS sensor and the existing series of observations from snow telemetry devices on the Iberian Peninsula. The results obtained in the comparison with MODIS indicate an error of 6.07% and $R^2 = 0.76$ in the snow probability values and kappa index values generally above 0.6 compared to the observations for most of the accumulation percentiles. These results prove the temporal and spatial consistency of the database compared to the observations. The database generated is able to reproduce the inter- and intrannual variability of the snowpack, being potentially useful for a large number of hydroclimatological studies, land management, winter tourism, ecology or risks associated with snow among others.

The newly generated database allowed us to study the different behaviors of the snowpack over the five main mountain ranges of the Iberian Peninsula (Cantabrian Range, Central System, Iberian System, Pyrenees and Sierra Nevada). Using the new generated data, the first climatology of the snow cover of the Iberian Peninsula has been developed. First, we calculated the average maximum accumulation, the average season duration and the coefficient of interannual variation of the accumulation maxima for each cell and each elevation in the whole database. Then a k-means

clustering algorithm was used to add similar climatologies over the different mountain ranges. We also studied how the values of snow probability and coefficient of variation change as a function of the elevation for each mountain range, as well as the intra-range variability. The results showed how the different behaviors of the snowpack are unevenly distributed along the elevational range of each mountain range. Snow values found above 1000m a.s.l. oscillate between areas with ephemeral or practically non-existent snow cover in contrast to areas with deep and long lasting snowpacks (198 days of snow presence and ~3m SD). The calculated snow indices suggest that, in terms of elevational bands, the Cantabrian Mountains and the Pyrenees have the largest and longest snow cover, followed by the Central and Iberian Systems. Sierra Nevada showed the shortest seasons and shallowest snow cover with the greatest inter-annual variability.

The winter precipitation and temperature of the Iberian Peninsula is highly affected by the synoptic patterns associated with the North Atlantic Oscillation index (NAO) and therefore must necessarily influence the interannual variability of the snow cover. We have studied the influence of the NAO on the duration and magnitude of the snowpack in the Iberian Peninsula as well as the spatial patterns of this relationship. For this purpose, we calculated from the database described above the series of maximum accumulation and annual duration. Then we correlated these snow indexes with the averaged NAO value of the months of December, January, February and March (DJFM-NAO). The results show very high negative correlation in all the main mountain ranges of the Iberian Peninsula. This is particularly evident on the slopes exposed to the advections fostered by the negative phases of the DJFM-NAO index, mostly in a southwestern and western direction. To prove this, we have used a non-parametric statistical test (Wilcoxon-Mann-Whitney test) between the correlation values of the snowpack indices and the DJFM-NAO of both slopes. Thus, we prove that the opposite slopes respond differently in all the main mountain ranges with the exception of Sierra Nevada where no differences between slopes were found. Strong relationships were found between the correlation values of the areas exposed to the advection and the geographical length and elevation. The correlations were generally greater at high elevations and tending to be located in the western areas of the mountain ranges. These results could potentially be used on a long-term high spatial resolution prediction of the magnitude and duration of the snowpack. Our findings prove the importance of the existence of long series in detecting temporal and spatial trends in the duration and magnitude of the snowpack.

Finally, the response of the snowpack to climate variability in different elevational bands has been studied. A factorial experiment was implemented, performing simulations of the snowpack by

means of FSM with progressive perturbations in the meteorological forcing simulated by WRF. The perturbation ranges of temperature were 0-4 °C in 0.5 °C increments, 0-40 Wm⁻² of short wave radiation in 5 Wm⁻² increments and ± 20% of precipitation in 5% increments, performing simulations within these disturbance ranges in all possible combinations. From the new SWE series generated we calculated the series of maximum annual SWE, duration of the snow season and average annual melting rate and used to estimate the percentage of change per increment of perturbation. The results have shown different sensitivities to climate variability but always with important losses of magnitude and duration of the snowpack at all elevation bands and study areas even in the situations of higher increase of precipitation. Sensitivity values of the melt rates were negative, suggesting longer and less intense melting periods, with obvious implications on the hydrology of areas influenced by the snow melt.

Capítulo 1: Introducción

1.1 La importancia del manto de nieve

Debido sus particulares características, el manto de nieve juega un papel crucial en una gran cantidad de procesos climáticos, ambientales y socio-económicos en numerosas zonas templadas y frías del planeta. El manto de nieve estacional cubre aproximadamente entre un mínimo de 2×10^6 km² y un máximo de 45×10^6 km² del Hemisferio Norte (Fig. 1) en invierno y verano respectivamente. Esto supone una cobertura de cerca del 50% de tierras emergidas en el hemisferio Norte (Déry and Brown, 2007), controlando directamente el balance energético del planeta Tierra y por ende condicionando de manera drástica el clima global. A modo de ejemplo, Barnett et al., 1988 realizaron una de las primeras simulaciones numéricas para testar el efecto del manto de nieve estacional de Eurasia en el clima global. Sus resultados relacionaron la variabilidad interanual del manto de nieve a escala continental con los monzones, el clima de Norte América, así como otros aspectos muy relacionados con el fenómeno de El Niño-Oscilación del Sur. Más recientemente, estas hipótesis han seguido siendo testadas y corroboradas. Vavrus, 2007 intentó cuantificar el efecto global del manto de nieve en el clima del planeta mediante el uso de modelos atmosféricos globales, comparando una simulación control con otra simulación sintética sin manto de nieve. Sus resultados sugirieron drásticas consecuencias sobre el clima, afectando no solo las temperaturas del suelo y su humedad, si no a grandes patrones atmosféricos en latitudes medias y regiones polares. Algunas de las implicaciones más notables fueron un drástico calentamiento atmosférico que legó a superar los 10 °C sobre la media durante el invierno en algunas zonas. El calentamiento global inducido por la falta de manto de nieve fue comparable a un tercio del inducido por doblar la cantidad de CO₂.

El aire contenido entre los cristales de hielo confiere al manto de nieve una gran capacidad aislante, resultando éste determinante para comprender la ecología de las zonas donde está presente. Las condiciones relativamente templadas del suelo bajo el manto de nieve, posibilitan una gran actividad biológica, incluyendo la actividad de plantas (Salisbury, 1985) y animales tanto vertebrados como invertebrados (Jones, 2001). Estas mismas características aislantes permiten la actividad microbiana siempre que se mantenga la temperatura del suelo por encima de aproximadamente -5 °C (Schimel and Clein, 1996), lo cual tiene implicaciones en los ciclos de

elementos básicos del suelo, como por ejemplo el nitrógeno (Brooks and Williams, 1999; Jones, 1999 entre otros).

Como recurso hidrológico, Barnett et al., 2005 estimaron que aproximadamente una sexta parte de la población mundial vive directamente en lugares en los que la fusión de nieve domina la hidrología de la región. Los mismos autores reconocen que esta estimación probablemente infravalora el grado de dependencia, ya que no incluye a las poblaciones que obtienen sus recursos hídricos fuera de las cuencas hidrológicas en las que viven. Más concretamente, Viviroli et al., 2007 estimaron que más de un 50% de las zonas montañosas del planeta juegan un papel esencial en las poblaciones aguas abajo de las cuencas de montaña, zonas en las que el ciclo hidrológico está profundamente influido por los procesos de acumulación y fusión nival.

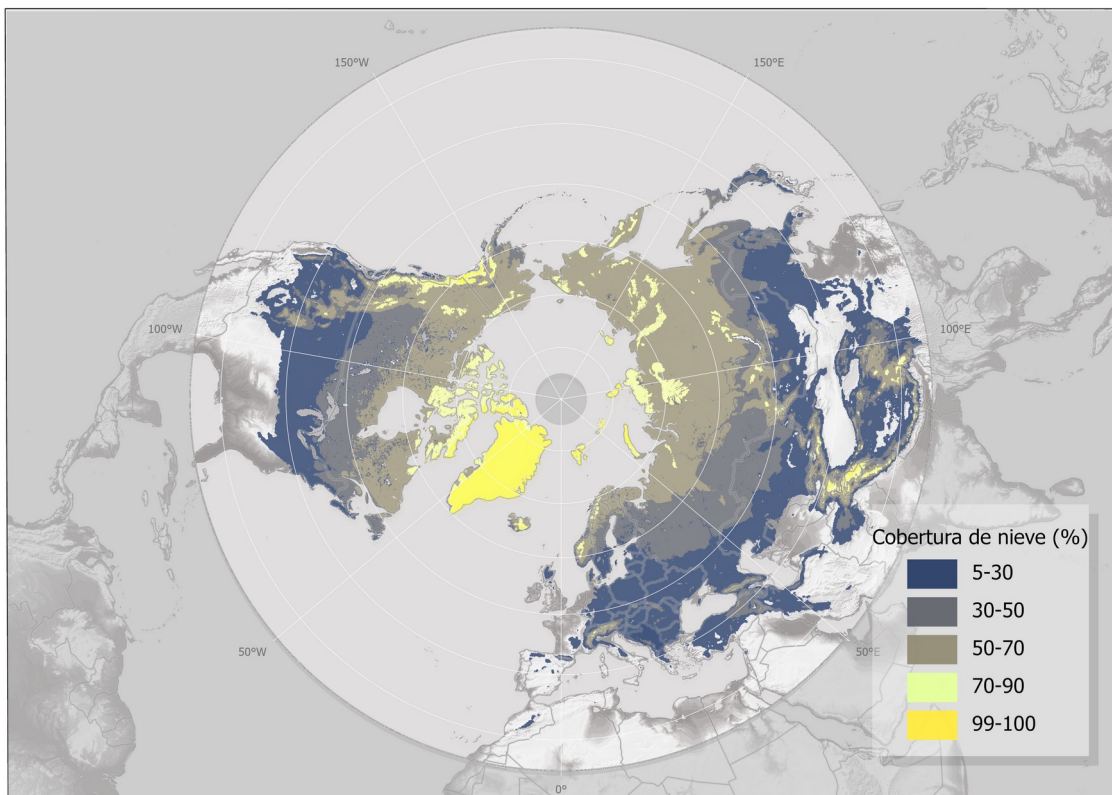


Figura 1: Promedio de cobertura de nieve del periodo 1999 - 2019 sobre el hemisferio norte calculado a partir el reanálisis ERA5-Land.

La importancia de la nieve como recurso hídrico, se vuelve especialmente crítica en las zonas montañosas con clima mediterráneo. La razón es que el clima mediterráneo está caracterizado por veranos secos, sucediendo la mayor parte de la precipitación anual durante los meses de invierno y

en menor medida otoño y primavera. El conjunto del periodo alcanza con frecuencia el 80% del total anual de las precipitaciones (Fayad et al., 2017), con valores que pueden llegar hasta el 90%, como ha sido cuantificado para la cordillera de Sierra Nevada (Estados Unidos) (Jepsen et al., 2012). A la concentración de las precipitaciones en la estación fría, hay que sumarle el hecho de que las montañas concentran buena parte de las precipitaciones debido al efecto orográfico, de tal forma que las zonas elevadas acumulan un manto de nieve profundo y de considerable persistencia a lo largo de la primavera (Alonso-González et al., 2019). Por ello, el manto de nieve en el Mediterráneo tiene la capacidad de mitigar el efecto de la fuerte estacionalidad pluviométrica sobre el régimen fluvial de los ríos de montaña, con caudales elevados durante la primavera que, en combinación con infraestructuras para la gestión de los recursos hídricos (embalses, canales, etc), resulta crucial para satisfacer la elevada demanda de agua durante los meses de verano (López-Moreno and García-Ruiz, 2004a), cuando las actividades turísticas, la agricultura y el sector energético producen un máximo de consumo de agua.

Debido a la influencia del manto de nieve en todos estos factores, resulta de gran interés conocer su variabilidad espacial y temporal, así como los factores que condicionan esta variabilidad. El manto de nieve presenta una gran variabilidad a diferentes escalas. A una escala local la distribución del manto de nieve está muy condicionada por las características topográficas del terreno, como pueden ser la pendiente, la curvatura o la exposición (López-Moreno et al., 2017; Revuelto et al., 2014), así como por los efectos de la redistribución por el viento (Winstral et al., 2002) o el bosque (Sanmiguel-Vallelado et al., 2020), jugando estos factores un importante papel en la formación de avalanchas de nieve (Schweizer et al., 2008). A escala regional, la variabilidad del manto de nieve está condicionada por la variabilidad climática. De esta manera los patrones atmosféricos tienen una gran influencia en la variabilidad interanual del espesor y duración del manto de nieve (Clark et al., 1999), ya que controlan los patrones espaciales y la variabilidad interanual de la precipitación y temperatura.

1.2 Información disponible del manto de nieve

A pesar de todas las implicaciones que el manto de nieve tiene en los procesos anteriormente explicados, existen grandes lagunas de conocimiento en su comportamiento a nivel regional. Dicha carencia se explica fundamentalmente por una falta generalizada de información cuantitativa sobre la duración y más aún el espesor y contenido en agua del manto de nieve, limitándose en la mayor

parte de los casos a registros de escasa consistencia espacial y referida a periodos de corta duración y con presencia de frecuentes lagunas.

A la situación general anteriormente mencionada hay excepciones con registros de larga duración, densidad espacial y calidad en los datos. Un ejemplo fue la base datos diaria de espesor de nieve en 284 estaciones de la antigua Unión Soviética conocida como *Historical Soviet Daily Snow Depth* (HSDSD)(Armstrong, 2001), que cubrió el periodo 1881-1995, si bien existen importantes lagunas especialmente en el periodo anterior a 1966. En la costa oeste de los Estados Unidos se ha medido el espesor de nieve y su contenido en agua de forma regular (quincenal o mensualmente) desde las primeras décadas del siglo XX, siguiendo un buen número de transectos predefinidos. Esta red evolucionó a principios de los años ochenta hacia la actualmente conocida como red SNOTEL (SNOW TELEmetry) (Schaefer and Paetzold, 2001), que cubre gran parte del oeste de Norte América mediante más de 800 estaciones automáticas que miden el espesor y su contenido en agua, así como otros parámetros meteorológicos como temperatura o precipitación. Sin embargo, esta red también posee problemas de representatividad espacial, pues las estaciones se localizan en zonas forestales y muchas veces situadas teniendo en cuenta la accesibilidad, quedando el piso alpino muy débilmente monitorizado (Molotch and Bales, 2006).

En Europa occidental, no existen redes de monitorización del manto de nieve como las anteriormente descritas, en cuanto a su cobertura espacial y duración temporal, aunque sí es posible encontrar información sobre el manto de nieve, en algunas ocasiones cubriendo varias décadas de longitud, recogidas por diferentes agencias meteorológicas o hidrológicas estatales y más locales tanto para fines operacionales como para la investigación. Sin embargo muchos de estos se refieren con frecuencia a zonas de baja altitud donde se encuentran los principales núcleos de población. Así, zonas de alta montaña donde se acumula la mayor parte del recurso nieve quedan muy débilmente monitorizadas. Un buen ejemplo de red de monitorización en Europa occidental es la dirigida por el Instituto para la Investigación de la Nieve y las Avalanchas (Suiza, WSL Institute for Snow and Avalanche Research SLF) iniciada en la década de 1960 y con mediciones continuas de espesor de nieve y equivalente en agua (SWE). Los datos son obtenidos manualmente dos veces al mes en diferentes puntos de los Alpes Suizos (Jonas et al., 2009). Otra fuente de información interesante son las bases de datos nivometeorológicas de las diferentes zonas experimentales repartidas por el continente Europeo. En ellas se cuenta con información de larga duración del manto de nieve así como de multitud de variables meteorológicas. Algunos buenos ejemplos de zonas de investigación del manto de nieve pueden ser la zona de observación Suiza Weissfluhjoch,

que cuenta con datos desde 1936 (Marty and Meister, 2012), la estación francesa Col du Porte (Lejeune et al., 2019), que cuenta con información desde 1960 o la finlandesa Sodankyla (Essery et al., 2016). Un completo informe sobre los esfuerzos de los diferentes estados europeos para monitorizar el manto de nieve lo podemos encontrar en el “*European Snow Booklet*”(Haberkorn et al., n.d.).

En el caso de la península ibérica, la monitorización del manto de nieve de forma regular y distribuida espacialmente comenzó en los años 80 (1986) en el Pirineo a través del programa ERHIN (Evaluación de los Recursos Hídricos Procedentes de la Innivación) (Arenillas et al., 2008; Pedrero, 1988) por parte del Ministerio de Medio Ambiente y Medio Rural y Marino. En el marco de este programa se instalaron alrededor de 100 jalones en los que se medía el espesor de nieve tres veces al año (enero, marzo y finales de abril o principios de mayo) y la densidad en alrededor de un tercio de las balizas (López-Moreno and Nogués-Bravo, 2005). Posteriormente el proyecto se expandió a otras cordilleras españolas como la Cordillera Cantábrica, Sistema Central y Sierra Nevada. A parte de las mediciones periódicas, un total de 29 telenivómetros se instalaron en las principales cordilleras de la península ibérica, con 19 más propuestos para instalar en una fase más avanzada sin determinar. Estos telenivómetros tienen capacidad para medir en tiempo real tanto el espesor como el SWE, y transmitir remotamente la información. Desgraciadamente, este ambicioso programa se ejecutó con un éxito moderado, pues la mayor parte de los telenivómetros nunca llegaron a funcionar de forma continua siendo los que dan servicio a la cuenca del Ebro los únicos de los que actualmente se puede obtener información adecuada. En cualquier caso, los datos procedentes de las balizas han permitido realizar diversos trabajos científicos que han ayudado a avanzar en el conocimiento de la dinámica del manto de nieve y su relación con la hidroclimatología de la península ibérica. Algunos ejemplos los podemos encontrar en estudios hidrológicos (Sanmiguel-Vallelado et al., 2017), estudios de la variabilidad de los eventos de nevadas (Navarro-Serrano and López-Moreno, 2017), estudios de tendencias (López-Moreno, 2005; Morán-Tejeda et al., 2013), validación *in situ* de información por satélite (Juan Collados-Lara et al., 2016), o incluso utilizar la información procedente de los jalones para reproducir el manto de nieve de manera distribuida (Collados-Lara et al., 2020, 2017; López-Moreno and Nogués-Bravo, 2006, 2005) entre otros. De forma semejante a la red ERHIN, pero en la vertiente francesa de los Pirineos, Meteofrance ha instalado la red NIVOSÊ, con 9 medidores automáticos de espesor del manto de nieve junto a estaciones automáticas de alta montaña.

Además del programa ERHIN, en la península ibérica existen muy pocas iniciativas de medición del manto de nieve. En el Pirineo Central, se encuentra la Cuenca Experimental de Izas (Revuelto et al., 2017). Esta cuenca cuenta con un sistema de motorización automática de todo tipo de variables meteorológicas entre las que se incluye un medidor de espesor del manto de nieve. Esta cuenca experimental tiene la particularidad de que, a mayores de variables meteorológicas, cuenta con esporádicas mediciones de alta resolución del manto de nieve mediante láser escáner terrestre así como fotografías de la cobertura del manto de nieve cada tres horas. Estos datos, junto a los procedentes del aforo del caudal que existe en la salida de la cuenca, proporcionan una base de datos muy completa que destaca internacionalmente. Además, en el Pirineo Oriental, el servicio meteorológico de Cataluña (Meteocat), cuenta con 17 estaciones automáticas de montaña. Otra zona de medición del manto de nieve interesante dentro de la península ibérica es la red de monitorización de Guadaleo (Sierra Nevada)(Polo et al., 2019), que cuenta con información de varias estaciones automáticas con imágenes de alta resolución temporal, desde diferentes puntos de vista, del estado de nieve. Además, en Sierra Nevada existe el Observatorio de Cambio Global de Sierra Nevada que cuenta con 10 estaciones meteorológicas automáticas de montaña. En cualquier caso, si ya es muy complicado encontrar series de mediciones de nieve en Pirineos o Sierra Nevada, en el resto de cordilleras ibéricas son prácticamente inexistentes, con algunos ejemplos de estaciones automáticas como las pertenecientes a la red de motorización de Guadarrama, GuMNet (*Guadarrama Monitoring Network*).

A pesar de las mejoras que se han mencionado en el seguimiento de la nieve en la península ibérica, la información disponible es aún insuficiente para realizar estudios regionales sobre la variabilidad espacial y estacional del manto de nieve en la península. A la problemática de la longitud de las series, hay que sumarle la gran variabilidad espacial del manto de nieve especialmente en las zonas de terreno complejo. Este hecho hace que las mediciones puntuales del manto de nieve no tengan que ser necesariamente representativas de sus inmediaciones, siendo muy recomendable distribuir especialmente las mediciones (J. I. López-Moreno et al., 2011a). Esta limitación tiene obvias implicaciones a escala regional, donde se pretende analizar el comportamiento a nivel de cordillera, por lo que es necesario el uso de datos distribuidos y de un número suficiente de años. Además, el carácter mediterráneo del clima de montaña de la península ibérica, tiene como consecuencia un manto de nieve de una gran variabilidad inter- e intranual comparado con el manto de nieve de otras regiones frías (Fayad et al., 2017), por lo que una buena resolución temporal es también

indispensable. Prueba de todo ello, ha sido la ausencia hasta ahora de una climatología peninsular del manto de nieve, un recurso básico para buena parte del territorio mencionado.

1.2 Alternativas a las observaciones

La problemática de la falta de datos anteriormente descrita, no es exclusiva de la península ibérica. En general se podría decir que las observaciones de nieve son una rareza en la mayor parte de las montañas y zonas frías del mundo, especialmente si se comparan estas con otras variables meteorológicas. Ante este escenario de falta de datos, existen básicamente dos alternativas para obtener información del manto de nieve; las técnicas de teledetección y la simulación numérica del manto de nieve

1.2.1 Uso de información por satélite en el estudio del manto de nieve

La teledetección ha sido y sigue siendo una herramienta muy común a la hora de obtener información de la cobertura del manto de nieve, habiendo sido usada desde la aparición de los primeros satélites de observación de la superficie terrestre (Lucas and Harrison, 1990). Los productos de cobertura de nieve, se calculan mediante el índice espectral llamado Índice Diferencial Normalizado de Nieve (NDSI), el cual utiliza bandas del espectro visible (verde) y del infrarrojo de onda corta (Hall and Riggs, 2011). Es posible encontrar estas bandas en los sensores pasivos de varias constelaciones de satélites, lo que quiere decir que es posible generar productos de cobertura de nieve de múltiples sensores. En cualquier caso, para cumplir con los requisitos necesarios para realizar climatologías, no hay demasiados satélites elegibles. Una de las mayores limitaciones es la fecha de lanzamiento del satélite, o lo que es lo mismo, la longitud temporal de las series de datos disponibles, que deberá ser lo mayor posible, lo cual ya limita muchísimo el número de productos interesantes a día de hoy. Otro requisito importante es una buena resolución temporal, ya que el efecto combinado de la cobertura de nubes, imposibilitando obtener información de la superficie, junto con resoluciones temporales muy groseras, generan enormes lagunas temporales de información. Esto es particularmente problemático en el estudio de la nieve, debido al hecho de que las temporadas de mayor cobertura de nieve estarán necesariamente relacionadas con las temporadas con coberturas de nubes más persistentes. Además la gran variabilidad del manto de nieve, especialmente en cotas bajas, es la causante de que resoluciones temporales demasiado groseras no sean capaces de captar adecuadamente la dinámica de la cobertura de nieve (Dietz et al., 2012). Por último, otro aspecto a tener en cuenta es la resolución espacial, ya que existe una gran

incertidumbre asociada a las diferentes resoluciones en el cálculo de las superficies cubiertas de nieve (Paul et al., 2013), especialmente en áreas de terreno complejo como la península ibérica.

De todos los posibles candidatos, el sensor MODIS a bordo de los satélites Aqua y Terra es el que probablemente muestre un mejor compromiso en su longitud de series disponibles, resolución temporal y espacial (Fig. 2). La información disponible se remonta al año 2000, con un tiempo de revisita diario (con una imagen procedente del satélite Aqua y otra del satélite Terra con unas horas de diferencia) y con una resolución espacial de 500m. Estos productos han sido muy utilizados en diferentes zonas del planeta con ejemplos en los Andes para realizar climatologías de la cobertura del manto de nieve (Saavedra et al., 2017), así como para estudiar la variabilidad interanual de la nieve (Saavedra et al., 2018), en los Alpes australianos (Thompson, 2016), Tibet (Li et al., 2018), Alaska (Lindsay et al., 2015), o Austria (Parajka and Blöschl, 2008) entre otros muchos. En los Pirineos, Gascoin et al., 2015 realizaron una climatología de la cobertura del manto de nieve a partir de los productos MODIS diarios, llenando las lagunas de información producidas por las nubes. El corto periodo de revisita de MODIS, permitió el desarrollo de un algoritmo de relleno de datos que mediante el uso de ventanas temporales y espaciales, así como un árbol de regresión en su última fase, capaz de completar la información faltante generando así productos con resolución diaria. En este trabajo, además de validar el uso de MODIS para cadenas montañosas de la escala de las presentes en la península ibérica, relacionaron las anomalías en la cobertura del manto de nieve con la caída de la producción hidroeléctrica española de la temporada 2011/2012.

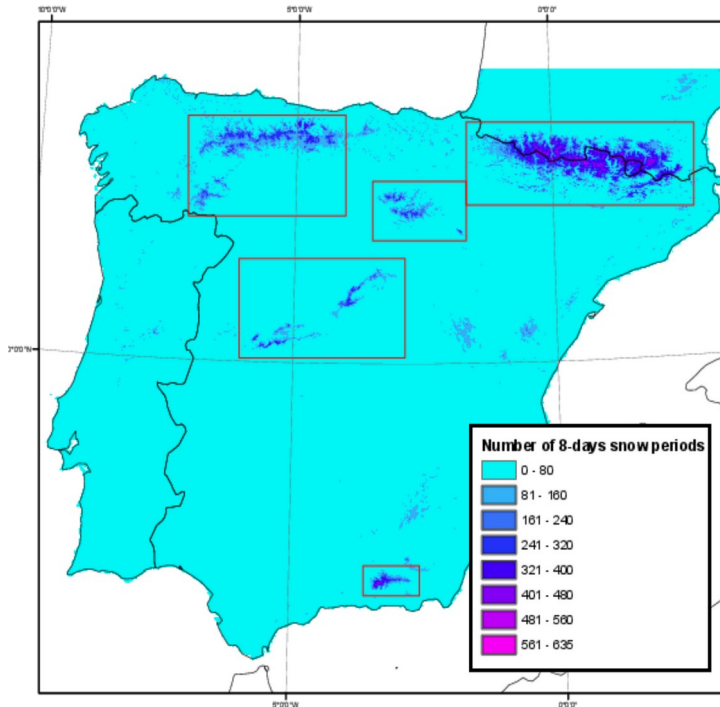


Figura 2: Número de períodos de 8 días con presencia de nieve para el total de la serie de MODIS para el periodo 2001/2015 (Gascoin et al. 2015).

Una gran limitación de la teledetección para el estudio de nieve es la dificultad de obtener información del espesor o del SWE. Existen algunas experiencias mediante el uso de sensores pasivos de microondas en combinación con observación de espesor del manto de nieve para generar imágenes con información del SWE. Un producto de uso muy común de este tipo es *GlobSnow* de la Agencia Espacial Europea. Estos productos cuentan con información de SWE de todo el Hemisferio Norte a resolución diaria desde 1979. Constituye de esta manera una interesante fuente de información para estudios a nivel continental, pero su limitada resolución espacial, de tan solo 25km, y el hecho de que los errores se incrementan en zonas con manto de nieve poco profunda (~35 mm de error de SWE en mantos de menos de 150 mm de SWE (Takala et al., 2011)) hacen que no sea muy recomendable para trabajar en zonas de terreno complejo, y mucho menos en una zona como la península ibérica con grandes extensiones de terreno con un manto de nieve efímero y muy comúnmente poco profundo. El NASA *Airborne Snow Observatory* (Painter et al., 2016), genera productos semanales de muy alta resolución espacial de SWE sobre extensas zonas de Sierra Nevada (California, EEUU). Para conseguir esto, realizan mediciones del espesor de nieve

mediante LIDAR aerotrasportado junto con mediciones del albedo de la nieve mediante cámaras multiespectrales. Estos datos son posteriormente asimilados en un modelo de balance de masa y energía (Ver apartado 1.2.2 Uso de simulaciones numéricas del manto de nieve para generar información del espesor de nieve y del SWE) para producir los mapas de SWE. A pesar de la interesante información obtenida, el desorbitado coste de realizar mediciones LIDAR semanales limita su aplicación en otras zonas del planeta.

Actualmente es posible obtener información del espesor del manto de nieve de zonas remotas a muy alta resolución (cercana a los 4m horizontales) mediante el uso de técnicas estereoscópicas a partir de la constelación de satélites Pléiades (Martí et al., 2016; Shaw et al., 2020). A pesar de producir prometedores resultados, esta novedosa técnica presenta importantes limitaciones temporales que no permiten una gran resolución temporal, a la que se suma un error vertical superior a los 30cm que dificultan de nuevo su aplicación en mantos de nieve poco profundos. Todo esto quiere decir, que en términos del estudio de la climatología del manto de nieve en la península ibérica mediante información por satélite, las posibilidades se reducen al estudio de la cobertura del manto de nieve, lo cual es una gran limitación debido a la poca representatividad que la cobertura tiene en los procesos hidrológicos si se compara con información que proporciona el SWE (Ceballos-Barbancho et al., 2018).

1.2.2 Uso de simulaciones numéricas del manto de nieve para generar información del espesor de nieve y del SWE

En muchas ocasiones, la simulación numérica resulta la única alternativa viable para reconstruir la información del SWE y espesor del manto de nieve a alta resolución temporal. Existen dos grandes métodos a la hora de simular el manto de nieve: el método grados-día y el de balance de energía. Los métodos grados-día, en sus diferentes variaciones, intentan simular la fusión neta calculada a partir de la temperatura al que se le aplica un valor (grados-día) estimado empíricamente, que se sustraerá a la masa de nieve acumulada, que se calcula a partir de la precipitación caída en los meses precedentes por debajo de un determinado umbral térmico (Hock, 2003). En ocasiones a estos métodos se les introduce más complejidad incluyendo otras variables en la estimación de la tasa de fusión (Pellicciotti et al., 2005), o discerniendo de forma más compleja la separación de la fase sólida y líquida de la precipitación. Estos métodos han sido ampliamente utilizados en glaciología y nivología debido a su simplicidad, que se traduce en una gran facilidad de implementación con un coste computacional muy pequeño. Además, es posible utilizarlos con un forzamiento atmosférico

sencillo, siendo únicamente necesario datos de precipitación y temperatura. El mayor problema que presentan estos modelos es que no tienen en cuenta los procesos físicos de tipo radiativo y turbulento que influyen de forma determinante en la dinámica del manto de nieve. Por ejemplo, no tienen en cuenta procesos de sublimación, los cuales se ha llegado a observar que en Sierra Nevada ocurren durante un 60% del tiempo en el que encontramos manto de nieve (Herrero et al., 2016). Otros procesos como el rehielo del agua en fase líquida dentro del manto de nieve, la compactación, el efecto de la radiación o el intercambio turbulento de energía (producidos en los cambios de fase de la superficie nivosa) tampoco estarían representados en un modelo de grados día.

En contraposición a los modelos de grados-día, el manto de nieve se puede simular mediante un balance de masa y energía, en el que los componentes de los flujos de masa y energía son resueltos a partir de un forzamiento meteorológico. Estos modelos de base física, simulan el manto de nieve mediante un conjunto de ecuaciones que simulan diferentes procesos del manto de nieve. En estos modelos se calcula el balance de energía mediante:

$$\frac{\partial Q}{\partial t} = Q_{SW} + Q_{LW} + Q_H + Q_L + Q_P + Q_G$$

Donde $\partial Q / \partial t$ es el ratio de energía, Q_{SW} es el flujo neto de radiación de onda corta, Q_{LW} es el flujo neto de energía en onda larga, Q_H es el flujo de calor sensible, Q_L es el flujo de calor latente, Q_P es el flujo de calor procedente de la precipitación y Q_G es el flujo de calor procedente del suelo. De manera análoga, el balance de masa es calculado mediante:

$$\frac{\partial M}{\partial t} = M_S + M_L - M_{Sb} - M_{rff} + M_R + M_A$$

Donde $\partial M / \partial t$ es el ratio de masa, M_S es el flujo de precipitación sólida, M_L es el flujo de precipitación en forma líquida, M_{Sb} es el flujo de masa perdido por sublimación, Q_{rff} es el flujo de masa que se escapa del manto en forma líquida (principalmente fusión), M_R es el flujo de masa que se recongela dentro del manto de nieve y M_A es el flujo de masa a consecuencia del transporte por viento.

La complejidad de los modelos de balance de energía, radica en la manera en la que sus parametrizaciones resuelven cada uno de los componentes de los balances de masa y energía, que puede variar tremadamente. Estos balances de energía se implementan en los modelos en un número variable de capas que van desde las más sencillas de una sola capa, como el usado por

muchos modelos atmosféricos globales (ECMWF, 2019), a múltiples capas (Niu et al., 2011), llegando algunos a tener una gran complejidad a costa de un gran esfuerzo computacional y siendo destinados principalmente a su uso en la simulación de situaciones de avalanchas (Vionnet et al., 2012).

El mayor problema de los modelos de nieve de base física es disponer de información meteorológica suficiente para forzar las simulaciones. Estos modelos suelen requerir diferentes tipos de variables meteorológicas para resolver cada uno de los componentes del balance de energía, entre las cuales deberán de estar presentes como mínimo la temperatura del aire, la humedad atmosférica, viento, presión atmosférica, precipitación y radiación en onda corta. Habiendo visto anteriormente la dificultad de disponer de observaciones meteorológicas y nivológicas adecuadas en zonas de alta montaña (Raleigh et al., 2016), su aplicación en la mayor parte de las montañas en general, y en la península ibérica en particular, resulta muy compleja.

La única alternativa viable para encontrar información meteorológica para forzar modelos de balance de masa y energía y poder realizar simulaciones de varios años del manto de nieve la encontramos en los datos procedentes de simulaciones atmosféricas, que para reproducir períodos pasados se denominan de reanálisis. Los reanálisis atmosféricos son bases de datos realizadas mediante modelos atmosféricos globales. Estos modelos son forzados por datos históricos procedentes de muy diversas fuentes de información incluyendo estaciones meteorológicas convencionales, información por satélite, globos sonda meteorológicos, estaciones meteorológicas o boyas marinas entre otras. Existen multitud de reanálisis diferentes que cubren diferentes períodos de tiempo con multitud de particularidades diferentes. Si bien todos ellos tienen muchas aplicaciones en el área de la climatología, prácticamente todos tienen en común la poca resolución espacial disponible, que a día de hoy puede llegar a ser en el mejor de los casos de 0.25° (~ 30 km) siendo comunes resoluciones cercanas o superiores a 1° (~ 110 km). Esto imposibilita totalmente su uso para simular el manto de nieve en terreno complejo debido al enorme suavizado de la topografía que representa (Mass et al., 2002). No obstante, es posible incrementar su resolución mediante modelos atmosféricos regionales. Estos modelos funcionan de manera análoga a los modelos atmosféricos globales, con la particularidad de que es posible lanzarlos en zonas delimitadas del territorio con un modelo de elevaciones muy superior al del reanálisis original, y utilizando las condiciones iniciales y de contorno, de un modelo atmosférico global previo. El uso de este tipo de datos para realizar simulaciones físicas del balance de energía no es nuevo, por ejemplo van Pelt et al., 2016 utilizaron un procedimiento similar para Svalbard utilizando las salidas del modelo

climático regional HIRLAM como forzamiento del modelo de balance de masa y energía *Snowmodel* (Liston and Elder, 2006a). De manera análoga, Wu et al., 2016 generaron productos de SWE en las montañas de Altai, donde usaron las salidas del modelo climático WRF (Skamarock et al., 2008) como forzamiento de un modelo tipo grados día, ajustado mediante información por satélite.

A pesar de las mejoras de resolución de los modelos atmosféricos regionales, las resoluciones alcanzadas cuando se simulan períodos de tiempo largos (más de 30 años) no son suficientes para resolver adecuadamente todos los campos meteorológicos de las zonas de terreno complejo con un coste computacional asumible. Existen diferentes maneras de sortear esta barrera computacional, mediante aproximaciones que, realizando algunas simplificaciones, consiguen mejorar todavía más la resolución de las simulaciones atmosféricas con un coste computacional asumible. Un ejemplo de estas soluciones alternativas es el modelo MICROMET (Liston and Elder, 2006b), el cual interpola espacialmente las variables meteorológicas de superficie de un modelo atmosférico (o una red de estaciones meteorológicas), y las corrige con la altura sobre un modelo digital de elevaciones, generando nuevos campos meteorológicos de mayor resolución. Estos productos pueden ser de mucha utilidad si se asume la incertidumbre introducida por la interpolación estadística o por otras simplificaciones como el uso de gradientes térmicos y pluviométricos, especialmente si se cuenta con datos observados para asimilar en el modelo. Otra técnica muy usada han sido las simulaciones semidistribuidas, en las que se reproducen los campos meteorológicos necesarios para forzar un modelo del manto de nieve en un punto con unas características de exposición, elevación o pendiente concretas (Revuelto et al., 2018), habiendo sido esta técnica previamente utilizada en los Pirineos para el estudio del efecto del cambio climático en el manto de nieve (López-Moreno et al., 2009).

1.3 El manto de nieve en la península ibérica

A pesar de que no existe una climatología de nieve a nivel regional de toda la península ibérica, sí que existen trabajos previos que describen diversos aspectos de la dinámica del manto de nieve, especialmente en los Pirineos y Sierra Nevada. La península ibérica tiene una topografía muy compleja con varias cordilleras montañosas que pueden resumirse en cinco macizos donde la nieve posee un papel relevante desde un punto de vista hidrológico, ecológico y socioeconómico: Cordillera Cantábrica, Sistema Central, Sistema Ibérico, Pirineos y Sierra Nevada. Estas cordilleras rodean dos importantes mesetas que hacen de la península ibérica una de las regiones más elevadas

de Europa. A pesar de su baja latitud, nevadas ocasionales son comunes en la mayor parte del territorio, siendo muy frecuentes en varias ciudades importantes de la mitad norte de la península (Merino et al., 2014). Existen registros de nevadas incluso cerca del nivel del mar en la zona de Levante (Mora et al., 2016), Barcelona o Gerona (Aran et al., 2010). En cualquier caso, a pesar de que estos eventos suelen tener una repercusión muy elevada, ya que suceden en zonas de alta densidad de población, la realidad es que la península ibérica cuenta con un manto de nieve estacional únicamente en las zonas montañosas, dónde sí persiste hasta el final de la primavera y principios de verano, incluso en las zonas más meridionales y áridas como Sierra Nevada (Pimentel et al., 2017). Estas zonas montañosas ejercen un gran control sobre las zonas aguas abajo (López and Jústribó, 2010) como ha sido confirmado en los Pirineos (López-Moreno and García-Ruiz 2004). De esta manera, el ciclo hidrológico está, en las épocas de fusión, mucho más relacionado con las acumulaciones de nieve existentes en cotas altas que con la precipitación en forma líquida, con importantes implicaciones también en las avenidas, las cuales son amplificadas a consecuencia de la fusión de nieve (Morán-Tejeda et al., 2019).

Aparte de la importancia hidrológica anteriormente descrita, no hay que olvidar el impacto que el manto de nieve posee directamente sobre la economía de la península ibérica, y más concretamente en zonas muchas veces afectadas por la despoblación o la falta de motores económicos. El turismo relacionado de alguna manera con la nieve, y más concretamente el esquí alpino, ha demostrado ser una fuente de riqueza con potencial para recuperar la demografía de las zonas donde se consolida (Lasanta et al., 2007). En cualquier caso, las zonas rurales montañosas donde se asienta un manto de nieve estacional, están sufriendo una continuada despoblación, y es precisamente en ellas donde la nieve juega un papel como motor económico en forma de turismo deportivo, o de cualquier otro tipo. Esta es la razón por la que la gestión del territorio en las zonas rurales de la montaña Ibérica ha pasado en muchas ocasiones por la gestión de las actividades directamente relacionadas con la nieve por parte de los entes públicos y políticos (Gilaberte-Búrdalo et al., 2017). Otros sectores socioeconómicos afectados por la variabilidad espacio temporal de la nieve, tienen relación con la producción forestal, la cual está influenciada por los patrones de acumulación del manto de nieve (Sanmiguel-Vallelado et al., 2019) o la gestión del riesgo tanto en el transporte, el cual se ha demostrado aumenta considerablemente con las nevadas (Mills et al., 2011) o por avalanchas. Las avalanchas representan uno de los mayores riesgos en zonas montañosas, a las que se les asocia alrededor de 1900 muertes en Europa y Norte América en el periodo desde 2000/2001 hasta 2009/2010 (Schweizer et al., 2015).

La variabilidad intranual e interanual de los eventos de nieve está muy asociada a los diferentes patrones sinópticos atmosféricos (Esteban et al., 2005; Navarro-Serrano and López-Moreno, 2017). La Oscilación del Atlántico Norte (NAO) es un índice de teleconexión que se define como la diferencia de presión atmosférica para el dipolo centrado en Islandia y las Islas Azores. En la cuenca Mediterránea, la NAO es el principal índice de teleconexión que determina los patrones espaciales y la magnitud de la precipitación y la temperatura (Fig.3) (Corte-Real et al., 1995; Hurrell, 1995; J. I. López-Moreno et al., 2011b). Es por esto que el manto de nieve estacional estará necesariamente relacionado con la NAO, o más concretamente con el índice NAO promedio de la temporada de acumulación. López-Moreno and Vicente-Serrano (2007) y posteriormente Buisan et al.(2015) comprobaron una clara correlación negativa entre el índice NAO y la acumulación de nieve en el Pirineo Central, si bien con coeficientes muy variables en altura y localización geográfica. A una escala espacial mucho más amplia, López-Moreno et al. (2011) utilizaron datos climáticos en rejilla (0.5° de resolución) proporcionados por la Unidad de Investigación Climática de la universidad de East Anglia (CRU, Mitchell and Jones, 2005) junto con información observada del manto de nieve de los Pirineos y Alpes, para valorar la relación que existe entre el índice NAO y el manto de nieve a escala regional para las montañas que rodean la cuenca del Mediterráneo. Quedó demostrada la influencia de la NAO en el manto de nieve, pero con varias puntualizaciones. Por ejemplo, el efecto de la NAO de invierno en el manto de nieve tiende a perder relevancia cuanto más hacia el este se encuentra una determinada cordillera. Además de esto, el efecto de la NAO invernal en el manto presenta un claro gradiente altitudinal, a consecuencia de que en las cotas bajas la presencia de nieve está más marcada por el régimen térmico que por el pluviométrico. Esto se produce a consecuencia de que los patrones sinópticos asociados a las fases de NAO negativa favorecen los flujos de viento procedentes del sur y sur oeste, por lo que propician advecciones de humedad, pero con condiciones térmicas templadas.

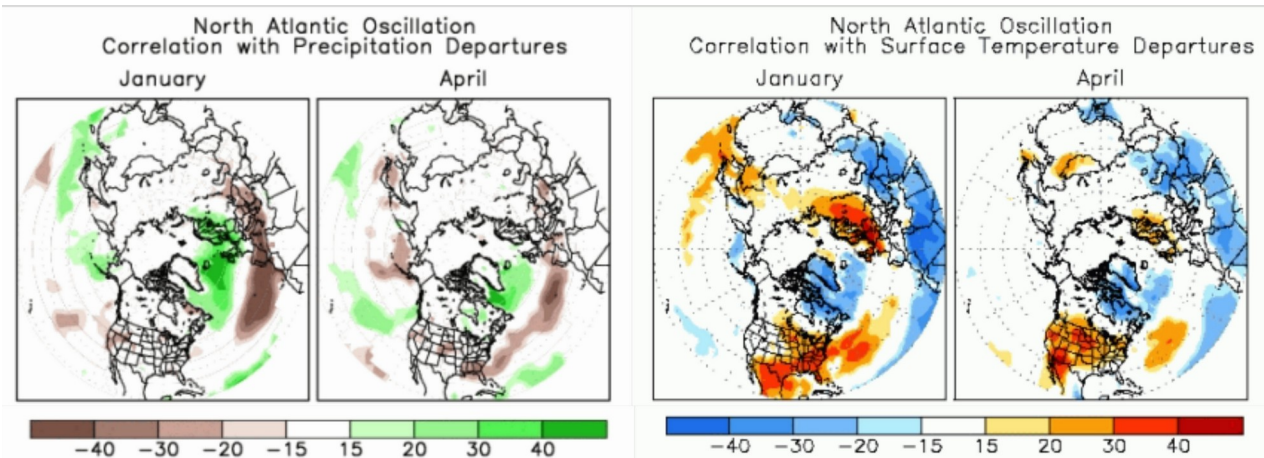


Figura 3: Patrones de correlación entre el índice NAO y la precipitación y temperatura en el Hemisferio Norte. Modificado de NOAA/ National Weather Service.

Esta relación entre el índice NAO y el manto de nieve tiene grandes implicaciones. A día de hoy, las predicciones estacionales a largo plazo mediante simulaciones atmosféricas presentan una gran incertidumbre a consecuencia de la no-linealidad de las ecuaciones involucradas en cualquier modelo atmosférico numérico moderno. Esto hace muy difícil poder predecir con exactitud la cantidad de nieve que estará presente en el futuro a medio plazo de manera directa. En cambio, la predicción de los grandes patrones sinópticos atmosféricos mediante el uso de indicadores empíricos (Scaife et al., 2014; Wang et al., 2017), con una antelación temporal entre uno y varios años, sí ha mejorado notablemente (Dunstone et al., 2016). De esta manera, potencialmente sería posible obtener una aproximación a la cantidad de nieve disponible con mucha antelación, con todas las implicaciones que ello tiene para la gestión de los recursos hídricos y la economía.

A pesar de la certidumbre que se tenía en la influencia de la NAO invernal en el manto de nieve, la falta de datos o, como en el caso del trabajo de López-Moreno et al., 2011, la falta de resolución, no han permitido un estudio en profundidad de cómo esta influencia se distribuye espacialmente, información fundamental para el uso operacional de la NAO invernal como predictor del manto de nieve.

1.4 Impactos de la variabilidad climática en el manto de nieve de la península ibérica

No es solo crucial conocer las características actuales del manto de nieve, si no entender como estas características pueden evolucionar en el futuro. Debido a su naturaleza, el manto de nieve responde de manera muy clara a la variabilidad climática. En el actual proceso de calentamiento en el que nos encontramos, son de esperar importantes cambios en el manto de nieve que potencialmente tendrán efectos sobre un alto porcentaje de la población mundial (Barnett et al., 2005). A parte de las claras implicaciones que el cambio climático tendrá en el manto de nieve en términos de duración y magnitud, recientes estudios han demostrado como el manto de nieve puede responder de manera muy compleja a los procesos de calentamiento. Por ejemplo, Musselman et al., 2017 observaron que bajo condiciones más cálidas las tasas de fusión tienden a ralentizarse, hipótesis que ha sido confirmada para el conjunto del hemisferio norte (Wu et al., 2018). Esta respuesta implica periodos de fusión más largos, con importantes impactos en la gestión de los recursos hídricos entre otros. Otro ejemplo de cómo de compleja es la respuesta del manto de nieve a los procesos de calentamiento lo encontramos en Harpold and Brooks, (2018). En este trabajo se demuestra que los procesos de fusión asociados al calentamiento están controlados en realidad por la humedad atmosférica que controla el flujo de masa en forma de sublimación y por lo tanto una importante parte del balance de energía. Diferentes repuestas del manto de nieve a la variabilidad climática se pueden producir incluso dentro de áreas catalogadas como climáticamente iguales. López-Moreno et al. (2017), demostraron como la sensibilidad del manto de nieve al calentamiento puede ser muy diferente incluso en zonas catalogadas como clima mediterráneo, con diferencias de una disminución de entre unos 6 días $^{\circ}\text{C}^{-1}$ de duración y un 9% $^{\circ}\text{C}^{-1}$ de máximo de acumulación, hasta 28 días $^{\circ}\text{C}^{-1}$ y un 19% $^{\circ}\text{C}^{-1}$ de máximo de acumulación en las zonas más sensibles. Todas estas respuestas tan diferenciadas se producen a consecuencia de los diferentes pesos de los componentes de los respectivos balances de masa y energía de cada lugar.

A demás del incremento de temperatura asociado al cambio climático, existen otras fuentes de variabilidad climática que influyen directamente en el balance de masa y energía de la nieve. Por ejemplo, existe una gran incertidumbre sobre como las precipitaciones pueden evolucionar en las próximas décadas (Monjo et al., 2016), a pesar de que la disminución de la nieve a causa del cambio climático puede estar muy relacionada con la disminución de las precipitaciones (Irannejhad et al., 2016). Por otro lado, hay una tendencia muy clara en el incremento de la

radiación en onda corta sobre la península ibérica, cuando se analizan datos observados. Este incremento se achaca al efecto mixto de una atmósfera con cada vez con menos aerosoles, y un descenso de la nubosidad sobre la península (Vicente-Serrano et al., 2017), efecto que ha sido también observado para la totalidad de Europa (Sanchez-Lorenzo et al., 2017). Todos estos factores representan una gran fuente de incertidumbre sobre como el manto de nieve podría evolucionar en las próximas décadas, a la que habría que sumar el efecto de la altitud, ya que se ha probado que la sensibilidad del manto de nieve es mayor en los lugares cerca de la isoterma 0 °C (Pierce and Cayan, 2013), y que resulta crucial en una zona de topografía tan compleja como es la península ibérica.

1.5 Objetivos

Todo lo expuesto en los apartados anteriores, pone de manifiesto la necesidad de entender en profundidad la forma en que el manto de nieve se comporta a nivel regional, dado el importante papel que este juega en múltiples aspectos de la península ibérica. En este contexto se desarrolla la presente tesis doctoral, la cual tiene como objetivo principal conocer el comportamiento del manto de nieve a nivel regional, así como su respuesta a la variabilidad climática. Expuestas previamente las dificultades y las herramientas disponibles para completar este objetivo, así como un resumen del conocimiento actual que se tiene sobre el manto de nieve en la península ibérica, nos planteamos los siguientes objetivos secundarios, que se han materializado en diferentes etapas del trabajo, habiendo sido cada uno de ellos objeto de una publicación científica:

- 1- Generar una base de datos del manto de nieve semidistribuida a resolución diaria consistente con las observaciones disponibles que cubran un periodo mínimo de 30 años, permitiendo así realizar estudios climáticos robustos.
- 2- Estudiar las características del manto de nieve a nivel regional en las principales cordilleras de la península ibérica, realizando la primera climatología de nieve del mismo territorio.
- 3- Estudiar el efecto que los patrones sinópticos asociados a las diferentes fases de la Oscilación del Atlántico Norte (NAO) durante los meses de invierno tienen sobre los patrones espaciales de magnitud y duración del manto de nieve en la península ibérica.
- 4- Estudiar las diferencias en los valores de sensibilidad del manto de nieve respecto a la variabilidad de la temperatura, precipitación y radiación en onda corta a lo largo de un gradiente altitudinal sobre la península ibérica.

Cada uno de los próximos capítulos tiene como objetivo completar respectivamente cada uno de estos puntos, correspondiéndose con las cuatro etapas de la tesis doctoral. El último capítulo de la tesis doctoral está constituido por unas conclusiones generales de todo el trabajo, donde también se tratarán posibles líneas de investigación futuras.

Referencias:

- Alonso-González, E., López-Moreno, J.I., Navarro-Serrano, F., Sanmiguel-Vallelado, A., Revuelto, J., Domínguez-Castro, F., Ceballos, A., 2020. Snow climatology for the mountains in the Iberian Peninsula using satellite imagery and simulations with dynamically downscaled reanalysis data. *Int. J. Climatol.* 40, 477–491. <https://doi.org/10.1002/joc.6223>
- Aran, M., Rigo, T., Bech, J., 2010. Analysis of the hazardous low-altitude snowfall, 8th March 2010, in Catalonia. ... Sept. 1-4, 2010 ... 12, 2010.
- Arenillas, M., Cobos, G., Navarro, J., 2008. Datos sobre la nieve y los glaciares en las cordilleras españolas. El programa ERHIN (1984--2008). Ed. Minist. Medio Ambient. y Medio Rural y Mar. Madrid.
- Armstrong, R., 2001. Historical Soviet daily snow depth version 2 (HSDSD). Natl. Snow Ice Data Center, Boulder, CO. CD-ROM.
- Barnett, T.P., Adam, J.C., Lettenmaier, D.P., 2005. Potential impacts of a warming climate on water availability in snow-dominated regions. *Nature* 438, 303–309. <https://doi.org/10.1038/nature04141>
- Barnett, T.P., Dümenil, L., Schlese, U., Roeckner, E., 1988. The effect of eurasian snow cover on global climate. *Science* (80-.). 239, 504–507. <https://doi.org/10.1126/science.239.4839.504>
- Brooks, P.D., Williams, M.W., 1999. Snowpack controls on nitrogen cycling and export in seasonally snow-covered catchments. *Hydrol. Process.* 13, 2177–2190.
- Buisan, S.T., Saz, M.A., López-Moreno, J.I., 2015. Spatial and temporal variability of winter snow and precipitation days in the western and central Spanish Pyrenees. *Int. J. Climatol.* 35, 259–274. <https://doi.org/10.1002/joc.3978>
- Ceballos-Barbancho, A., Llorente-Pinto, J.M., Alonso-González, E., López-Moreno, J.I., 2018. Dinámica del manto de nieve en una pequeña cuenca de montaña mediterránea: El caso del río tormes (cuenca del duero, españa)1. *Rev. Geogr. Norte Gd.* 2018, 9–34. <https://doi.org/10.4067/s0718-34022018000300009>
- Clark, M.P., Serreze, M.C., Robinson, D.A., 1999. Atmospheric controls on Eurasian snow extent. *Int. J. Climatol.* 19, 27–40. [https://doi.org/10.1002/\(SICI\)1097-0088\(199901\)19:1<27::AID-JOC346>3.0.CO;2-N](https://doi.org/10.1002/(SICI)1097-0088(199901)19:1<27::AID-JOC346>3.0.CO;2-N)
- Collados-Lara, A.J., Pardo-Igúzquiza, E., Pulido-Velazquez, D., 2020. Optimal design of snow stake networks to estimate snow depth in an alpine mountain range. *Hydrol. Process.* 34, 82–95. <https://doi.org/10.1002/hyp.13574>

Collados-Lara, A.J., Pardo-Igúzquiza, E., Pulido-Velazquez, D., 2017. Spatiotemporal estimation of snow depth using point data from snow stakes, digital terrain models, and satellite data. *Hydrol. Process.* 31, 1966–1982. <https://doi.org/10.1002/hyp.11165>

Corte-Real, J., Zhang, X., Wang, X., 1995. Large-scale circulation regimes and surface climatic anomalies over the Mediterranean. *Int. J. Climatol.* 15, 1135–1150. <https://doi.org/10.1002/joc.3370151006>

Déry, S.J., Brown, R.D., 2007. Recent Northern Hemisphere snow cover extent trends and implications for the snow-albedo feedback. *Geophys. Res. Lett.* 34. <https://doi.org/10.1029/2007GL031474>

Dietz, A.J., Kuenzer, C., Gessner, U., Dech, S., 2012. Remote sensing of snow - a review of available methods. *Int. J. Remote Sens.* 33, 4094–4134. <https://doi.org/10.1080/01431161.2011.640964>

Dunstone, N., Smith, D., Scaife, A., Hermanson, L., Eade, R., Robinson, N., Andrews, M., Knight, J., 2016. Skilful predictions of the winter North Atlantic Oscillation one year ahead. *Nat. Geosci.* 9, 809–814. <https://doi.org/10.1038/ngeo2824>

ECMWF, 2019. PART IV: PHYSICAL PROCESSES, in: IFS Documentation CY46R1, IFS Documentation. ECMWF, p. 4.

Essery, R., Kontu, A., Lemmetyinen, J., Dumont, M., Ménard, C.B., 2016. A 7-year dataset for driving and evaluating snow models at an Arctic site (Sodankylä, Finland). *Geosci. Instrumentation, Methods Data Syst.* 5, 219–227. <https://doi.org/10.5194/gi-5-219-2016>

Esteban, P., Jones, P.D., Martín-Vide, J., Mases, M., 2005. Atmospheric circulation patterns related to heavy snowfall days in Andorra, Pyrenees. *Int. J. Climatol.* 25, 319–329. <https://doi.org/10.1002/joc.1103>

Fayad, A., Gascoin, S., Faour, G., López-Moreno, J.I., Drapeau, L., Page, M. Le, Escadafal, R., 2017. Snow hydrology in Mediterranean mountain regions: A review. *J. Hydrol.* 551, 374–396. <https://doi.org/10.1016/j.jhydrol.2017.05.063>

Gascoin, S., Hagolle, O., Huc, M., Jarlan, L., Dejoux, J.F., Szczypta, C., Martí, R., Sánchez, R., 2015. A snow cover climatology for the Pyrenees from MODIS snow products. *Hydrol. Earth Syst. Sci.* 19, 2337–2351. <https://doi.org/10.5194/hess-19-2337-2015>

Gilaberte-Búrdalo, M., López-Moreno, J.I., Morán-Tejeda, E., Jerez, S., Alonso-González, E., López-Martín, F., Pino-Otín, M.R., 2017. Assessment of ski condition reliability in the Spanish and

Andorran Pyrenees for the second half of the 20th century. *Appl. Geogr.* 79, 127–142. <https://doi.org/10.1016/j.apgeog.2016.12.013>

Haberkorn, A., Fierz, C., Marty, C., Macelloni, G., Morin, S., Schöner, W., n.d. The European Snow Booklet. <https://doi.org/doi:10.16904/envidat.59>

Hall, D.K., Riggs, G.A., 2011. Normalized-difference snow index (Ndsi). *Encycl. Earth Sci. Ser. Part 3*, 779–780. https://doi.org/10.1007/978-90-481-2642-2_376

Harpold, A.A., Brooks, P.D., 2018. Humidity determines snowpack ablation under a warming climate. *Proc. Natl. Acad. Sci. U. S. A.* 115, 1215–1220. <https://doi.org/10.1073/pnas.1716789115>

Herrero, J., Polo, M.J., Eugster, W., 2016. Evaposublimation from the snow in the Mediterranean mountains of Sierra Nevada (Spain). *Cryosphere* 10.

Hock, R., 2003. Temperature index melt modelling in mountain areas. *J. Hydrol.* 282, 104–115. [https://doi.org/10.1016/S0022-1694\(03\)00257-9](https://doi.org/10.1016/S0022-1694(03)00257-9)

Hurrell, J.W., 1995. Decadal trends in the North Atlantic oscillation: Regional temperatures and precipitation. *Science (80-.).* 269, 676–679. <https://doi.org/10.1126/science.269.5224.676>

Irannezhad, M., Ronkanen, A.K., Kløve, B., 2016. Wintertime climate factors controlling snow resource decline in Finland. *Int. J. Climatol.* 36, 110–131. <https://doi.org/10.1002/joc.4332>

Jepsen, S.M., Molotch, N.P., Williams, M.W., Rittger, K.E., Sickman, J.O., 2012. Interannual variability of snowmelt in the Sierra Nevada and Rocky Mountains, United States: Examples from two alpine watersheds. *Water Resour. Res.*

Jonas, T., Marty, C., Magnusson, J., 2009. Estimating the snow water equivalent from snow depth measurements in the Swiss Alps. *J. Hydrol.* 378, 161–167.

Jones, H., 2001. *Snow ecology: an interdisciplinary examination of snow-covered ecosystems.* Cambridge University Press.

Jones, H.G., 1999. The ecology of snow-covered systems: a brief overview of nutrient cycling and life in the cold. *Hydrol. Process.* 13, 2135–2147. [https://doi.org/10.1002/\(sici\)1099-1085\(199910\)13:14/15<2135::aid-hyp862>3.0.co;2-y](https://doi.org/10.1002/(sici)1099-1085(199910)13:14/15<2135::aid-hyp862>3.0.co;2-y)

Juan Collados-Lara, A., Pardo-Iguzquiza, E., Pulido-Velazquez, D., 2016. Estimation of snowpack matching ground-truth data and MODIS satellite-based observations by using regression kriging, in: EGU General Assembly Conference Abstracts.

Lasanta, T., Laguna, M., Vicente-Serrano, S.M., 2007. Do tourism-based ski resorts contribute to the homogeneous development of the Mediterranean mountains? A case study in the Central Spanish Pyrenees. *Tour. Manag.* 28. <https://doi.org/10.1016/j.tourman.2007.01.003>

Lejeune, Y., Dumont, M., Panel, J.-M., Lafaysse, M., Lapalus, P., Le Gac, E., Lesaffre, B., Morin, S., 2019. 57 years (1960--2017) of snow and meteorological observations from a mid-altitude mountain site (Col de Porte, France, 1325 m of altitude). *Earth Syst. Sci. Data* 11, 71.

Li, C., Su, F., Yang, D., Tong, K., Meng, F., Kan, B., 2018. Spatiotemporal variation of snow cover over the Tibetan Plateau based on MODIS snow product, 2001–2014. *Int. J. Climatol.* 38, 708–728. <https://doi.org/10.1002/joc.5204>

Lindsay, C., Zhu, J., Miller, A.E., Kirchner, P., Wilson, T.L., 2015. Deriving snow cover metrics for Alaska from MODIS. *Remote Sens.* 7, 12961–12985. <https://doi.org/10.3390/rs71012961>

Liston, G.E., Elder, K., 2006a. A distributed snow-evolution modeling system (snowmodel). *J. Hydrometeorol.* 7, 1259–1276. <https://doi.org/10.1175/JHM548.1>

Liston, G.E., Elder, K., 2006b. A meteorological distribution system for high-resolution terrestrial modeling (MicroMet). *J. Hydrometeorol.* 7, 217–234. <https://doi.org/10.1175/JHM486.1>

López-Moreno, J.I., 2005. Recent variations of snowpack depth in the central Spanish Pyrenees. *Arctic, Antarct. Alp. Res.* 37, 253–260. [https://doi.org/10.1657/1523-0430\(2005\)037\[0253:RVOSDI\]2.0.CO;2](https://doi.org/10.1657/1523-0430(2005)037[0253:RVOSDI]2.0.CO;2)

López-Moreno, J. I., Fassnacht, S.R., Beguería, S., Latron, J.B.P., 2011a. Variability of snow depth at the plot scale: Implications for mean depth estimation and sampling strategies. *Cryosphere* 5, 617–629. <https://doi.org/10.5194/tc-5-617-2011>

López-Moreno, J.I., García-Ruiz, J.M., 2004a. Influence of snow accumulation and snowmelt on streamflow in the central Spanish Pyrenees / Influence de l'accumulation et de la fonte de la neige sur les écoulements dans les Pyrénées centrales espagnoles. *Hydrol. Sci. J.* 49. <https://doi.org/10.1623/hysj.49.5.787.55135>

López-Moreno, J.I., García-Ruiz, J.M., 2004b. Influence de l'accumulation et de la fonte de la neige sur les écoulements dans les Pyrénées centrales espagnoles. *Hydrol. Sci. J.* 49, 787–802.

López-Moreno, J. I., Gascoin, S., Herrero, J., Sproles, E.A., Pons, M., Alonso-González, E., Hanich, L., Boudhar, A., Musselman, K.N., Molotch, N.P., Sickman, J., Pomeroy, J., 2017. Different sensitivities of snowpacks to warming in Mediterranean climate mountain areas. *Environ. Res. Lett.* 12. <https://doi.org/10.1088/1748-9326/aa70cb>

López-Moreno, J.I., Goyette, S., Beniston, M., 2009. Impact of climate change on snowpack in the Pyrenees: Horizontal spatial variability and vertical gradients. *J. Hydrol.* 374, 384–396. <https://doi.org/10.1016/j.jhydrol.2009.06.049>

López-Moreno, J.I., Nogués-Bravo, D., 2006. Interpolating local snow depth data: An evaluation of methods. *Hydrol. Process.* 20, 2217–2232. <https://doi.org/10.1002/hyp.6199>

López-Moreno, J.I., Nogués-Bravo, D., 2005. A generalized additive model for the spatial distribution of snowpack in the Spanish Pyrenees. *Hydrol. Process.* 19, 3167–3176. <https://doi.org/10.1002/hyp.5840>

López-Moreno, Juan I., Revuelto, J., Alonso-González, E., Sanmiguel-Vallelado, A., Fassnacht, S.R., Deems, J., Morán-Tejeda, E., 2017. Using very long-range terrestrial laser scanner to analyze the temporal consistency of the snowpack distribution in a high mountain environment. *J. Mt. Sci.* 14, 823–842. <https://doi.org/10.1007/s11629-016-4086-0>

López-Moreno, J.I., Vicente-Serrano, S.M., 2007. Atmospheric circulation influence on the interannual variability of snow pack in the Spanish Pyrenees during the second half of the 20th century. *Nord. Hydrol.* 38, 33–44. <https://doi.org/10.2166/nh.2007.030>

López-Moreno, J. I., Vicente-Serrano, S.M., Morán-Tejeda, E., Lorenzo-Lacruz, J., Kenawy, A., Beniston, M., 2011b. Effects of the North Atlantic Oscillation (NAO) on combined temperature and precipitation winter modes in the Mediterranean mountains: Observed relationships and projections for the 21st century. *Glob. Planet. Change* 77, 62–76. <https://doi.org/10.1016/j.gloplacha.2011.03.003>

López-Moreno, Juan I., Vicente-Serrano, S.M., Morán-Tejeda, E., Lorenzo-Lacruz, J., Zabalza, J., Kenawy, A. El, Beniston, M., 2011. Influence of Winter North Atlantic Oscillation Index (NAO) on Climate and Snow Accumulation in the Mediterranean Mountains, in: *Advances in Global Change Research*. Springer, Dordrecht, pp. 73–89. https://doi.org/10.1007/978-94-007-1372-7_6

López, R., Justribó, C., 2010. L'importance hydrologique de la montagne. Un cas d'étude régional: Le bassin de l'Èbre, nordest Péninsule Ibérique. *Hydrol. Sci. J.* 55, 223–233. <https://doi.org/10.1080/02626660903546126>

Lucas, R.M., Harrison, A.R., 1990. Snow observation by satellite: A review. *Remote Sens. Rev.* 4, 285–348. <https://doi.org/10.1080/02757259009532109>

Marti, R., Gascoin, S., Berthier, E., De Pinel, M., Houet, T., Laffly, D., 2016. Mapping snow depth in open alpine terrain from stereo satellite imagery. *Cryosphere* 10, 1361–1380. <https://doi.org/10.5194/tc-10-1361-2016>

Marty, C., Meister, R., 2012. Long-term snow and weather observations at Weissfluhjoch and its relation to other high-altitude observatories in the Alps. *Theor. Appl. Climatol.* 110, 573–583.

Mass, C.F., Ovens, D., Westrick, K., Colle, B.A., 2002. Does increasing horizontal resolution produce more skillful forecasts? The results of two years of real-time numerical weather prediction over the Pacific Northwest. *Bull. Am. Meteorol. Soc.* 83, 407-430+341. [https://doi.org/10.1175/1520-0477\(2002\)083<0407:DIHRPM>2.3.CO;2](https://doi.org/10.1175/1520-0477(2002)083<0407:DIHRPM>2.3.CO;2)

Merino, A., Fernández, S., Hermida, L., López, L., Sánchez, J.L., García-Ortega, E., Gascón, E., 2014. Snowfall in the northwest Iberian Peninsula: Synoptic circulation patterns and their influence on snow day trends. *Sci. World J.* 2014, 1–14. <https://doi.org/10.1155/2014/480275>

Mills, B.N., Andrey, J., Hambly, D., 2011. Analysis of precipitation-related motor vehicle collision and injury risk using insurance and police record information for Winnipeg, Canada. *J. Safety Res.* 42, 383–390. <https://doi.org/10.1016/j.jsr.2011.08.004>

Mitchell, T.D., Jones, P.D., 2005. An improved method of constructing a database of monthly climate observations and associated high-resolution grids. *Int. J. Climatol.* 25, 693–712. <https://doi.org/10.1002/joc.1181>

Molotch, N.P., Bales, R.C., 2006. SNOTEL representativeness in the Rio Grande headwaters on the basis of physiographics and remotely sensed snow cover persistence. *Hydrol. Process.* 20, 723–739. <https://doi.org/10.1002/hyp.6128>

Monjo, R., Gaitán, E., Pórtoles, J., Ribalaygua, J., Torres, L., 2016. Changes in extreme precipitation over Spain using statistical downscaling of CMIP5 projections. *Int. J. Climatol.* 36, 757–769. <https://doi.org/10.1002/joc.4380>

Mora, J.Á.N., Martín, J.R., García, M.M., de Pablo Davila, F., Rivas Soriano, L., 2016. Climatological characteristics and synoptic patterns of snowfall episodes in the central Spanish Mediterranean area. *Int. J. Climatol.* 36, 4488–4496. <https://doi.org/10.1002/joc.4645>

Morán-Tejeda, E., Fassnacht, S.R., Lorenzo-Lacruz, J., López-Moreno, J.I., Garc\'ia, C., Alonso-González, E., Collados-Lara, A.-J., 2019. Hydro-Meteorological Characterization of Major Floods in Spanish Mountain Rivers. *Water* 11, 2641.

Morán-Tejeda, E., Herrera, S., Ignacio López-Moreno, J., Revuelto, J., Lehmann, A., Beniston, M., 2013. Evolution and frequency (1970-2007) of combined temperature-precipitation modes in the Spanish mountains and sensitivity of snow cover. *Reg. Environ. Chang.* 13, 873–885. <https://doi.org/10.1007/s10113-012-0380-8>

- Musselman, K.N., Clark, M.P., Liu, C., Ikeda, K., Rasmussen, R., 2017. Slower snowmelt in a warmer world. *Nat. Clim. Chang.* 7, 214–219. <https://doi.org/10.1038/nclimate3225>
- Navarro-Serrano, F., López-Moreno, J.I., 2017. Análisis espacio-temporal de los eventos de nevadas en el pirineo Español y su relación con la circulación atmosférica. *Cuad. Investig. Geogr.* 43, 233–254. <https://doi.org/10.18172/cig.3042>
- Niu, G.Y., Yang, Z.L., Mitchell, K.E., Chen, F., Ek, M.B., Barlage, M., Kumar, A., Manning, K., Niyogi, D., Rosero, E., Tewari, M., Xia, Y., 2011. The community Noah land surface model with multiparameterization options (Noah-MP): 1. Model description and evaluation with local-scale measurements. *J. Geophys. Res. Atmos.* 116, D12109. <https://doi.org/10.1029/2010JD015139>
- Painter, T.H., Berisford, D.F., Boardman, J.W., Bormann, K.J., Deems, J.S., Gehrke, F., Hedrick, A., Joyce, M., Laidlaw, R., Marks, D., Mattmann, C., McGurk, B., Ramirez, P., Richardson, M., Skiles, S.M.K., Seidel, F.C., Winstral, A., 2016. The Airborne Snow Observatory: Fusion of scanning lidar, imaging spectrometer, and physically-based modeling for mapping snow water equivalent and snow albedo. *Remote Sens. Environ.* 184, 139–152. <https://doi.org/10.1016/j.rse.2016.06.018>
- Parajka, J., Blöschl, G., 2008. Spatio-temporal combination of MODIS images - Potential for snow cover mapping. *Water Resour. Res.* 44. <https://doi.org/10.1029/2007WR006204>
- Paul, F., Barrand, N.E., Baumann, S., Berthier, E., Bolch, T., Casey, K., Frey, H., Joshi, S.P., Konovalov, V., Le Bris, R., Mölg, N., Nosenko, G., Nuth, C., Pope, A., Racoviteanu, A., Rastner, P., Raup, B., Scharrer, K., Steffen, S., Winsvold, S., 2013. On the accuracy of glacier outlines derived from remote-sensing data. *Ann. Glaciol.* 54, 171–182. <https://doi.org/10.3189/2013AoG63A296>
- Pedrero, A., 1988. El Programa ERHIN. La nieve en el Pirineo español, Madrid, MOPU 9–28.
- Pellicciotti, F., Brock, B., Strasser, U., Burlando, P., Funk, M., Corripio, J., 2005. An enhanced temperature-index glacier melt model including the shortwave radiation balance: Development and testing for Haut Glacier d’Arolla, Switzerland. *J. Glaciol.* 51, 573–587. <https://doi.org/10.3189/172756505781829124>
- Pierce, D.W., Cayan, D.R., 2013. The uneven response of different snow measures to human-induced climate warming. *J. Clim.* 26, 4148–4167. <https://doi.org/10.1175/JCLI-D-12-00534.1>
- Pimentel, R., Herrero, J., Polo, M.J., 2017. Quantifying snow cover distribution in semiarid regions combining satellite and terrestrial imagery. *Remote Sens.* 9, 995.
- Polo, M.J., Herrero, J., Pimentel, R., Pérez-Palazón, M.J., 2019. The Guadaleo Monitoring Network (Sierra Nevada, Spain): 14 years of measurements to understand the complexity of snow

dynamics in semiarid regions. *Earth Syst. Sci. Data* 11, 393–407. <https://doi.org/10.5194/essd-11-393-2019>

Raleigh, M.S., Livneh, B., Lapo, K., Lundquist, J.D., 2016. How does availability of meteorological forcing data impact physically based snowpack simulations? *J. Hydrometeorol.* 17, 99–120. <https://doi.org/10.1175/JHM-D-14-0235.1>

Reuelto, J., Azorin-Molina, C., Alonso-González, E., Sanmiguel-Vallelado, A., Navarro-Serrano, F., Rico, I., Ignacio López-Moreno, J., 2017. Meteorological and snow distribution data in the Izas Experimental Catchment (Spanish Pyrenees) from 2011 to 2017. *Earth Syst. Sci. Data* 9, 993–1005. <https://doi.org/10.5194/essd-9-993-2017>

Reuelto, J., Lecourt, G., Lafayse, M., Zin, I., Charrois, L., Vionnet, V., Dumont, M., Rabatel, A., Six, D., Condom, T., Morin, S., Viani, A., Sirguey, P., 2018. Multi-criteria evaluation of snowpack simulations in complex alpine terrain using satellite and in situ observations. *Remote Sens.* 10, 1171. <https://doi.org/10.3390/rs10081171>

Reuelto, J., López-Moreno, J.I., Azorin-Molina, C., Vicente-Serrano, S.M., 2014. Topographic control of snowpack distribution in a small catchment in the central Spanish Pyrenees: Intra- and inter-annual persistence. *Cryosphere* 8, 1989–2006. <https://doi.org/10.5194/tc-8-1989-2014>

Saavedra, F.A., Kampf, S.K., Fassnacht, S.R., Sibold, J.S., 2018. Changes in Andes snow cover from MODIS data, 2000–2016. *Cryosphere* 12, 1027–1046. <https://doi.org/10.5194/tc-12-1027-2018>

Saavedra, F.A., Kampf, S.K., Fassnacht, S.R., Sibold, J.S., 2017. A snow climatology of the Andes Mountains from MODIS snow cover data. *Int. J. Climatol.* 37, 1526–1539.

Salisbury, F.B., 1985. Plant growth under snow. *Aquil. Ser. Bot. SER. BOT.].* 1985.

Sanchez-Lorenzo, A., Enriquez-Alonso, A., Wild, M., Trentmann, J., Vicente-Serrano, S.M., Sanchez-Romero, A., Posselt, R., Hakuba, M.Z., 2017. Trends in downward surface solar radiation from satellites and ground observations over Europe during 1983–2010. *Remote Sens. Environ.* 189. <https://doi.org/10.1016/j.rse.2016.11.018>

Sanmiguel-Vallelado, A., Camarero, J.J., Gazol, A., Morán-Tejeda, E., Sangüesa-Barreda, G., Alonso-González, E., Gutiérrez, E., Alla, A.Q., Galván, J.D., López-Moreno, J.I., 2019. Detecting snow-related signals in radial growth of *Pinus uncinata* mountain forests. *Dendrochronologia* 57, 125622. <https://doi.org/10.1016/j.dendro.2019.125622>

Sanmiguel-Vallelado, A., Morán-Tejeda, E., Alonso-González, E., López-Moreno, J.I., 2017. Effect of snow on mountain river regimes: an example from the Pyrenees. *Front. Earth Sci.* 11, 515–530. <https://doi.org/10.1007/s11707-016-0630-z>

Sanmiguel-Vallelado, A., López-Moreno, J.I., Morán-Tejeda, E., Alonso-González, E., Navarro-Serrano, F.M., Rico, I., Camarero, J.J., 2020. Variable effects of forest canopies on snow processes in a valley of the central Spanish Pyrenees. *Hydrol. Process.* <https://doi.org/10.1002/hyp.13721>

Scaife, A.A., Arribas, A., Blockley, E., Brookshaw, A., Clark, R.T., Dunstone, N., Eade, R., Fereday, D., Folland, C.K., Gordon, M., Hermanson, L., Knight, J.R., Lea, D.J., MacLachlan, C., Maidens, A., Martin, M., Peterson, A.K., Smith, D., Vellinga, M., Wallace, E., Waters, J., Williams, A., 2014. Skillful long-range prediction of European and North American winters. *Geophys. Res. Lett.* 41, 2514–2519. <https://doi.org/10.1002/2014GL059637>

Schaefer, G.L., Paetzold, R.F., 2001. SNOTEL (SNOWpack TELEmetry) and SCAN (soil climate analysis network), in: Proc. Intl. Workshop on Automated Wea. Stations for Appl. in Agr. and Water Resour. Mgmt.

Schimel, J.P., Clein, J.S., 1996. Microbial response to freeze-thaw cycles in tundra and taiga soils. *Soil Biol. Biochem.* 28, 1061–1066.

Schweizer, J., Bartelt, P., van Herwijnen, A., 2015. Snow Avalanches, in: Snow and Ice-Related Hazards, Risks, and Disasters. Elsevier, pp. 395–436. <https://doi.org/10.1016/B978-0-12-394849-6.00012-3>

Schweizer, J., Kronholm, K., Jamieson, J.B., Birkeland, K.W., 2008. Review of spatial variability of snowpack properties and its importance for avalanche formation. *Cold Reg. Sci. Technol.* 51, 253–272. <https://doi.org/10.1016/j.coldregions.2007.04.009>

Shaw, T.E., Gascoin, S., Mendoza, P.A., Pellicciotti, F., McPhee, J., 2020. Snow Depth Patterns in a High Mountain Andean Catchment from Satellite Optical Tristereoscopic Remote Sensing. *Water Resour. Res.* 56, e2019WR024880.

Skamarock, W.C., Klemp, J.B., Dudhia, J.B., Gill, D.O., Barker, D.M., Duda, M.G., Huang, X.-Y., Wang, W., Powers, J.G., 2008. A description of the Advanced Research WRF Version 3, NCAR Technical Note TN-475+STR. Tech. Rep. 113. <https://doi.org/10.5065/D68S4MVH>

Takala, M., Luojus, K., Pulliainen, J., Derksen, C., Lemmetyinen, J., Kärnä, J.P., Koskinen, J., Bojkov, B., 2011. Estimating northern hemisphere snow water equivalent for climate research through assimilation of space-borne radiometer data and ground-based measurements. *Remote Sens. Environ.* 115, 3517–3529. <https://doi.org/10.1016/j.rse.2011.08.014>

- Thompson, J.A., 2016. A modis-derived snow climatology (2000-2014) for the Australian Alps. *Clim. Res.* 68, 25–38. <https://doi.org/10.3354/cr01379>
- van Pelt, W.J.J., Kohler, J., Liston, G.E., Hagen, J.O., Luks, B., Reijmer, C.H., Pohjola, V.A., 2016. Multidecadal climate and seasonal snow conditions in Svalbard. *J. Geophys. Res. Earth Surf.* 121, 2100–2117. <https://doi.org/10.1002/2016JF003999>
- Vavrus, S., 2007. The role of terrestrial snow cover in the climate system. *Clim. Dyn.* 29, 73–88. <https://doi.org/10.1007/s00382-007-0226-0>
- Vicente-Serrano, S.M., Rodríguez-Camino, E., Domínguez-Castro, F., El Kenawy, A., Azorín-Molina, C., 2017. An updated review on recent trends in observational surface atmospheric variables and their extremes over Spain. *Cuad. Investig. Geogr.* 43, 209–232. <https://doi.org/10.18172/cig.3134>
- Vionnet, V., Brun, E., Morin, S., Boone, A., Faroux, S., Le Moigne, P., Martin, E., Willemet, J.M., 2012. The detailed snowpack scheme Crocus and its implementation in SURFEX v7.2. *Geosci. Model Dev.* 5, 773–791. <https://doi.org/10.5194/gmd-5-773-2012>
- Viviroli, D., Dürr, H.H., Messerli, B., Meybeck, M., Weingartner, R., 2007. Mountains of the world, water towers for humanity: Typology, mapping, and global significance. *Water Resour. Res.* 43. <https://doi.org/10.1029/2006WR005653>
- Wang, L., Ting, M., Kushner, P.J., 2017. A robust empirical seasonal prediction of winter NAO and surface climate. *Sci. Rep.* 7, 279. <https://doi.org/10.1038/s41598-017-00353-y>
- Winstral, A., Elder, K., Davis, R.E., 2002. Spatial snow modeling of wind-redistributed snow using terrain-based parameters. *J. Hydrometeorol.* 3, 524–538. [https://doi.org/10.1175/1525-7541\(2002\)003<0524:SSMOWR>2.0.CO;2](https://doi.org/10.1175/1525-7541(2002)003<0524:SSMOWR>2.0.CO;2)
- Wu, X., Che, T., Li, X., Wang, N., Yang, X., 2018. Slower Snowmelt in Spring Along With Climate Warming Across the Northern Hemisphere. *Geophys. Res. Lett.* 45, 12,331–12,339. <https://doi.org/10.1029/2018GL079511>
- Wu, X., Shen, Y., Wang, N., Pan, X., Zhang, W., He, J., Wang, G., 2016. Coupling the WRF model with a temperature index model based on remote sensing for snowmelt simulations in a river basin in the Altay Mountains, north-west China. *Hydrol. Process.* 30, 3967–3977. <https://doi.org/10.1002/hyp.10924>

Capítulo 2: Rejillas de datos diarios de espesor de nieve y equivalente en agua de nieve de la Península Ibérica desde 1980 hasta 2014.

Resumen: En este trabajo presentamos observaciones de nieve y una base de datos diaria en rejilla que se generó a partir de un reanálisis al que previamente se le mejoró la resolución en la Península Ibérica. La península Ibérica presenta un manto de nieve estacional de larga duración en sus diferentes cordilleras, y en la mayor parte de su territorio se producen nevadas invernales. Sin embargo, solo hay observaciones directas limitadas de la profundidad de la nieve (SD) y del equivalente en agua de la nieve (SWE), lo que dificulta el análisis de la dinámica de la nieve y de los patrones espacio-temporales de las nevadas. Utilizamos los datos meteorológicos de los reanálisis como forzamiento de un modelo de balance de energía de la nieve de base física para simular el SWE y el SD en la Península Ibérica desde 1980 hasta 2014. Más concretamente, el reanálisis ERA-interim se redujo a una resolución de 10 km utilizando el modelo de Weather research and Forecast (WRF). Los resultados de WRF se utilizaron directamente, o como entrada a otros submodelos, para obtener los datos necesarios para lanzar el modelo Factorial Snow Model (FSM). Para mejorar la resolución de las salidas de WRF, utilizamos gradientes térmicos y ajustes higrobarométricos para simular series de nieve en bandas de elevación de 100 m por cada celda de 10 km en la Península Ibérica. Las series de nieve fueron validadas utilizando datos del sensor satelital MODIS y observaciones terrestres. La simulación de nieve reprodujo con precisión la variabilidad interanual del manto nivoso así como la variabilidad espacial de la acumulación y la fusión, incluso en terreno complejo. Así pues, el conjunto de datos presentado puede ser útil para muchas aplicaciones, entre ellas la ordenación del territorio, los estudios hidrometeorológicos, la fenología de la flora y la fauna, el turismo invernal y la gestión de riesgos. Los datos presentados aquí pueden descargarse gratuitamente de Zenodo (<https://doi.org/10.5281/zenodo.854618>). A continuación, se describe detalladamente el procedimiento, la validación de los datos, la evaluación de la incertidumbre y las posibles aplicaciones y limitaciones de la base de datos

Cita completa:

Alonso-González, E., López-Moreno, J. I., Gascoin, S., García-Valdecasas Ojeda, M., Sanmiguel-Vallelado, A., Navarro-Serrano, F., Revuelto, J., Ceballos, A., Esteban-Parra, M. J., and Essery, R.: Daily gridded datasets of snow depth and snow water equivalent for the Iberian Peninsula from 1980 to 2014, *Earth Syst. Sci. Data*, 10, 303–315, <https://doi.org/10.5194/essd-10-303-2018>, 2018.

Daily gridded datasets of snow depth and snow water equivalent for the Iberian Peninsula from 1980 to 2014

Esteban Alonso-González¹, J. Ignacio López-Moreno¹, Simon Gascoin², Matilde García-Valdecasas Ojeda³, Alba Sanmiguel-Vallelado¹, Francisco Navarro-Serrano¹, Jesús Revuelto⁴, Antonio Ceballos⁵, María Jesús Esteban-Parra³, and Richard Essery⁶

1. Instituto Pirenaico de Ecología, Consejo Superior de Investigaciones Científicas (IPE-CSIC), Zaragoza, Spain.
2. Centre d'Etudes Spatiales de la Biosphère (CESBIO), UPS/CNRS/IRD/CNES, Toulouse, France.
3. Departamento de Física Aplicada, Facultad de Ciencias, Universidad de Granada, Granada, Spain.
4. Météo-France – CNRS, CNRM (UMR3589), Centre d'Etudes de la Neige, Grenoble, France.
5. Dept. Geografía, Universidad de Salamanca, Salamanca, Spain
6. School of GeoSciences.
6. University of Edinburgh, Edinburgh, UK.

Correspondence: Esteban Alonso-González (e.alonso@ipe.csic.com)

Received: 11 September 2017 – Discussion started: 20 October 2017

Revised: 28 December 2017 – Accepted: 8 January 2018 – Published: 20 February 2018

Abstract. We present snow observations and a validated daily gridded snowpack dataset that was simulated from downscaled reanalysis of data for the Iberian Peninsula. The Iberian Peninsula has long-lasting seasonal snowpacks in its different mountain ranges, and winter snowfall occurs in most of its area. However, there are only limited direct observations of snow depth (SD) and snow water equivalent (SWE), making it difficult to analyze snow dynamics and the spatiotemporal patterns of snowfall. We used meteorological data from downscaled reanalyses as input of a physically based snow energy balance model to simulate SWE and SD over the Iberian Peninsula from 1980 to 2014. More specifically, the ERA-Interim reanalysis was downscaled to 10 km resolution using the Weather Research and Forecasting (WRF) model. The WRF outputs were used directly, or as input to other submodels, to obtain data needed to drive the Factorial Snow Model (FSM). We used lapse rate coefficients and hygrobarometric adjustments to simulate snow series at 100 m elevations bands for each 10 km grid cell in the Iberian Peninsula. The snow series were validated using data from MODIS satellite sensor and ground observations. The overall simulated snow series accurately reproduced the interannual variability of snowpack and the spatial variability of snow accumulation and melting, even in very complex topographic terrains. Thus, the presented dataset may be useful for many applications, including land management, hydrometeorological

studies, phenology of flora and fauna, winter tourism, and risk management. The data presented here are freely available for download from Zenodo (<https://doi.org/10.5281/zenodo.854618>). This paper fully describes the work flow, data validation, uncertainty assessment, and possible applications and limitations of the database.

1 Introduction

Seasonal snowpack exerts an important control on the hydrology and economy of many mountainous and cold regions worldwide (Barnett et al., 2005). Snow variability also affects different ecological processes, such as species composition, distribution, and phenology (Keller et al., 2000; Wipf et al., 2009). For example, snowpack on Mediterranean mountains is a crucial source of water during the dry season (Fayad et al., 2017; García-Ruiz et al., 2011; Viviroli et al., 2007). Long-term data are required to analyze the spatiotemporal dynamics of snowpack, to assess the importance of snow as a resource, and to understand the effect of climatic fluctuations. However, there are only limited in situ observations of snowpack for most mountain regions (Raleigh et al., 2016). Currently, remote-sensing techniques can only reliably provide information about snow cover based on observations in the visible spectrum (Dietz et al., 2012). Current spaceborne sensors do not provide accurate data on snow water equivalent (SWE) and/or snow depth (SD) in mountainous regions (Dozier et al., 2016). Microwave imaging has a coarse resolution (grid cell size: 25 km), so does not characterize snowpack variability in the Mediterranean mountains, which have a high spatial heterogeneity not captured with this resolution. There are also spatial and temporal limitations when attempting to estimate snowpack using close-range remote-sensing techniques such as LIDAR (Revuelto et al., 2016).

There are limited in situ snow observations and meteorological data at high elevations in the Iberian Peninsula. Although the number of monitored sites has increased in recent years, there are no long-term series and there is in-sufficient characterization of snowpack dynamics at a regional scale. However, snowpack in the Iberian Peninsula is an important hydrological and also economical resource. An area of 19456.4 km² in the Iberian Peninsula lies above 1500 m a.s.l., mostly in the five most important mountain ranges (Pyrenees, Cantabrian Mountains, Central System, Iberian Range, and Sierra Nevada). At this elevation, snow-pack occurs for at least 4 months of the year (López-Moreno et al., 2011) making it a critical resource for water management in the largest

hydrological basins (Morán-Tejeda et al., 2014). Snowpack influences the interannual variability of water resources (López-Moreno and García-Ruiz, 2004) and the timing of the winter low flows and spring peak flows (Sanmiguel-Vallelado et al., 2017). Moreover, winter tourism (mainly skiing) has been increasingly important to the economy of mountain valleys in recent decades, and the large interannual fluctuations of snowpack in the different mountain regions of the Iberian Peninsula affect the economic viability of tourism (Gilaberte-Búrdalo et al., 2014, 2017).

The importance of snow to the environment and economy of the Iberian Peninsula, and the lack of data on snowpack in this region, motivated us to use meteorological outputs from downscaled reanalysis data to simulate snowpack at different elevations in the Iberian Peninsula. Atmospheric reanalyses, based on data assimilation and modeling (Saha et al., 2010), can provide important information about the temporal evolution of the atmosphere. Meteorological variables obtained from reanalysis data can be used as inputs for models of snow mass and energy balance which can be applied to describe the behavior of the snowpack over large areas (Brun et al., 2013; Krogh et al., 2015; Wegmann et al., 2017). However, the coarse resolution (cell size: around tens of kilo-meters) implies these simulations may have insufficient spatial resolution for characterizing the topographical complexity of mountain areas (Mass et al., 2002). To overcome this limitation, regional climate models (RCMs) are often used to obtain better representations of surface climatology, because they downscale physically reanalysis products (García-Valdecasas Ojeda et al., 2017; Kryza et al., 2017; Warrach-Sagi et al., 2013). Previous studies have used RCMs to study SD and SWE dynamics at finer resolutions (grid cell size: 5 to 11 km) when they are driven with reanalyses, and the resolution increases further (grid cell size: 1 km) when using forecasted data (Bellaire et al., 2011; van Pelt et al., 2016; Quéno et al., 2016; Wu et al., 2016).

van Pelt et al. (2016) used the High Resolution Limited Area Model (HIRLAM) in Svalbard (Norway), with forcing by ERA-40 and ERA-Interim reanalysis, and then used the meteorological simulation as driving data for SnowModel (Liston and Elder, 2006a). Their results support the usefulness of the methodology extracting snowpack trends from these data. Wu et al. (2016) used a similar procedure to describe the behavior of snowpack over the Altai Mountains in China. They coupled outputs from the Weather Research and Forecasting (WRF) model (Skamarock et al., 2008) driven by NCEP/NCAR reanalysis with a temperature index model (based on remote sensing), and their results had low error values. To increase the spatial resolution of the WRF out-puts, they used the MICROMET model (Liston and Elder, 2006b), a submodel of SnowModel in which WRF outputs are interpolated to a new grid, and then corrected physically according to topography.

Wrzesien et al. (2017) tested the capability of WRF to estimate SWE over complex terrain concluding that WRF simulations can be used over areas with few observational data.

We used a different approach, in an effort to make our database more computationally practicable and to avoid the uncertainties of the statistical interpolations of climatological variables over complex areas. More specifically, we projected WRF outputs to different elevation bands to generate simulations for multiple elevations. This procedure allows one to study the elevation dependent characteristics of the snowpack over different mountain ranges, preserving the WRF output resolution.

Our procedure uses the physically based Factorial Snow Model (FSM; Essery, 2015), which is fed by ERA-Interim reanalysis (Berrisford et al., 2011), and downscaled by the WRF model. The final products of our analysis are simulated daily time series of SD and SWE at different elevations from 1980 to 2014.

2. Data and methods

We used an existing WRF simulation (cell size: 10 km) for the whole Iberian Peninsula (Fig. 1), with a 3 h time step from January 1979 to November 2014, as input data for the FSM. Most inputs of the FSM were extracted directly from the WRF simulation, but some were calculated using other submodels. We projected the WRF outputs and derived variables to different elevation bands, from 500 to 2900 m a.s.l. at steps of 100 m, from the WRF pixel elevation using several hygrometric and psychrometric formulas and elevation lapse rates. FSM outputs were aggregated at a daily time step in order to increase the manageability of the data. Validation was performed at different steps of the workflow using different observational data sources. Figure 2 shows the work-flow completely, which is described in more detail below. Appendix A lists all the abbreviations used in this study.

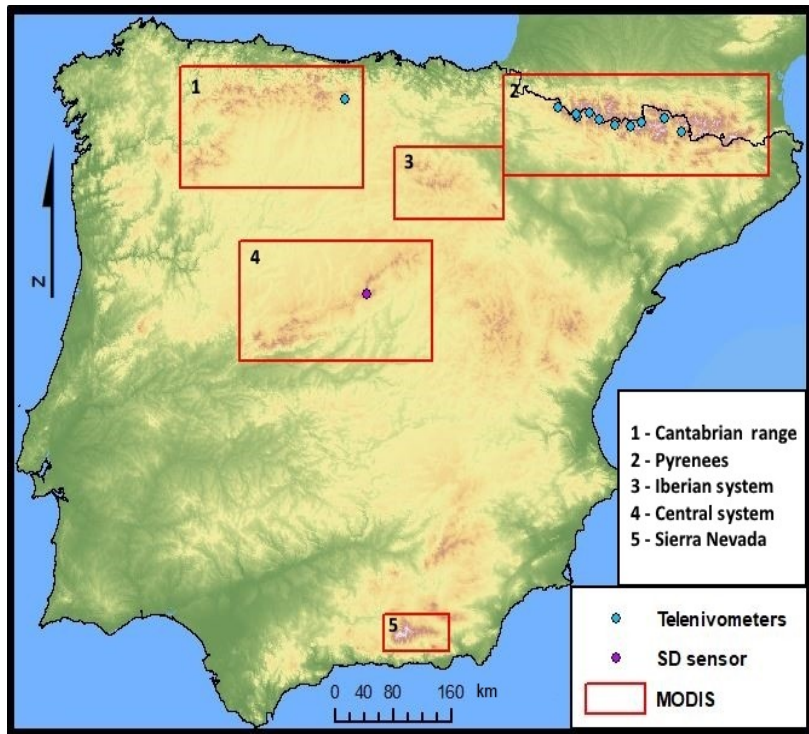


Figure 1: Digital elevation model (DEM) of the Iberian Peninsula and locations of the telenivometers, Cotos Pass SD sensor, and MODIS study areas.

2.1 Meteorological driving data

The meteorological variables were calculated using the WRF model, a mesoscale climate model. Previous researchers used this model to simulate climate at regional scales for analysis of past, present, and future conditions (Chen et al., 2011; Heikkilä et al., 2011). The spatial resolution of our simulation is 0.088 (10 km) and the time step is 3 h. ERA-Interim reanalysis (Berrisford et al., 2011) was used as driving data for the WRF model. With this procedure all meteorological variables for running snowpack models were generated for the whole Iberian Peninsula. The WRF configuration was described in detail by García-Valdecasas Ojeda et al. (2017). This simulation provided the following variables: wind speed (U_a), surface temperature (T), precipitation (Pr), relative humidity (RH), shortwave incoming radiation (SW), and atmospheric pressure (Ps).

2.2 Snow energy and mass balance model

SD and SWE time series were obtained using a mass and energy balance snowpack model. The FSM is a multi-physics snow model that simulates the accumulation and melting of snow (Essery, 2015). This model allows selection of two options for parameterizations of five different process, thereby enabling 32 different model configurations. The configuration used to develop our simulations decreases snow albedo and increases snow density at different rates for cold and melting snow, calculates thermal conductivity as a function of snow density, adjusts the turbulent exchange coefficient as a function of the bulk Richardson number, and allows retention and refreezing of liquid water inside the snowpack.

The model works with different numbers and thicknesses of layers, depending on snowpack depth. Thus, it assumes a single layer when snow depth is less than 0.2 m, and a maximum of three layers when the depth is greater than 0.5 m. This configuration allows the model to characterize the highly variable climatological conditions of the Iberian mountains. In addition to the variables provided by the WRF simulation (listed in Sect. 2.1), the FSM also needs estimates of snow rate (S_f), rain rate (R_f), and longwave incoming radiation (LW). To avoid the expense of rerunning WRF in this study, these variables have been reconstructed from available WRF simulation outputs.

To calculate S_f and R_f , we used a psychrometric energy balance method (PPPM; Harder and Pomeroy, 2013), which uses relative humidity and air temperature to calculate the surface temperature of falling hydrometeors. From this value, the fraction of liquid precipitation is as follows:

$$f_r(T_i) = \frac{1}{1 + bc^{(T_i)}}$$

where f_r is the percentage of liquid precipitation, T_i is the temperature ($^{\circ}\text{C}$) of the falling hydrometeor, and b and c are derived from statistical fits (2.50286 and 0.125006, respectively, for hourly time intervals). T_i is calculated from Eq. (2), which we solved numerically using the method described by Brent and Richard (1972):

$$T_i = T_a + \frac{D}{\lambda_t} L (\rho_{(T_a)} - \rho_{sat})$$

where T_a is the temperature (K), D is the diffusivity of water vapor in air ($\text{m}^2 \text{s}^{-1}$), λ_t is the thermal conductivity of air ($\text{W m}^{-1} \text{K}^{-1}$), L is the latent heat of sublimation or vaporization (J kg^{-1}), and ρ_{Ta} and $\rho_{\text{sat(Ti)}}$ (kg m^{-3}) are respectively the vapor densities in free atmosphere and at the saturated hydrometeor surface. This methodology gives the percentage of liquid precipitation; the percentage of solid precipitation is directly calculated from fr .

Incoming longwave radiation (W m^{-2}) was estimated from the Stefan–Boltzmann law:

$$L_{\downarrow} = \varepsilon \sigma (T_a)^4$$

where σ is the Stefan–Boltzmann constant and ε is the emissivity of the atmosphere.

Emissivity was calculated as a function of elevation and cloud cover, as proposed by Liston and Elder (2006b), who used a variation of the methodology described by Iziomon et al. (2003). Thus, emissivity is calculated as follows:

$$\varepsilon = 1,083(1 + Z_s cc^2)[1 - X_s \exp(-Y_s e / T_a)]$$

where e (Pa) is the atmospheric vapor pressure, cc is the fractional cloud cover, and X_s , Y_s , and Z_s are coefficients that are corrected with elevation:

$$C_s = C_1 \quad z < 200 \text{ m a.s.l.},$$

$$C_s = C_1 + (z - z_1) \left(\frac{C_2 - C_1}{z_2 - z_1} \right) \quad 200 \text{ m a.s.l.} \leq 3000 \text{ m},$$

$$C_s = C_2 \quad 3000 \text{ m a.s.l.} < z$$

where z (m) is the elevation above sea level, and X_s , Y_s , and Z_s can be substituted for C , with $X_1=0.35$, $X_2=0.51$, $Y_1=0.100 \text{ Kpa}^{-1}$, $Y_2=0.130 \text{ KPa}^{-1}$, $Z_1=0.224$, $Z_2=1.100$, $z_1=200 \text{ m a.s.l.}$, and $z_2=3000 \text{ m a.s.l.}$

Different parameterizations using SW were tested to estimate cc , from potential SW, a more accurate approach than the parameterization proposed by Liston and Elder (2006b), according to Gascoin et al. (2013). This approach uses the relationship between SW and potential SW radiation that is restricted to daylight hours. Thus, in this work, we used the parameterization proposed by Walcek (1994) for cc estimation, which is the original parameterization proposed by Liston and Elder (2006b).

$$cc = 0.832 \left(\frac{(RH_{700} - 100)}{41.6} \right)$$

where RH_{700} is the relative humidity at 700 mb. The methodology used to project RH to 700 mb elevation is described below. To scale the snow simulations to different elevations, we first used the internationally accepted standard air temperature lapse rate ($\beta=0.0065\text{ K m}^{-1}$; Barry and Chorley, 1987; ISO, 1975) to project the surface air temperature. For RH, the methodology proposed by Liston and Elder (2006b) was used, in which a lapse rate is applied to the dew point temperature (HR_m). First, we calculated the dew point temperature from RH and the saturation vapor pressure. Then, we applied the standard air temperature lapse rate to the dew point temperature, and recalculated the RH at the target elevation from the scaled dew point temperature and the saturation vapor pressure. Once we rescaled temperature and RH, we calculated the precipitation phase and LW radiation at the different elevations. Finally, to estimate the scaled surface air pressure we used a generalization of the barometric formula for scenarios that consider air temperature lapse rates (Berberan-Santos et al., 1997):

$$p_{(z)} = p_{(0)} \left(1 - \frac{(\beta z)}{T_a} \right)^{(mg/R\beta)}$$

where $p_{(0)}$ is the surface air pressure, z is the elevation difference (m), m is the molecular mass of air ($0.0289644\text{ kg mol}^{-1}$), and R is the universal gas constant ($8.31432\text{ J K}^{-1}\text{ mol}^{-1}$).

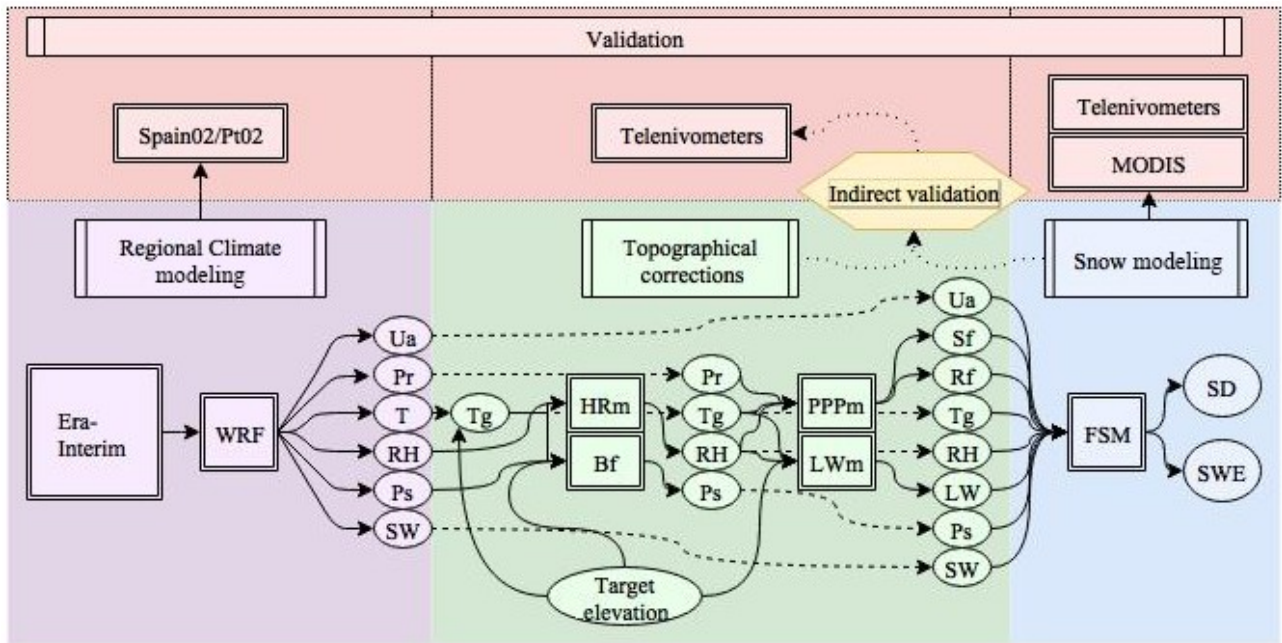


Figure 2: Simulation workflow. Squared boxes represent modeling steps and rounded boxes represent meteorological variables. Variables that are not inputs or outputs of a model are indicated by dotted lines (see a glossary of abbreviations used in Appendix A).

2.3 Validation procedure

Validation was performed at different resolutions and at different steps of the workflow, using all available observational data (Fig. 2). Previous studies (Argüeso et al., 2012; García-Valdecasas-Ojeda et al., 2016) simulated temperature and precipitation using WRF at different timescales compared with the grids, based on observations from Spain02 (Herrera et al., 2012) and PT02 (Belo-Pereira et al., 2011), high resolution precipitation and temperature precipitation and temperature, even for extreme events. Subsequent research showed that the downscaling made by WRF provided improved accuracy compared to ERA-Interim data, due to the higher resolution (García-Valdecasas Ojeda et al., 2017).

In this work, we used the Moderate-Resolution Imaging Spectroradiometer (MODIS) satellite sensor to validate our snow cover product for the period September 2000 to November 2014. Similarly, we used data from telenivometers, which were available in the Pyrenees from October 2009 to June 2014.

First, we compared MODIS data with the SD and SWE time series (10 km resolution). MODIS snow maps were generated using the same workflow for each mountain range in the study area (Pyrenees, Cantabrian Mountains, Central System, Iberian Range, and Sierra Nevada). We downloaded all the available MOD10A1 and MYD10A1 products (version 5) from the National Snow and Ice Data Center (Hall et al., 2006). The original granules were mosaicked and reprojected from the sinusoidal system to the Universal Trans-verse Mercator (UTM) reference system. Then, we ran a gapfilling algorithm, using the binary snow product to avoid data losses due to cloud cover (Gascoin et al., 2015). This provided gap-free daily maps showing the presence and absence of snow in each mountain range from 2000 to 2014. From these maps, the probability of snow was calculated as follows:

$$P_{(\text{Snow})} = \frac{N_s}{N} \times 100$$

where $P_{(\text{Snow})}$ is the probability of snow (%), N_s is the number of days with snow, and N is the total number of days of the period.

Snow probability maps were also calculated from the FSM snow cover maps. In this work, we chose a threshold of 0.11 m for SD and a threshold of 40 mm for SWE (Gascoin et al., 2015) in the FSM time series. This allowed us to generate snow cover maps from FSM outputs. Then, we aggregated the MODIS pixels (500 m) to the simulation grid (10 km), with averaging of the values of MODIS pixels to make them comparable.

We also used data from 11 telenivometers, which measure subhourly SWE and SD using gamma ray attenuation and acoustic sensors. These data were provided by the ERHIN program (Estimación de Recursos Hídricos Procedentes de la Nieve) of the Hydrological Ebro River Basin Authority (Navarro-Serrano and López-Moreno, 2017). Ten telenivometers were located in the Pyrenees, and one in the Cantabrian Mountains. A complete description of the telenivometers and their locations can be found at www.saihhebro.com. We also used a SD sensor in the Central System mountain range (Durán et al., 2017), which is from the National Meteorological Agency of Spain (AEMET). We projected the meteorological variables from the WRF simulation to elevations of the different telenivometers for simulations. Figure 3 shows a comparison of the modeled and observed SD time series at these 10 sites.

It must be noted that it is challenging to validate gridded products from ground-based data (Snauffer et al., 2016). Snowpack can have large variability over small distances (López-Moreno et al., 2015;

Meromy et al., 2013). This implies that punctual measurements may not be representative of the 10 km resolution data, even when comparing a simulation at the same elevation as the telenivometer. In addition, snow measurements always include biases from the different measuring devices (Kinar and Pomeroy, 2015). Thus, we focused on the temporal patterns of snowpack during the season. More specifically, we compared the accumulation patterns during the season, assuming that accumulation and melting rates were similar in the simulated and observational data, but that SD and SWE likely differ between the telenivometer and the simulation.

Thus, we first compared different percentiles of SD and SWE in the telenivometer and the simulated time series. Then, using each percentile as a threshold for snow presence, we converted the series into binary data, allowing use of the kappa test (Cohen, 1960) for each percentile. The kappa coefficient ranges from 1 and < 0, but it is difficult to assign an agreement criterion based on kappa value. Thus, we used the thresholds proposed by Landis and Koch (1977), which basically agree with values proposed by Fleiss et al. (1969; <0.00: poor; 0.00–0.20: slight; 0.21–0.4: fair; 0.41–0.60: moderate; 0.61–0.80: substantial; and 0.81–1.00: almost perfect). We examined percentile values between 10 and 90 %, as more representative of snow accumulation during the sea-son.

3 Results

3.1 Validation

Our analysis of the probability of snow presence from MODIS and FSM shows that the outputs had good correlations (Fig. 4). This analysis compared the probability of snow at each pixel (10 km 10 km) from MODIS and FSM outputs for the SWE and SD time series from September 2000 to November 2014. The mean coefficient (R^2) was 0.76, and a mean absolute error was 6.3 %. This analysis also shows the correlations for each mountain range, and the distribution of errors for SWE and SD (simulated less observed).

These results also show there are no significant differences in the errors of $P_{(Snow)}$ for the different mountain ranges. However, the correlation was not strong for the Sierra Nevada range, probably due to its limited snow cover, although this remained inside the variability of the scatter plot.

Validation of these results with telenivometers indicated kappa values for thresholds in the 10th to 90th percentiles of each season (Fig. 5). The kappa values were mostly above 0.6, although accuracy declined for the highest percentiles.

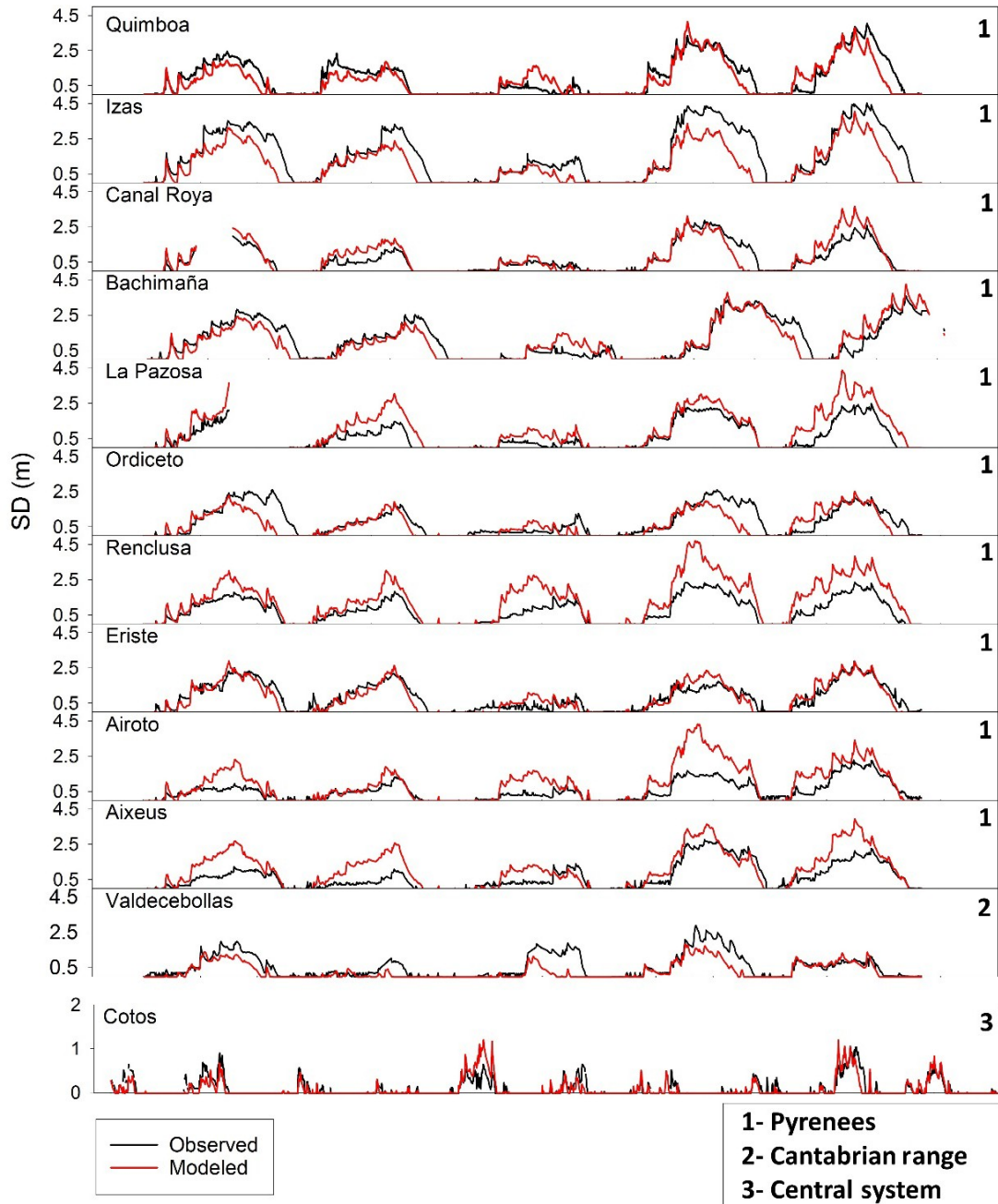


Figure 3: Comparison between modeled (red) and observed (black) SD time series for each telenivometer and the Cotos SD sensor.

The kappa coefficient does not account for the displacement magnitude of the different percentiles, and a difference of a few days at the time of peak accumulation may cause a sharp decrease in the kappa value. This is the reason for the loss of accuracy at the highest percentiles. Thus, we further analyzed these data to determine the time of the year when snowpack exceeded the 90th, 75th, and 50th percentiles at each telenivometer in the observed (OBS) and simulated (SIM) series (Fig. 5c). This analysis shows that, despite small temporal shifts, the simulated snow series accurately represents the temporal patterns when different snow percentiles are exceeded.

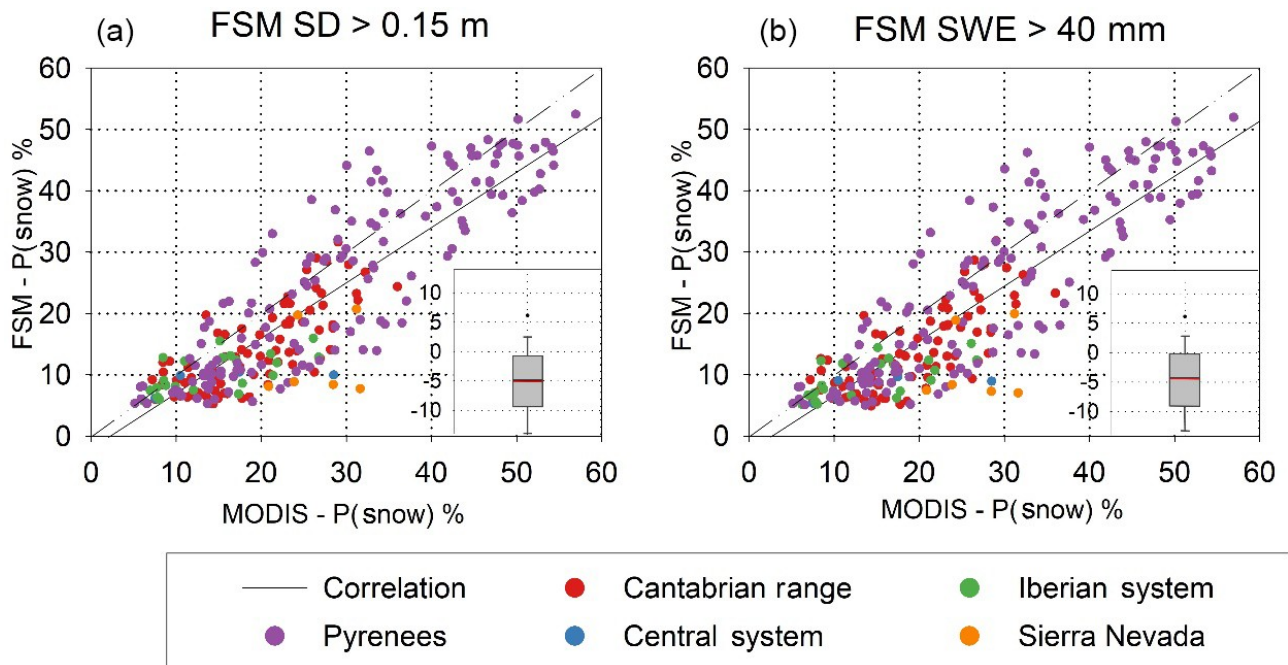


Figure 4: Correlation between the long-term (2000–2015) mean probability of snow depth (a) and snow water equivalent (b) from MODIS data and from FSM output. Box plot insets show the frequency distributions of errors (%), with the central red lines indicating average errors, boxes indicating the 25th and 75th percentiles, bars indicating the 10th and 90th percentiles, and dots indicating the 5th and 95th percentiles.

The biggest shift in the position of the 90th and 75th percentiles was during the 2011/2012 season. This season was extremely dry on the Iberian Peninsula, and there were very few snowfall events (Fig. 3). Thus, a small bias in the simulation of a single event during this time could lead to a large error in prediction of the magnitude and timing of SD and SWE maxima.

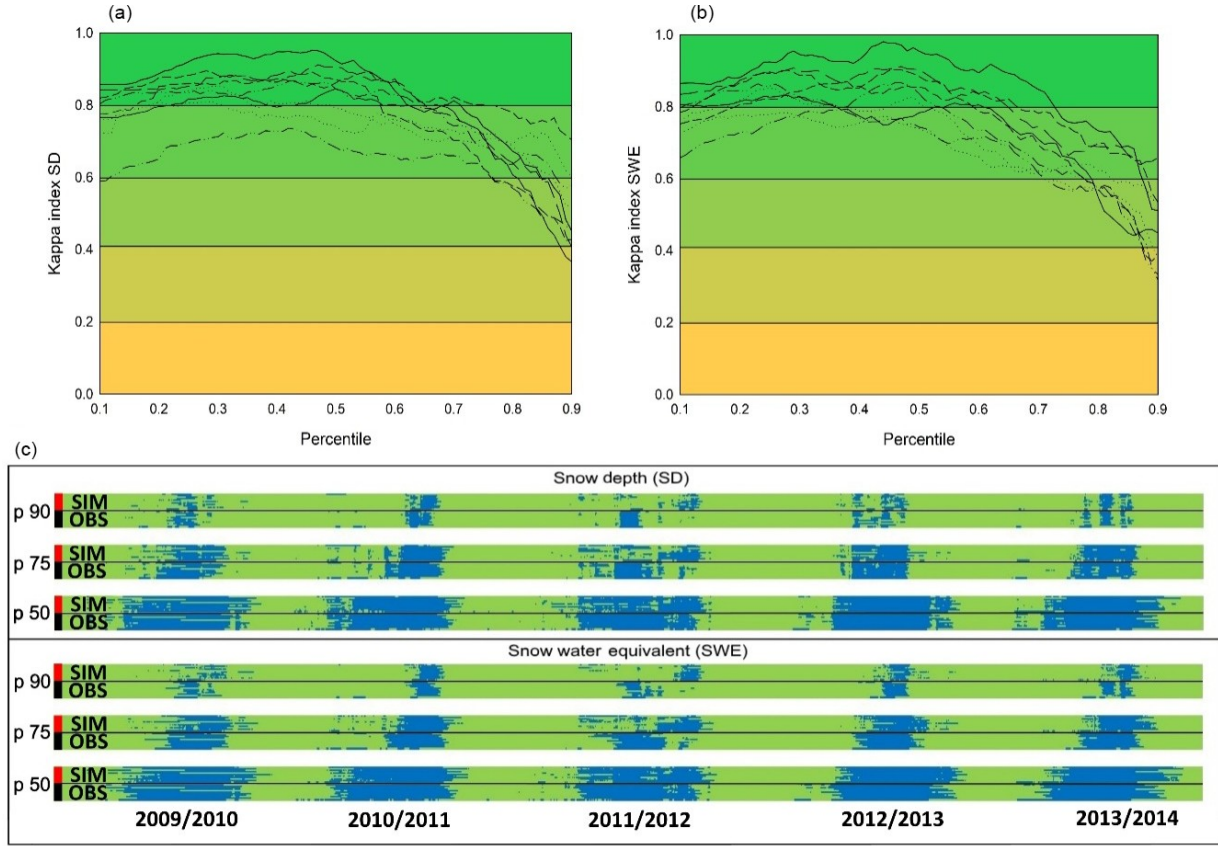


Figure 5: Kappa values derived from comparison of observed and simulated series for different percentiles of snow depth (a) and snow water equivalent (b), and periods of the year (blue) when snowpack exceeds the 90th, 75th, and 50th percentiles (c). In (c), each pair of bands shows the times when the different percentiles in the observed (OBS) and simulated (SIM) series at each telenivometer exceeded the indicated percentile.

3.2 Gridded snow dataset: applications and limitations

The final products of the models are daily gridded datasets (resolution: 0.088° , ~ 10 km) of SD and SWE at elevations from 500 to 2900 m a.s.l. (100 m intervals) from 1980 to 2014. The datasets (ncdf4 format) cover the entire Iberian Peninsula, including the north side of the Pyrenees in France. Each dataset contains information of the entire Iberian Peninsula and a mask that covers pixels that do not present areas at the elevations of the simulation estimated from a 250 m resolution DEM.

This snow database provides new opportunities for studies of snow in the Iberian Peninsula. In particular, the temporal resolution and the duration of the series show significant improvements over previous observational data. Also, the geographic data generated on SD and SWE provides the opportunity to obtain more snow and hydrologically relevant information than available from remote sensing alone. It is also possible to develop different snow products at different elevations, allowing for comparison of different elevations and different regions. For example, Fig. 6 shows the long-term average interannual maximum SD and SWE at three different elevations.

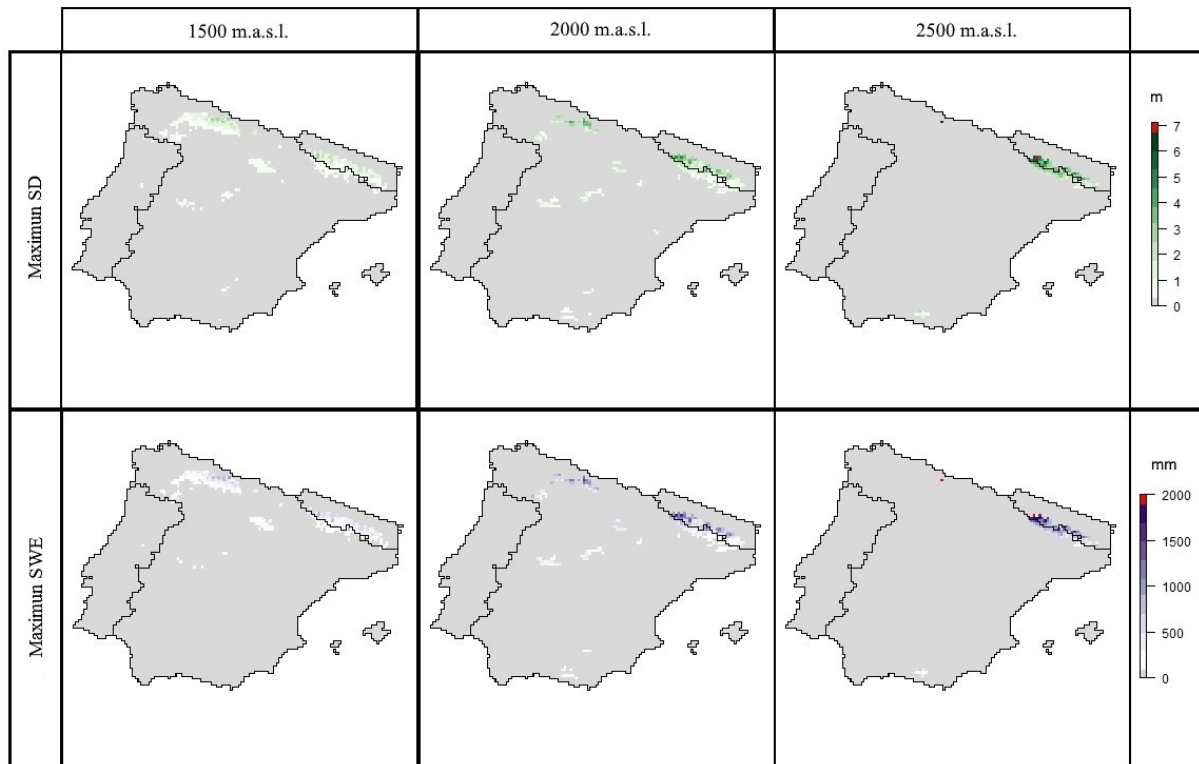


Figure 6: Long-term (1980–2014) average maximum SWE and SD grids at 1500, 2000, and 2500 m a.s.l.

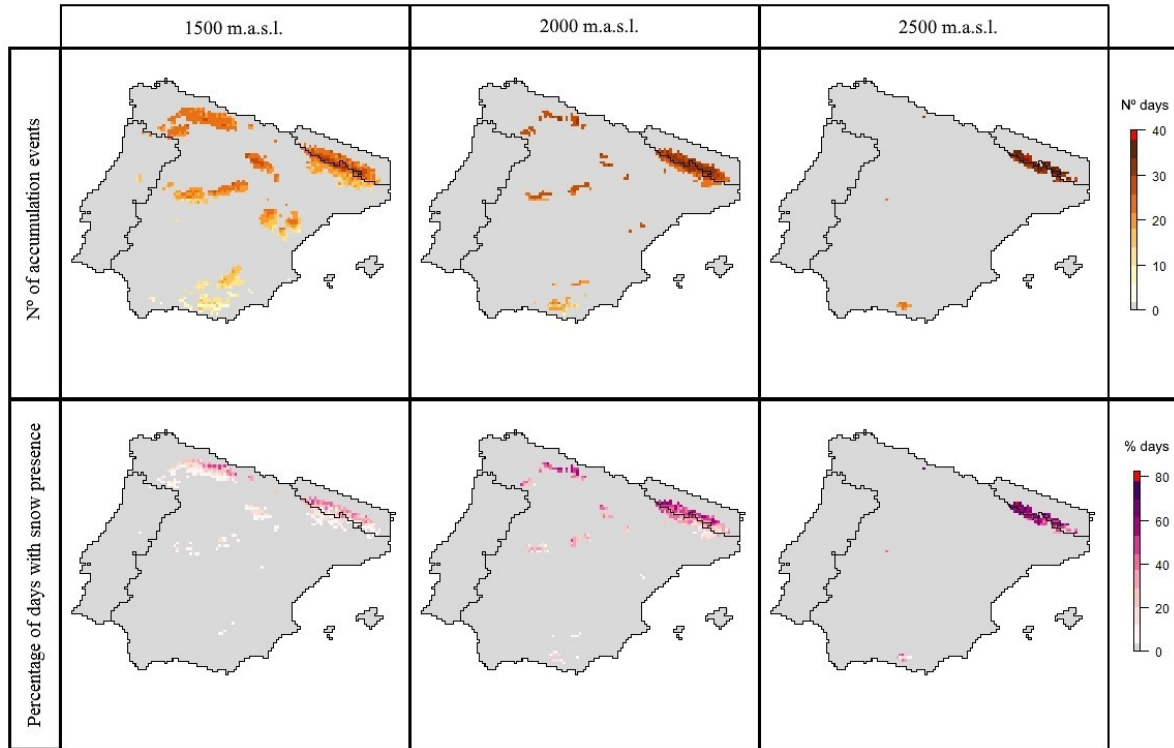


Figure 7: Long-term (1980–2014) average number of snowfall events and percentage of snow presence at 1500, 2000, and 2500 m a.s.l.

Figure 7 shows examples of other snow variables that can be derived from the database: average number of snowfall events and percentage of days with snow cover at three elevations. These analyses are particularly useful for the development of different snow climatologies for the whole Iberian Peninsula, or for specific areas, in studies that rely on ecological data (e.g., phenology or distribution of plants and animals, forest growth), studies that require hydrological parameters for different catchments, and studies that determine risk maps for snow-related events.

It is also possible to extract daily time series for different areas or elevations at each pixel. For example, Fig. 8 compares SWE series at three elevations in the pixel at the highest peak of the Pyrenees (Aneto Peak, 3404 m a.s.l.). Thus, these series allows for the study of different annual snow accumulation and melting patterns at a specific location and how elevation influences snow

evolution. Similarly, it enables one to study the existence of temporal trends or the occurrence of extreme snowfall and melting events.

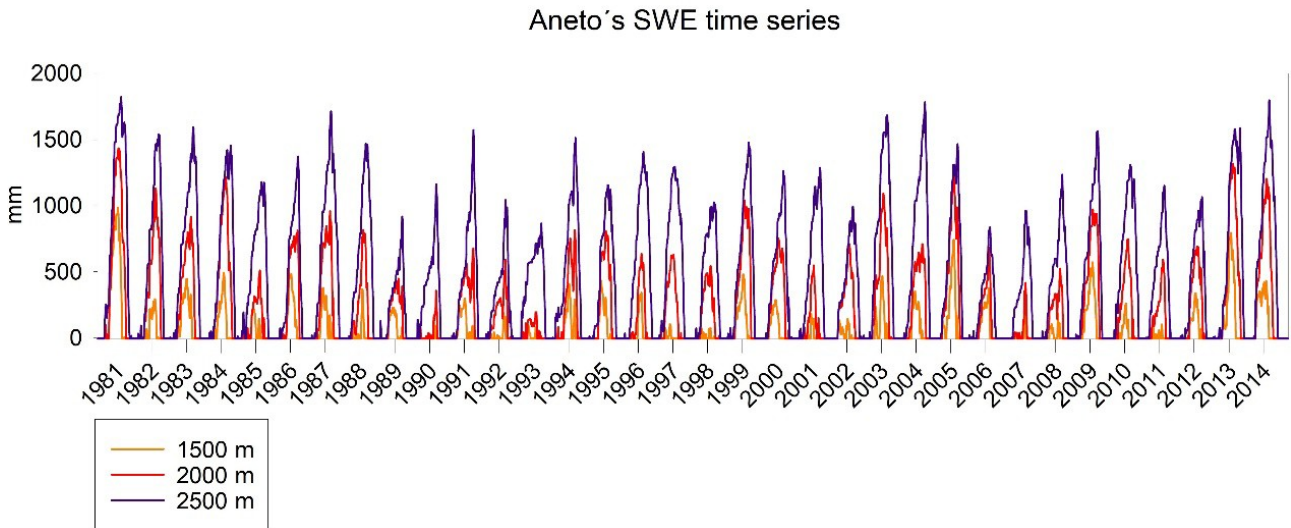


Figure 8: Comparison of SWE time series at 1500, 2000, and 2500 m a.s.l. at Aneto Peak.

The database contains uncertainties that are not easy to quantify, due to the limited amount of observational data. Biases may be due to uncertainty of the boundary conditions from the ERA-Interim reanalysis (Chaudhuri et al., 2013) since errors from the WRF downscaling model are difficult to quantify in mountain areas (Gutmann et al., 2012), and uncertainties that typically result from simulations of snow mass and energy balance from meteorological data (Essery et al., 1999, 2013; Magnusson et al., 2015). The use of the standard air temperature lapse rate could also be a source of uncertainty. Although other studies have observed a decrease in the lapse rate during winter months, this effect is result of thermic inversions that are not considered to be due to the spatial resolution of the simulation.

Despite these limitations, we had very satisfactory results when testing the duration and the interannual variability of the snowpack against MODIS and telenivometer data, which provided reliable observations during several snow seasons. This way, the database presents a reliable validation for more than a third of the time period generated. When using this database, it is important to consider that it was based on the assumption of flat topography within each 10 km 10 km pixel. Therefore, this dataset is not suitable for studies of snow variability due to terrain aspect, slope, and snow redistribution processes, such as avalanches and wind transport.

4. Data availability

The data presented here are freely available for download from Zenodo (<https://doi.org/10.5281/zenodo.854618>). SD and SWE datasets are in ncdf4 format, with one file for each elevation band. The observational information used to validate the main data is also available for download. All telenivometer data are in CSV format. Daily snow cover (derived from MODIS) is provided as five multiband GeoTiff files (one file for each mountain range, each band is a date), and a CSV file indicates the date of each band.

The FSM code is freely available from <https://github.com/RichardEssery/FSM> (Essery, 2015).

5. Conclusions

We presented a new daily gridded database of SD and SWE for the Iberian Peninsula from 1980 to 2014 period at a resolution of 0.088 (10 km). The database consists of 50 ncdf4 files for SD and SWE from 500 to 2900 m a.s.l., and an-other 2 files of WRF simulation DEMs, summing more than 652 000 maps. A mask label of “no data” is included if the grid is not found at the elevation of the simulated elevation band.

The scarcity of snow observations in the Iberian Peninsula made it necessary to couple a dynamic downscaling of ERA-Interim reanalysis using the WRF model by use of a snow energy and mass balance model (FSM). Input data of FSM provided directly, or estimated from WRF outputs, were avail-able for the average elevation of each 10 km 10 km pixel, and these data were transformed to achieve an elevation off-set at 100 m intervals.

Despite some uncertainties, the database is consistent with available observational data. More specifically, validation with MODIS data indicated an error of 6.07 % and an R^2 of 0.76 from the analysis of the mean presence of snow. The database also provides good representation of the temporal patterns of the telenivometers, with kappa values generally over 0.6, and above 0.4 for all analyzed percentiles.

This database will be an important resource for studies of many different hydrological, environmental, and economic processes in Mediterranean areas. Thus, we expect the database presented here will be useful for future snow-related studies at regional scales on the Iberian Peninsula, and for a broad community of researchers and land managers working in areas where snowfall occurs.

Acknowledgements. Esteban Alonso-González is supported by the Spanish Ministry of Economy and Competitiveness (BES-2015-071466). This study was funded by the Spanish Ministry of Economy and Competitiveness projects CGL2014-52599-P 10 (Estudio del manto de nieve en la montaña española y su respuesta a la variabilidad y cambio climático) and CGL2017-82216-R (HIDROIBERNIEVE) and (with additional support from the European Community funds, FEDER) CGL2013-48539-R (Impactos del cambio climático en los recursos hídricos de la cuenca del Duero a alta resolución). Also, the Regional Government of Andalusia has funded this research with the project P11-RNM-7941 (Impactos del Cambio Climático en la cuenca del Guadalquivir, LICUA). The authors would like to express thanks to Hydrological Ebro River Basin Authority (CHE) for providing telenivometer data. Development of FSM is supported by NERC grant NE/P011926/1. Cotos snow data were provided by Consejería de Medio Ambiente, Administración Local y Ordenación del Territorio de la Comunidad de Madrid, from the meteorological network of Parque Natural de Peñalara. The authors sincerely thank Jan Magnusson for his help on the first steps of the use of FSM code.

References

- Argüeso, D., Hidalgo-Muñoz, J. M., Gámiz-Fortis, S. R., Esteban-Parra, M. J., and Castro-Díez, Y.: Evaluation of WRF Mean and Extreme Precipitation over Spain: Present Climate (1970–99), *J. Climate*, 25, 4883–4897, <https://doi.org/10.1175/JCLI-D-11-00276.1>, 2012.
- Barnett, T. P., Adam, J. C., and Lettenmaier, D. P.: Potential impacts of a warming climate on water availability in snow-dominated regions, *Nature*, 438, 303–309, <https://doi.org/10.1038/nature04141>, 2005.
- Barry, R. and Chorley, R. J.: *Atmosphere, weather and climate*, Methuen & Co. Ltd., London., 1987.
- Bellaire, S., Jamieson, J. B., and Fierz, C.: Forcing the snow-cover model SNOWPACK with forecasted weather data, *The Cryosphere*, 5, 1115–1125, <https://doi.org/10.5194/tc-5-1115-2011>, 2011.
- Belo-Pereira, M., Dutra, E., and Viterbo, P.: Evaluation of global precipitation data sets over the Iberian Peninsula, *J. Geophys. Res.*, 116, D20101, <https://doi.org/10.1029/2010JD015481>, 2011.
- Berberan-Santos, M. N., Bodunov, E. N., and Pogliani, L.: On the barometric formula, *Am. J. Phys.*, 65, <https://doi.org/10.1119/1.18555>, 1997.
- Berrisford, P., Dee, D. P., Poli, P., Brugge, R., Fielding, K., Fuentes, M., Kållberg, P. W., Kobayashi, S., Uppala, S., and Simmons, A.: The ERA-Interim archive Version 2.0, *ERA Rep. Ser.*, 23, 2011.
- Brent, R. P. and Richard P.: Algorithms for minimization without derivatives, Prentice-Hall, 1972.
- Brun, E., Vionnet, V., Boone, A., Decharme, B., Peings, Y., Valette, R., Karbou, F., and Morin, S.: Simulation of Northern Eurasian Local Snow Depth, Mass, and Density Using a Detailed Snowpack Model and Meteorological Reanalyses, *J. Hydrometeorol.*, 14, 203–219, <https://doi.org/10.1175/JHM-D-12-012.1>, 2013.
- Chaudhuri, A. H., Ponte, R. M., Forget, G., and Heim-bach, P.: A Comparison of Atmospheric Reanalysis Surface Products over the Ocean and Implications for Uncertainties in Air–Sea Boundary Forcing, *J. Climate*, 26, 153–170, <https://doi.org/10.1175/JCLI-D-12-00090.1>, 2013.
- Chen, F., Kusaka, H., Bornstein, R., Ching, J., Grimmond, C. S. B., Grossman-Clarke, S., Loridan, T., Manning, K. W., Martilli, A., Miao, S., Sailor, D., Salamanca, F. P., Taha, H., Tewari, M., Wang,

X., Wyszogrodzki, A. A., and Zhang, C.: The integrated WRF/urban modelling system: development, evaluation, and applications to urban environmental problems, *Int. J. Climatol.*, 31, 273–288, <https://doi.org/10.1002/joc.2158>, 2011.

Cohen, J.: A Coefficient of Agreement for Nominal Scales, *Educ. Psychol. Meas.*, 20, 37–46, <https://doi.org/10.1177/001316446002000104>, 1960.

Dietz, A. J., Kuenzer, C., Gessner, U., and Dech, S.: Remote sensing of snow – a review of available methods, *Int. J. Remote Sens.*, 33, 4094–4134, <https://doi.org/10.1080/01431161.2011.640964>, 2012.

Dozier, J., Bair, E. H., and Davis, R. E.: Estimating the spatial distribution of snow water equivalent in the world's mountains, *Wiley Interdiscip. Rev. Water*, 3, 461–474, <https://doi.org/10.1002/wat2.1140>, 2016.

Durán, L., Rodríguez-Muñoz, I., and Sánchez, E.: The Peñalara Mountain Meteorological Network (1999–2014): Description, Preliminary Results and Lessons Learned, *Atmosphere*, 8, 203, <https://doi.org/10.3390/atmos8100203>, 2017.

Essery, R.: A factorial snowpack model (FSM 1.0), *Geosci. Model Dev.*, 8, 3867–3876, <https://doi.org/10.5194/gmd-8-3867-2015>, 2015.

Essery, R., Martin, E., Douville, H., Fernández, A., and Brun, E.: A comparison of four snow models using observations from an alpine site, *Clim. Dynam.*, 15, 583–593, <https://doi.org/10.1007/s003820050302>, 1999.

Essery, R., Morin, S., Lejeune, Y., and Menard, C.: A comparison of 1701 snow models using observations from an alpine site, *Adv. Water Resour.*, 55, 131–148, <https://doi.org/10.1016/j.advwatres.2012.07.013>, 2013.

Fayad, A., Gascoin, S., Faour, G., López-Moreno, J. I., Drapeau, L., Le Page, M., and Escadafal, R.: Snow hydrology in Mediterranean mountain regions: A review, *J. Hydrol.*, 551, 374–396, <https://doi.org/10.1016/j.jhydrol.2017.05.063>, 2017.

Fleiss, J. L., Cohen, J., and Everitt, B. S.: Large sample standard errors of kappa and weighted kappa, *Psychol. Bull.*, 72, 323–327, <https://doi.org/10.1037/h0028106>, 1969.

García-Ruiz, J. M., López-Moreno, J. I., Vicente-Serrano, S. M., Lasanta-Martínez, T., and Beguería, S.: Mediterranean water re-sources in a global change scenario, *Earth-Sci. Rev.*, 105, 121– 139, <https://doi.org/10.1016/j.earscirev.2011.01.006>, 2011.

García-Valdecasas-Ojeda, M., De Franciscis, S., Raquel Gámiz-Fortis, S., Castro-Díez, Y., and Esteban-Parra, M. J.: Evaluation of high-resolution WRF climate simulations for hydrological variables over Iberian Peninsula, *Geophys. Res. Abstr.*, 14153, EGU General Assembly 2016, Vienna, Austria, 2016.

García-Valdecasas Ojeda, M., Gámiz-Fortis, S. R., Castro-Díez, Y., and Esteban-Parra, M. J.: Evaluation of WRF capability to detect dry and wet periods in Spain using drought indices, *J. Geophys. Res.-Atmos.*, 122, 1569–1594, <https://doi.org/10.1002/2016JD025683>, 2017.

Gascoin, S., Lhermitte, S., Kinnard, C., Bortels, K., and Liston, G. E.: Wind effects on snow cover in Pascua-Lama, Dry Andes of Chile, *Adv. Water Resour.*, 55, 25–39, <https://doi.org/10.1016/j.advwatres.2012.11.013>, 2013.

Gascoin, S., Hagolle, O., Huc, M., Jarlan, L., Dejoux, J.-F., Szczypta, C., Marti, R., and Sánchez, R.: A snow cover climatology for the Pyrenees from MODIS snow products, *Hydrol. Earth Syst. Sci.*, 19, 2337–2351, <https://doi.org/10.5194/hess-19-2337-2015>, 2015.

Gilaberte-Búrdalo, M., López-Martín, F., Pino-Otín, M. R., and López-Moreno, J. I.: Impacts of climate change on ski industry, *Environ. Sci. Policy*, 44, 51–61, <https://doi.org/10.1016/j.envsci.2014.07.003>, 2014.

Gilaberte-Búrdalo, M., López-Moreno, J. I., Morán-Tejeda, E., Jerez, S., Alonso-González, E., López-Martín, F., and Pino-Otín, M. R.: Assessment of ski condition reliability in the Spanish and Andorran Pyrenees for the sec-ond half of the 20th century, *Appl. Geogr.*, 79, 127–142, <https://doi.org/10.1016/j.apgeog.2016.12.013>, 2017.

Gutmann, E. D., Rasmussen, R. M., Liu, C., Ikeda, K., Gochis, D. J., Clark, M. P., Dudhia, J., and Thompson, G.: A Com-parison of Statistical and Dynamical Downscaling of Winter Precipitation over Complex Terrain, *J. Climate*, 25, 262–281, <https://doi.org/10.1175/2011JCLI4109.1>, 2012.

Hall, K., D., Riggs, G. A., and Salomonson., V. V.: MODIS/Terra Snow Cover Daily L3 Global 500m Grid V005, 2006.

Harder, P. and Pomeroy, J.: Estimating precipitation phase using a psychrometric energy balance method, *Hydrol. Process.*, 27, 1901–1914, <https://doi.org/10.1002/hyp.9799>, 2013.

Heikkilä, U., Sandvik, A., and Sorteberg, A.: Dynamical down-scaling of ERA-40 in complex terrain using the WRF regional climate model, *Clim. Dynam.*, 37, 1551–1564, <https://doi.org/10.1007/s00382-010-0928-6>, 2011.

Herrera, S., Gutiérrez, J. M., Ancell, R., Pons, M. R., Frías, M. D., and Fernández, J.: Development and analysis of a 50-year high-resolution daily gridded precipitation dataset over Spain (Spain02), *Int. J. Climatol.*, 32, 74–85, <https://doi.org/10.1002/joc.2256>, 2012.

ISO: ISO 2533:1975 – Standard Atmosphere, 108, available at: http://www.iso.org/iso/catalogue_detail?csnumber=7472 (last access: 1 February 2017), 1975.

Iziomon, M. G., Mayer, H., and Matzarakis, A.: Downward atmo-spheric longwave irradiance under clear and cloudy skies: Mea-surement and parameterization, *J. Atmos. Sol.-Terr. Phys.*, 65, 1107–1116, <https://doi.org/10.1016/j.jastp.2003.07.007>, 2003.

Keller, F., Kienast, F., and Beniston, M.: Evidence of re-sponse of vegetation to environmental change on high-elevation sites in the Swiss Alps, *Reg. Environ. Change*, 1, 70–77, <https://doi.org/10.1007/PL00011535>, 2000.

Kinar, N. J. and Pomeroy, J. W.: Measurement of the physi-cal properties of the snowpack, *Rev. Geophys.*, 53, 481–544, <https://doi.org/10.1002/2015RG000481>, 2015.

Krogh, S. A., Pomeroy, J. W., and McPhee, J.: Physi-cally Based Mountain Hydrological Modeling Using Reanal-yysis Data in Patagonia, *J. Hydrometeorol.*, 16, 172–193, <https://doi.org/10.1175/JHM-D-13-0178.1>, 2015.

Kryza, M., Wałaszek, K., Ojrzyńska, H., Szymański, M., Werner, M. and Dore, A. J.: High-Resolution Dynamical Downscaling of ERA-Interim Using the WRF Regional Climate Model for the Area of Poland. Part 1: Model Configuration and Statistical Evaluation for the 1981–2010 Period, *Pure Appl. Geophys.*, 174, 511–526, <https://doi.org/10.1007/s00024-016-1272-5>, 2017.

Landis, J. R. and Koch, G. G.: The Measurement of Observer Agreement for Categorical Data, *Biometrics*, 33, 159–174, <https://doi.org/10.2307/2529310>, 1977.

Liston, G. E. and Elder, K.: A Distributed Snow-Evolution Mod-eling System (SnowModel), *J. Hydrometeorol.*, 7, 1259–1276, <https://doi.org/10.1175/JHM548.1>, 2006a.

Liston, G. E. and Elder, K.: A Meteorological Distribution System for High-Resolution Terrestrial Modeling (MicroMet), *J. Hydrometeorol.*, 7, 217–234, <https://doi.org/10.1175/JHM486.1>, 2006b.

López-Moreno, J. I. and García-Ruiz, J. M.: Influence of snow accumulation and snowmelt on streamflow in the central Spanish Pyrenees Influence de l'accumulation et de la fonte de la neige sur les écoulements dans les Pyrénées centrales espagnoles, *Hydrol. Sci. J.*, 49, p. 802, <https://doi.org/10.1623/hysj.49.5.787.55135>, 2004.

López-Moreno, J. I., Goyette, S., Vicente-Serrano, S. M., and Beniston, M.: Effects of climate change on the intensity and frequency of heavy snowfall events in the Pyrenees, *Climatic Change*, 105, 489–508, <https://doi.org/10.1007/s10584-010-9889-3>, 2011.

López-Moreno, J. I., Revuelto, J., Fassnacht, S. R., Azorín-Molina, C., Vicente-Serrano, S. M., Morán-Tejeda, E., and Sexstone, G. A.: Snowpack variability across various spatio-temporal resolutions, *Hydrol. Process.*, 29, 1213–1224, <https://doi.org/10.1002/hyp.10245>, 2015.

Magnusson, J., Wever, N., Essery, R., Helbig, N., Winstral, A., and Jonas, T.: Evaluating snow models with varying process representations for hydrological applications, *Water Resour. Res.*, 51, 2707–2723, <https://doi.org/10.1002/2014WR016498>, 2015.

Mass, C. F., Ovens, D., Westrick, K., and Colle, B. A: Does Increasing Horizontal Resolution Produce More Skillful Forecasts?, *B. Am. Meteorol. Soc.*, 83, 407–430, [https://doi.org/10.1175/1520-0477\(2002\)083<0407:DIHRPM>2.3.CO;2](https://doi.org/10.1175/1520-0477(2002)083<0407:DIHRPM>2.3.CO;2), 2002.

Meromy, L., Molotch, N. P., Link, T. E., Fassnacht, S. R., and Rice, R.: Subgrid variability of snow water equivalent at operational snow stations in the western USA, *Hydrol. Process.*, 27, 2383–2400, <https://doi.org/10.1002/hyp.9355>, 2013.

Morán-Tejeda, E., Lorenzo-Lacruz, J., López-Moreno, J. I., Rahman, K., and Beniston, M.: Streamflow timing of mountain rivers in Spain: Recent changes and future projections, *J. Hydrol.*, 517, 1114–1127, <https://doi.org/10.1016/j.jhydrol.2014.06.053>, 2014.

Navarro-Serrano, F. M. and López-Moreno, J. I.: Spatio-temporal analysis of snowfall events in the Spanish Pyrenees and their relationship to atmospheric circulation, *Cuad. Investig. Geográfica*, 43, 233–254, <https://doi.org/10.18172/cig.3042>, 2017.

Quéno, L., Vionnet, V., Dombrowski-Etchevers, I., Lafaysse, M., Dumont, M., and Karbou, F.: Snowpack modelling in the Pyrenees driven by kilometric-resolution meteorological forecasts, *The Cryosphere*, 10, 1571–1589, <https://doi.org/10.5194/tc-10-1571-2016>, 2016.

Raleigh, M. S., Livneh, B., Lapo, K., and Lundquist, J. D.: How Does Availability of Meteorological Forcing Data Impact Physically Based Snowpack Simulations?, *J. Hydrometeorol.*, 17, 99–120, <https://doi.org/10.1175/JHM-D-14-0235.1>, 2016.

Revuelto, J., Jonas, T., and López-Moreno, J.-I.: Backward snow depth reconstruction at high spatial resolution based on time-lapse photography, *Hydrol. Process.*, 30, 2976–2990, <https://doi.org/10.1002/hyp.10823>, 2016.

Saha, S., Moorthi, S., Pan, H.-L., Wu, X., Wang, J., Nadiga, S., Tripp, P., Kistler, R., Woollen, J., Behringer, D., Liu, H., Stokes, D., Grumbine, R., Gayno, G., Wang, J., Hou, Y.-T., Chuang, H.-Y., Juang, H.-M. H., Sela, J., Iredell, M., Treadon, R., Kleist, D., Van Delst, P., Keyser, D., Derber, J., Ek, M., Meng, J., Wei, H., Yang, R., Lord, S., Van Den Dool, H., Kumar, A., Wang, W., Long, C., Chelliah, M., Xue, Y., Huang, B., Schemm, J.-K., Ebisuzaki, W., Lin, R., Xie, P., Chen, M., Zhou, S., Higgins, W., Zou, C.-Z., Liu, Q., Chen, Y., Han, Y., Cucurull, L., Reynolds, R. W., Rutledge, and Goldberg, G.: The NCEP Climate Forecast System Reanalysis, *B. Am. Meteorol. Soc.*, 91, 1015–1057, <https://doi.org/10.1175/2010BAMS3001.1>, 2010.

Sanmiguel-Vallelado, A., Morán-Tejeda, E., Alonso-González, E., and López-Moreno, J. I.: Effect of snow on mountain river regimes: an example from the Pyrenees, *Front. Earth Sci.*, 11, 515–530, <https://doi.org/10.1007/s11707-016-0630-z>, 2017.

Skamarock, W. C., Klemp, J. B., Dudhia, J., Gill, D. O., Barker, D. M., Dudhia, M. G., Huang, X., Wang, W., and Powers, Y.: A Description of the Advanced Research WRF Version 3, NCAR Tech. Note NCAR/TN-475CSTR, <https://doi.org/10.5065/D68S4MVH>, 2008.

Snauffer, A. M., Hsieh, W. W., and Cannon, A. J.: Comparison of gridded snow water equivalent products with in situ measurements in British Columbia, Canada, *J. Hydrol.*, 541, , 714–726, <https://doi.org/10.1016/j.jhydrol.2016.07.027>, 2016.

van Pelt, W. J. J., Kohler, J., Liston, G. E., Hagen, J. O., Luks, B., Reijmer, C. H., and Pohjola, V. A.: Multidecadal climate and seasonal snow conditions in Svalbard, *J. Geophys. Res.-Earth*, 121, 2100–2117, <https://doi.org/10.1002/2016JF003999>, 2016.

Viviroli, D., Dürr, H. H., Messerli, B., Meybeck, M., and Wein-gartner, R.: Mountains of the world, water towers for humanity: Typology, mapping, and global significance, *Water Resour. Res.*, 43, W07447, <https://doi.org/10.1029/2006WR005653>, 2007.

Walcek, C. J.: Cloud Cover and Its Relationship to Relative Humidity during a Springtime Midlatitude Cyclone, *Mon. Weather Rev.*, 122, 1021–1035, [https://doi.org/10.1175/1520-0493\(1994\)122<1021:CCAIRT>2.0.CO;2](https://doi.org/10.1175/1520-0493(1994)122<1021:CCAIRT>2.0.CO;2), 1994.

Warrach-Sagi, K., Schwitalla, T., Wulfmeyer, V., and Bauer, H.-S.: Evaluation of a climate simulation in Europe based on the WRF– NOAH model system: precipitation in Germany, *Clim. Dynam.*, 41, 755–774, <https://doi.org/10.1007/s00382-013-1727-7>, 2013.

Wegmann, M., Orsolini, Y., Dutra, E., Bulygina, O., Sterin, A., and Brönnimann, S.: Eurasian snow depth in long-term climate reanalyses, *The Cryosphere*, 11, 923–935, <https://doi.org/10.5194/tc-11-923-2017>, 2017.

Wipf, S., Stoeckli, V., and Bebi, P.: Winter climate change in alpine tundra: plant responses to changes in snow depth and snowmelt timing, *Climatic Change*, 94, 105–121, <https://doi.org/10.1007/s10584-009-9546-x>, 2009.

Wrzesien, M. L., Durand, M. T., Pavelsky, T. M., Howat, I. M., Margulis, S. A., and Huning, L. S.: Comparison of Methods to Estimate Snow Water Equivalent at the Mountain Range Scale: A Case Study of the California Sierra Nevada, *J. Hydrometeo-rol.*, 18, 1101–1119, <https://doi.org/10.1175/JHM-D-16-0246.1>, 2017.

Wu, X., Shen, Y., Wang, N., Pan, X., Zhang, W., He, J., and Wang, G.: Coupling the WRF model with a temperature index model based on remote sensing for snowmelt simulations in a river basin in the Altay Mountains, north-west China, *Hydrol. Pro-cess.*, 30, 3967–3977, <https://doi.org/10.1002/hyp.10924>, 2016.

Capítulo 3: Climatología de nieve de las montañas de la Península Ibérica mediante imágenes por satélite y simulaciones con mejoras de escala dinámicas.

Resumen: La presencia de un manto de nieve estacional determina la hidrología, geomorfología y ecología de amplias zonas de la Península Ibérica, con grandes implicaciones en la economía, el transporte y la gestión de riesgos. Por esta razón, es necesario contar con información fiable desde un punto de vista operacional y científico. Este es el caso de la Península Ibérica, donde la falta de datos ha impedido el estudio de la duración del manto de nieve, magnitud así como su variabilidad interanual. En este trabajo presentamos la primera climatología del manto de nieve de toda la península Ibérica. La escasez de observaciones in situ se ha solucionado mediante el uso de una nueva base de datos generada mediante información procedente del sensor satelital MODIS (2000-2014) y el modelo de base física Factorial Snow Model (FSM), forzado por las salidas del modelo climático regional Weather Research and Forecast (WRF) sobre la Península Ibérica cubriendo el periodo 1980-2014. El manto de nieve de las principales áreas montañosas (Pirineos, Cordillera Cantábrica, Sistema Central, Sistema Ibérico y Sierra Nevada) es descrito, estimado de la base de datos generada. La información del manto de nieve ha sido procesada usando un algoritmo de agrupamiento k-means, buscando similitudes en el manto de nieve a diferentes alturas. Los resultados han encontrado cuatro tipos diferentes de manto de nieve en términos de profundidad, duración y variabilidad interanual sobre las diferentes bandas altitudinales demostrando la variabilidad del manto de nieve de la península Ibérica. Los análisis han revelado zonas con nevadas efímeras en contraste con áreas con duraciones medias de 198 días de nieve al año y 3m de profundidad. Los coeficientes de variación del manto de nieve oscilaron entre 35,2 y 162,4%. Todos los índices analizados indican que la Cordillera Cantábrica y los Pirineos tienen los mantos de nieve más profundos y de mayor duración, seguidos por el Sistema Central e Ibérico. Sierra Nevada mostró el manto de nieve de menor duración y menor profundo con una mayor variabilidad interanual.

Cita completa:

Alonso-González, E., López-Moreno, J. I., Navarro-Serrano, F., Sanmiguel-Vallelado, A., Revuelto, J., Domínguez-Castro, F., & Ceballos, A. (2020). Snow climatology for the mountains in the Iberian Peninsula using satellite imagery and simulations with dynamically downscaled reanalysis data. *Int J Climatol.* 2020; 40: 477– 491. <https://doi.org/10.1002/joc.6223>

Snow climatology for the mountains in the Iberian Peninsula using satellite imagery and simulations with dynamically downscaled reanalysis data

Esteban Alonso-González¹, Juan Ignacio López-Moreno¹, Francisco Navarro-Serrano¹, Alba Sanmiguel-Vallelado¹, Jesús Revuelto², Fernando Domínguez-Castro¹, Antonio Ceballos³

1. Instituto Pirenaico de Ecología, Consejo Superior de Investigaciones Científicas (IPE-CSIC), Zaragoza, Spain
2. Météo-France – CNRS, CNRM (UMR3589), Centre d'Etudes de la Neige, Grenoble, France
3. Dept. Geografía, Universidad de Salamanca, Salamanca, Spain

Correspondence: Esteban Alonso-González (e.alonso@ipe.csic.com)

Received: 03 Diciembre 2018

Accepted: 02 July 2019

Abstract. The presence of a seasonal snowpack determines the hydrology, geomorphology and ecology of wide parts of the Iberian Peninsula, with strong implications for the economy, transport and risk management. Thus, reliable information on snow is necessary from a scientific and operational point of view. This is the case of the Iberian Peninsula where, lack of observation has impeded proper analysis of snow-pack duration, magnitude and interannual variability. In this study, we present the first snow climatology of the entire Iberian Peninsula. The scarcity of in situ observations has been overcome, using a newly developed remote sensing snow data-base from MODIS satellite sensors for the period 2000–2014 and a physically based snow model (Factorial Snow Model—FSM), driven by a regional atmospheric model (Weather Research and Forecast model—WRF) over the Iberian Peninsula for the period 1980–2014. The snowpack of the main mountain areas (Pyrenees, Cantabrian, Central, Iberian range and Sierra Nevada) are described, estimated from the generated databases. The information has been processed using a k-means cluster algorithm, looking for similarities in snow indices at different elevation bands. Results show four different types of snowpack in terms of depth, duration and interannual variability, lying over different elevation bands in the different ranges, proving the variability of the snowpack over Iberia. Analyses reveal areas characterized by ephemeral snowpacks, while in some sectors snowpack lasts, on average, 198 days per year with 3.02 m of peak snow depth. The coefficient of variation of interannual peak snow depth oscillated between 35.2 and 162.4%. All the analysed indices show that at common elevations the Cantabrian range and the Pyrenees host the deepest and longest

lasting snowpacks, followed by the Central and Iberian ranges. The Sierra Nevada exhibits the shortest, shallowest snowpack and more year-to-year variability.

1 Introduction

Snowpack has significant implications for many environmental processes at high latitudes and in most of the mountainous areas of the world. Thus, snow directly affects geomorphological processes (Carrera-Gómez and Valcárcel, 2018; González Trueba and Serrano, 2010), nutrient transport (Jones, 1999), plants and animal phenology (García-Hernández et al., 2016; Slatyer et al., 2017) and the surface energy balance (Lund et al., 2017). It also may become a risk source associated with heavy snowfall, avalanches, floods triggered by rain on snow events (Garvelmann et al., 2015; Würzer and Jonas, 2018), snow melt induced land-slides, cause transport problems or damage to infrastructure (García et al., 2009; Chueca Cía et al., 2014; García-Hernández et al., 2018). These events cause economic losses and even loss of life (Stethem et al., 2003; Höller, 2007; Pfeifer et al., 2018). Furthermore, seasonal snowpack exerts a critical role in various surface and groundwater hydrological processes (Viviroli et al., 2007), especially in those areas, such as the Mediterranean region, where the wet sea-son coincides with the snow accumulation period (Fayad et al., 2017). Additionally, snow, as it relates to tourism, has become a main economic support of mountain areas world-wide (Elsasser and Bürki, 2002). Thus, appropriate management of risks and natural resources of mountainous areas requires spatially comparable information on the duration, magnitude and temporal variability of the snowpack.

The orography of the Iberian Peninsula is complex, with several mountainous areas and two important elevated plateaus that make it one of the highest average elevation regions in Europe (Casas-Sainz and de Vicente, 2009). Snowfall can occur over most of its territory, even at the lowest elevations (Arndt et al., 2010; Bech et al., 2013). As an example, from 1947 to 2009, 16 snowfall events were recorded in Barcelona (13 m a.s.l.) and 18 in Gerona (69 m a.s.l.) areas (Aran et al., 2010). Few snow events are recorded at the coastal elevations of the Valencian Community during the snow season (Mora et al., 2016). Snowfall is not rare over the main cities of northern Spain during the winter, causing associated transportation risks and traffic collapse (Merino et al., 2014). Despite these occasional events at low elevation, a continuous seasonal snowpack appears only in the mountains, generally higher than 1,300–1,500 m a.s.l. (López-Moreno et al., 2009).

Mountainous areas host the headwaters of the main rivers of the Iberian Peninsula. Thus, snow exerts a strong hydrological influence on downstream sectors (López and Jústribó, 2010), controlling the interannual variability of river flows; López-Moreno and García-Ruiz, 2005) and reshaping the annual hygrograms. This has obvious implications on water management (Morán-Tejeda et al., 2014; Sanmiguel-Vallelado et al., 2017), which is expected to become more challenging in the future (Viviroli et al., 2011) due to climatological and landscape changes (García-Ruiz et al., 2011; Vicente-Serrano et al., 2014). The economy of many regions in the Iberian Peninsula has become dependent on the interannual variability of snow, which makes these regions highly vulnerable to climate change, since snow duration in this area is largely connected to climate warming (Gilaberte-Búrdalo et al., 2014, 2017).

There are some studies describing the behavior of the snowpack over different mountain ranges of Iberia. More specifically, most of these studies are focused on the Pyrenees and, to a lesser degree, in the Sierra Nevada (i.e., Herrero et al., 2011; Revuelto et al., 2014; Gascoin et al., 2015; López-Moreno et al., 2015; Quénol et al., 2016; Navarro-Serrano and López-Moreno, 2017) with just some mention of other mountain ranges in Iberia where snow plays an important role (i.e., Palacios et al., 2003; Serrano Cañas et al., 2016; Soteres García et al., 2016; Ceballos-Barbancho et al., 2018).

Most of the snow studies are limited by the limited snow data available. Topographical complexity and the spatial and temporal variability of the snowpack at different scales make it challenging to characterize the snowpack at regional scale from field measurements (López-Moreno et al., 2011a, 2013), which are, in turn, very scarce in the Iberian mountains. Daily snow observations in Spain rely on observatories from the National Meteorological Agency (AEMET), but information is generally restricted to the presence or absence of snow, less often providing snow depth (SD) (Buisan et al., 2015). In the last years, AEMET and some hydrological administrations have installed automatic stations at higher elevations. Despite the interest in this new information, available series are too short and too sparsely distributed over terrain to be used for generating sound regional information (Revuelto et al., 2017).

Remote sensing data can be useful for retrieving information on snow presence over large areas, but in most cases this information is limited to the snow cover area. Obtaining SD and Snow Water Equivalent (SWE) data from remote sensing techniques is an active research topic. However, this information is not always available, and there are not yet products able to retrieve information on snow depth or SWE under complex topography and at a spatial and, more importantly, temporal

scale useful for scientific and managerial purposes. The use of numerical mesoatmospheric models coupled online (Wrzesien et al., 2018) or offline (van Pelt et al., 2016; Wu et al., 2016) with snow modelling systems has proven consistent, replicating interannual and intraannual snowpack variability, allowing the development of consistent snow climatologies (Wrzesien et al., 2017; Revuelto et al., 2018).

Recently, Alonso-González et al. (2018) generated the first snow database for the whole of Iberia. The database was made by combining remote sensing data (Moderate-Resolution Imaging Spectroradiometer, MODIS) for the period 2000–2014 with simulations from a snow energy balance model (Factorial Snow Model, FSM) driven by the out-puts of a mesoatmospheric climate model (Weather Research and Forecast, WRF) at 0.088 (~10 km) resolution for the period 1980–2014. This was further rescaled at different elevation bands to estimate SD and SWE. The objectives here are: (a) to illustrate and quantify the main differences of the snow phenomena across the Iberian Peninsula; and (b) to characterize the snow cover duration, magnitude of the snow pack and its interannual variability exhibited in the last decades.

2 Study area

The Iberian Peninsula has a complex topography, dominated by two large central plateaus surrounded for several mountain ranges that exceed 2,000 m a.s.l. These mountain areas are well represented by five principal mountain ranges (Pyrenees, Cantabrian Mountains, Central, Iberian and Sierra Nevada; see Table 1 for a detailed description of position and elevation of each range) where seasonal snowpack develops every year. The Sierra Nevada (Mulhacén peak, 3,478 m a.s.l.) and the Pyrenees (Aneto peak, 3,404 m a.s.l.) mountain ranges reach the higher elevations of the Peninsula.

Table 1: Maximum elevation, location and area at different elevation ranges of the main mountain ranges of Iberia.

Study area	Max. elevation	Surface (Km ²)			
		1000 - 1500	1500 – 2000	2000 – 2500	>2500
Cantabrian	2648	11397	3211	143	<1
Central	2592	9772	2116	218	<1
Iberian	2314	7198	918	26	0
Sierra Nevada	3479	1510	902	388	190
Pyrenees	3404	9318	5560	3543	836

The distribution of the mountain ranges runs generally from west to east, localized at different latitudes and at different distances to the sea (Figure 1). This particular distribution and the contrasted air masses that affect the Iberian Peninsula (transition from Atlantic to Mediterranean patterns) generate different climatological areas over Iberia (Lopez-Bustins et al., 2008). The climatological particularities of each mountain range affect the energy balance of the snowpack in different ways, generating different behaviours of the snowpack and different responses to climate warming (López-Moreno et al., 2017a). All these different conditions also ensure the snowpack will exhibit very different duration and thicknesses at the different elevation bands when the mountain ranges are compared. In addition, the hypsometry of each mountain range (Figure 1) differs considerably in what may have noticeable impacts on the importance of the snow phenomena. Thus, the Pyrenees and Sierra Nevada exhibits much larger areas above 1,500–2,000 m where seasonal and long-lasting snowpacks generally exists.

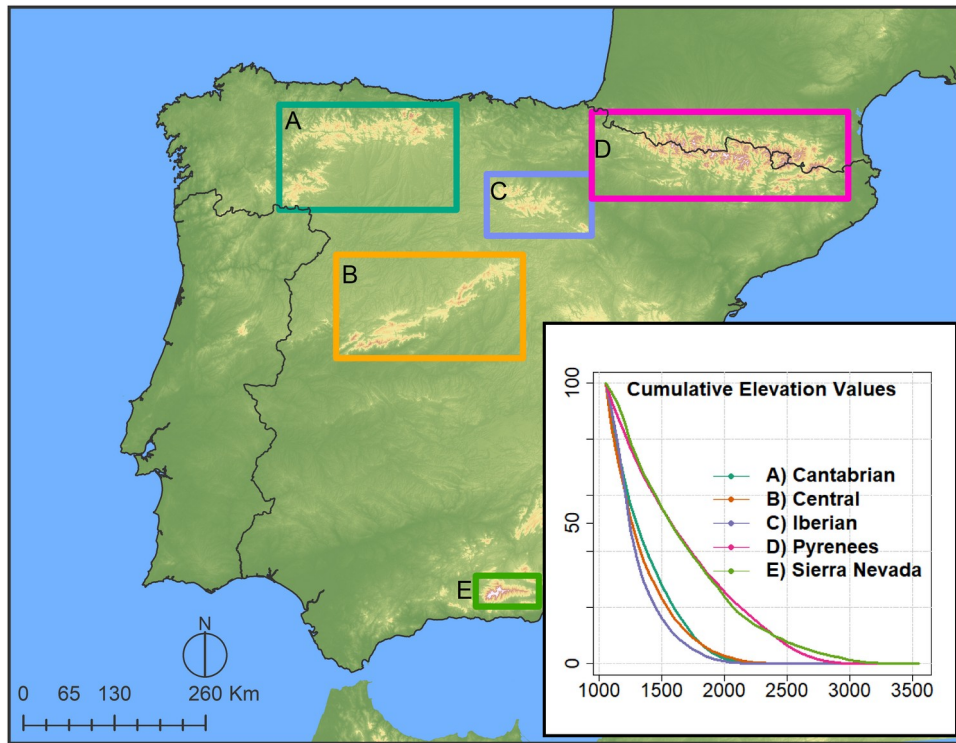


Figure 1: Distribution of the main mountain ranges over Iberia and its hypsography.

3 Data and methods

3.1 Remote sensing

To study the spatiotemporal variability of the snow cover, we used the MODIS database of snow cover maps for the Iberian Peninsula from MODIS images (Alonso-González et al., 2018). Raw data (from the National Snow and Ice Data Center (Hall et al., 2006) was subjected to a gap-filling procedure, based on the algorithm developed by Gascoin et al. (2015), in order to avoid data losses due to cloud cover. The gap-filling algorithm works in four steps. First, it combines the MOD10A1/MYD10A1 data. Then, it reclassifies each no-data pixel if it is surrounded by at least five snow or no-snow pixels. After that, it deduces the values of the no-data pixel with a temporal moving window for the preceding and antecedent grid. Finally, the remaining no-data pixels are reclassified using a classification tree in the last step. This provided gap-free daily maps showing the presence and absence of snow in each mountain range from 2000 to 2014 seasons. Gascoin et al. (2015) used this methodology to study snow cover dynamics over the Pyrenees and indicated the capability of

this product to detect reliable spatial patterns and temporal anomalies of the probability of snow cover presence on the ground. To avoid excessive computational expense and improve the precision of the final products, the five individual mountain range domains were analysed rather than the entire Iberian Peninsula (Figure 1).

These gap-filling products allow us to estimate the percentage of the year covered by snow, that is, the temporal snow probability ($P_{(Snow)}$), at a 500 m resolution. This index improves the visualization and inter-comparison of the calculations, so it refers directly to the average number of days covered by snow per year over the 15-year period of record. We have also estimated the temporal coefficient of variation (CV) of the interannual values of $P_{(Snow)}$.

To make remote sensing and simulations comparable (see Section 3.2, simulation of snow depth and snow water equivalent) we computed the two MODIS-based snow indexes, $P_{(Snow)}$ and CV for common elevation bands. We considered a common elevation band, the pixels inside the range ([elevation band value] \pm 50 m a.s.l.), to make it com-parable with the simulated products.

3.2 SD and SWE simulation

Climatology of SD and SWE was based on the snow product simulated using a physically-based snow energy balance model, that is, FSM (Essery, 2015) forced with meteorological data from downscaled reanalysis products. A full description of this snow database is provided in Alonso-González et al. (2018). More specifically, the global ERA-Interim reanalysis (Berrisford et al., 2011) at 0.75 (~80 km) resolution, was dynamically downscaled using the WRF model (Skamarock et al., 2008) to the spatial resolution of 0.088 (~10 km) from 1980 to 2014 and 3-h time resolution by García-Valdecasas Ojeda et al. (2017). These outputs provided spatially distributed surface meteorological information of 2 m temperature, shortwave radiation, 10-m wind speed and direction, surface atmospheric pressure, and precipitation. The surface meteorological information was scaled from the original elevation of each cell to 100-m elevation bands using hygrobarometric formulas and temperature lapse rates (Alonso-González et al., 2018). This methodology allows study of the snowpack at different elevations inside each 0.088 cell. Afterwards, we calculated snowfall rate, rainfall rate (Harder and Pomeroy, 2013) and longwave radiation (Izquierdo et al., 2003; Liston and Elder, 2006), which are also variables required as input of FSM to calculate the daily SD and SWE series. Alonso-González et al. (2018) proved the consistency of the temporal and

spatial variability of the simulated snow data when compared with in situ snow observations and MODIS data.

A k-means cluster algorithm (Hartigan and Wong, 1979) was used to classify the cells of the different mountain ranges, in order to identify similarities in the seasonal snow patterns between different mountain areas at different elevations. K-means algorithm is a common aggregation technique that iteratively reassigns the centroids of the groups until its global convergence; the centroids do not change (or they have little movement) in the following iterations. This is to ascertain if snowpack duration and magnitude in a mountain at a given elevation is comparable to other mountain ranges at the same or different elevation band. We considered all elevation bands over 1,000 m a.s.l., where most areas began to show shallow snowpacks. To achieve this, we calculated three different snow indices from the simulated series for every cell at all elevation bands of the semi-distributed snowpack database. (a) mean maximum accumulation, (b) mean snow season duration, and (c) coefficient of variation of the yearly maximum accumulation, to characterize the depth, duration, and interannual variability of the snowpack, respectively (López-Moreno et al., 2017a). The indices were previously standardized and the k-means algorithm was run ignoring the elevation values, allowing us to find similar snowpack characteristics at different elevations over different mountain ranges. The maximum accumulation was estimated from SD and SWE values, but no significant differences were found, so SD was chosen to improve results, visualization and interpretation. An array of 30 clustering tests was computed to determine the number of clusters. Following the majority rule (Charrad et al., 2014), four clusters was chosen as the most appropriate number.

Finally, the variability of the snowpack among the different analysed mountain ranges at comparable elevation bands was evaluated. We calculated the $P_{(Snow)}$ duration simulated with FSM for each cell at the common elevation band of 2,000 m a.s.l., assuming a snow cover detection threshold of 40 mm of SWE (Gascoin et al., 2015). In the Sierra Nevada, it was necessary to calculate the $P_{(Snow)}$ values at the 2,500 m a.s.l. common elevation band, due to low $P_{(Snow)}$ values in the 2,000 m a.s.l. band. Then, a simple spline interpolation was computed to study the inter-range spatial trends using the $P_{(Snow)}$ values across the mountain ranges. The spline interpolation technique fits a mathematical surface with the minimum possible curvature over each value of a numeric matrix, generating a smooth surface that contains exactly the values of the matrix. The maps were calculated for the Cantabrian Range, the Pyrenees and the Central Range at 2,000 and over 2,500 m a.s.l. for the Sierra Nevada. The interpolation for the Sierra Nevada was set at 2500 m a.s.l. because

at 2,000 m a.s.l. snow is too ephemeral for proper analysis of differences in snow probability. The Iberian Range is not in this analysis, as it does not have enough area at this elevation band to check differences at a regional scale.

4 Results and discussion

4.1 Probability of snow cover from MODIS

Elevation and latitude are the main variables affecting the $P_{(Snow)}$ over the Iberian Peninsula (e.g., Cantabrian $P_{(Snow)}$ distribution vs Sierra Nevada's $P_{(Snow)}$ distribution, Figure 2). There are also clear differences among the analysed mountains and the different areas within a particular mountain range (Figure 3).

At 1000 m a.s.l., $P_{(Snow)}$ is very low in all mountains (Figure 2) (ranging from 0.9% in the Sierra Nevada to 6% in the Pyrenees), corresponding to ephemeral snowpack after isolated snowfall events (Table 2). At 1,500 and 2,000 m a.s.l. $P_{(Snow)}$ exceeds 15 and 30%, respectively, in the Pyrenees, with very similar values in the Cantabrian mountains; while in the Sierra Nevada, probabilities are much lower for the same elevations (3.7 and 13.8% for 1,500 and 2,000 m, respectively). Indeed, the presented data suggest a shift of more than 500 m in the duration of the snowpack when the Sierra Nevada is compared to the Pyrenees or Cantabrian at 2,000 m and below (Table 2). This shift becomes less evident in the highest elevations, where the values of $P_{(Snow)}$ of the Sierra Nevada and the Pyrenees are closer but maintaining a difference of ~13% of $P_{(Snow)}$. At 2,900 m a.s.l. differences between the Pyrenees and the Sierra Nevada are markedly reduced, with probabilities of 64 and 50.9%, respectively. The Iberian and Central ranges exhibit intermediate values, at 1,500 m a.s.l. $P_{(Snow)}$ in the Iberian range (13.7%) clearly exceeding the Central range (7%). However, this relationship shifts at 2,000 m a.s.l. (27% in the Iberian range vs. 35% in central), probably because this elevation is very close to the summits and main ridges in the Iberian range, and the blowing wind can be very intense, whereas many summits and ridges of the Central range lie between 2,200 and 2,500 m a.s.l (see Figure 1). Considering all the mountains together, the $P_{(Snow)}$ ranges between 27 and 37% (Sierra Nevada 13.8%), indicating a long lasting seasonal snowpack in the Iberian Peninsula at an elevation of 2,000 m a.s.l. that could be a representative common elevation band for all the main mountain ranges.

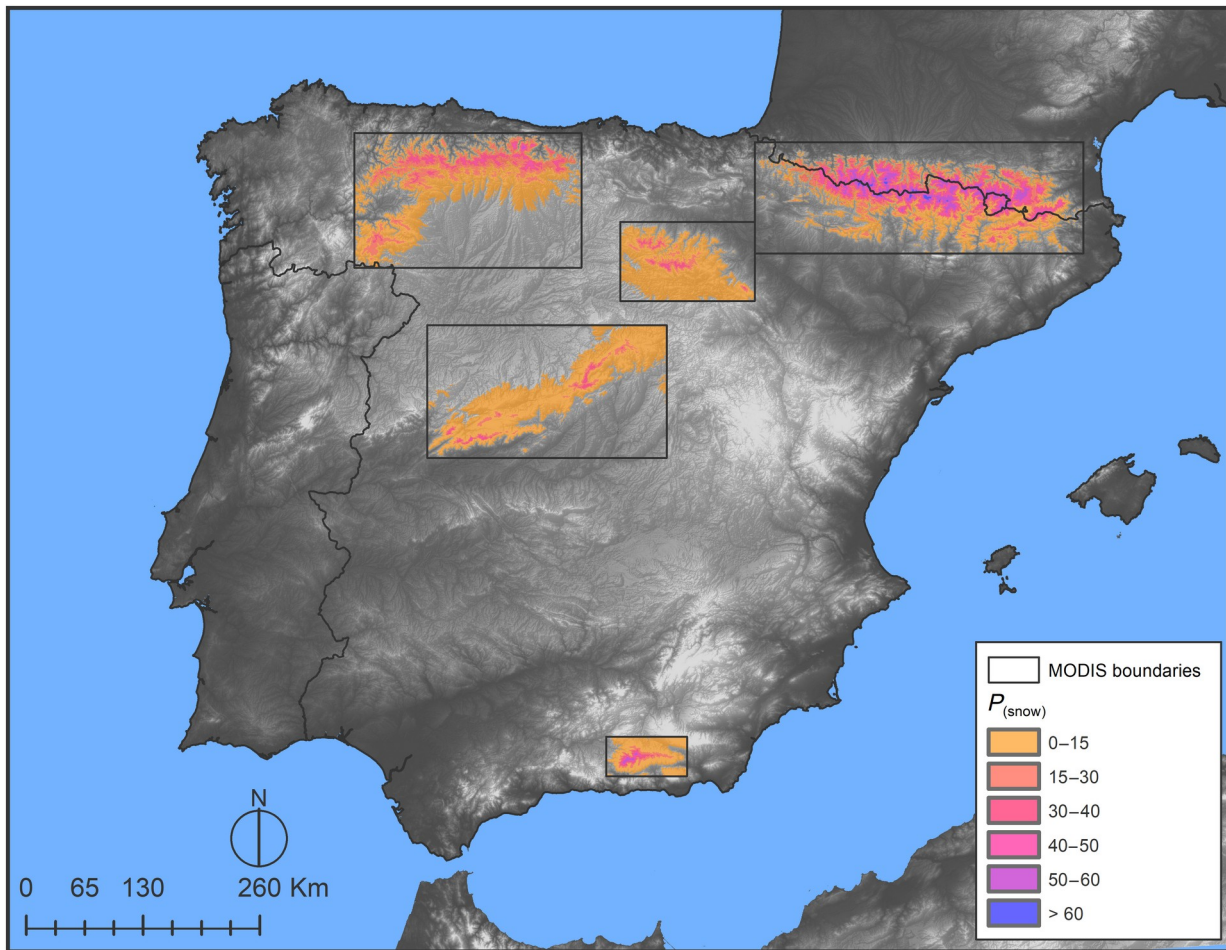


Figure 2: P_{Snow} over main mountain ranges of Iberia based on MODIS gap-filled products.

At 2,000 m, where a long lasting snowpack exists in all mountain areas except in the Sierra Nevada, where the snow limit lies very close to this elevation band, the Pyrenees show the largest dispersion (P_{Snow} range: 16–58%, Figure 3) due to its large extension and strong climatological gradients from Atlantic to Mediterranean conditions (López-Moreno and Nogués-Bravo, 2005). The Cantabrian range also has a considerable longitudinal length and a very strong north–south climatological gradient, also exhibiting a high spatial variability (P_{Snow} range: 21–55%); the Iberian range and Central range have the lowest variability values (P_{Snow} ranges: 23–42% and 16–39%, respectively). Due to its small size, the Sierra Nevada exhibits the lowest range in the P_{Snow} values (P_{Snow} range: 15–25%), even though it exhibits the largest CV at 2,500 and 2,900 m a.s.l. (CV values: 33.5 and 50.9%, respectively). This variability is a consequence of the very strong differences in

precipitation and incoming radiation between its northern and southern slopes (Huete-Morales et al., 2018).

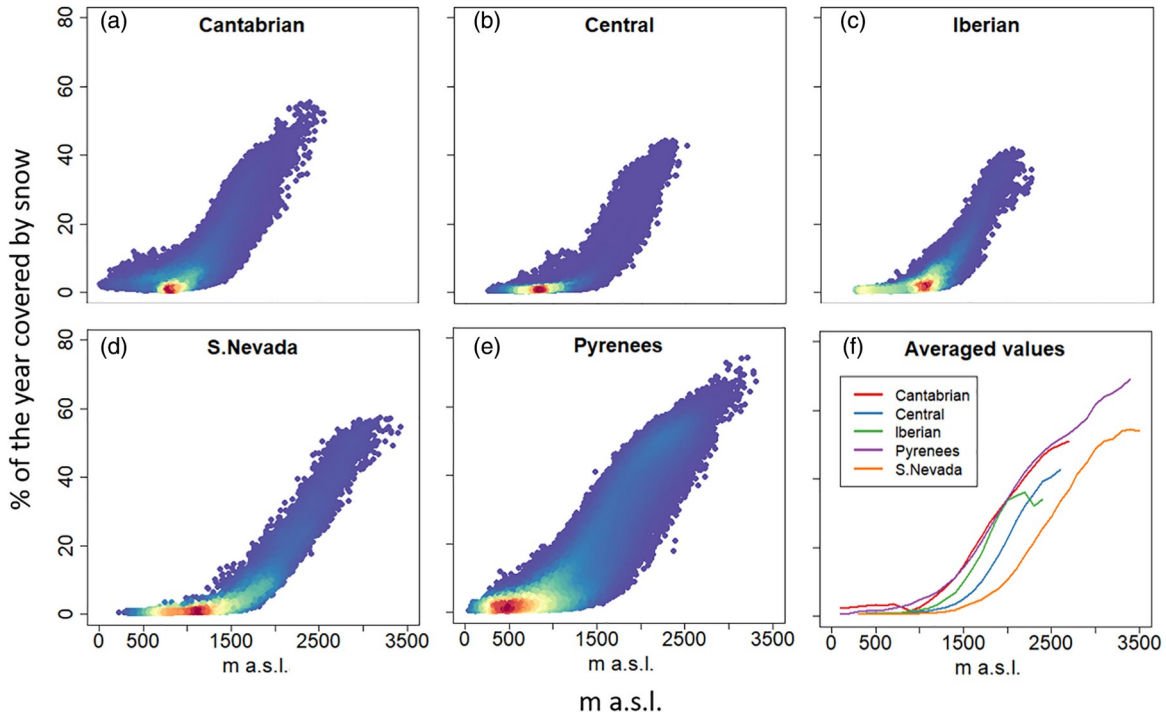


Figure 3: (a-e) Distribution $P_{(\text{Snow})}$ values per elevation over the main mountain ranges of the Iberian Peninsula from MODIS data. (f) Intercomparison of mean values of $P_{(\text{Snow})}$ for each mountain range. The colours of the scatterplots indicates the relative density of points, ranging from blue (lower density) to red (higher density).

Monthly distribution of $P_{(\text{Snow})}$ at the common elevation band of 2,000 m a.s.l. varies through the different mountain ranges, reaching maximum values at Pyrenees and Sierra Nevada (Figure 4). In addition, $P_{(\text{Snow})}$ monthly values for the elevation band of 2,900 m a.s.l. for the Sierra Nevada and the Pyrenees, remarks an evident slower snowmelt at Sierra Nevada (Figure 4).

Table 2: Mean values of $P_{(Snow)}$ (%) and averaged interannual coefficient of variation CV (%) for each mountain range at common elevation bands (m a.s.l.).

	1000 m a.s.l.		1500 m a.s.l.		2000 m a.s.l.		2500 m a.s.l.		2900 m a.s.l.	
	$P_{(Snow)}$	CV								
Cantabrian	4.3	60.6	19.0	33.1	37.0	13.7	50.1	6.2	-	-
Central	1.5	32.1	7.0	43.3	27.8	19.8	-	-	-	-
Iberian	2.2	44.5	13.7	26.9	35.1	11.1	-	-	-	-
Sierra Nevada	0.9	47.9	3.7	53.1	13.8	34.2	33.5	18.0	50.9	6.9
Pyrenees	5.8	64.3	17.6	48.0	38.3	21.5	51.7	9.6	64.0	4.74

The inter-comparison at 2,000 m a.s.l. elevation band highlights again the great spatial variability of the Pyrenees mentioned above, the longer persistence of the snowpack in the Pyrenees, Cantabrian range and Iberian Range, and the shorter persistence of the snowpack in the Central range and, in particular, in the Sierra Nevada. The differences between the Pyrenees and the Sierra Nevada are also very marked at 2900 m a.s.l (Figure 4f), especially at the beginning and end of the snow season, when $P_{(Snow)}$ values have at least a 1-month lag, showing a much later snowpack in the Pyrenees.

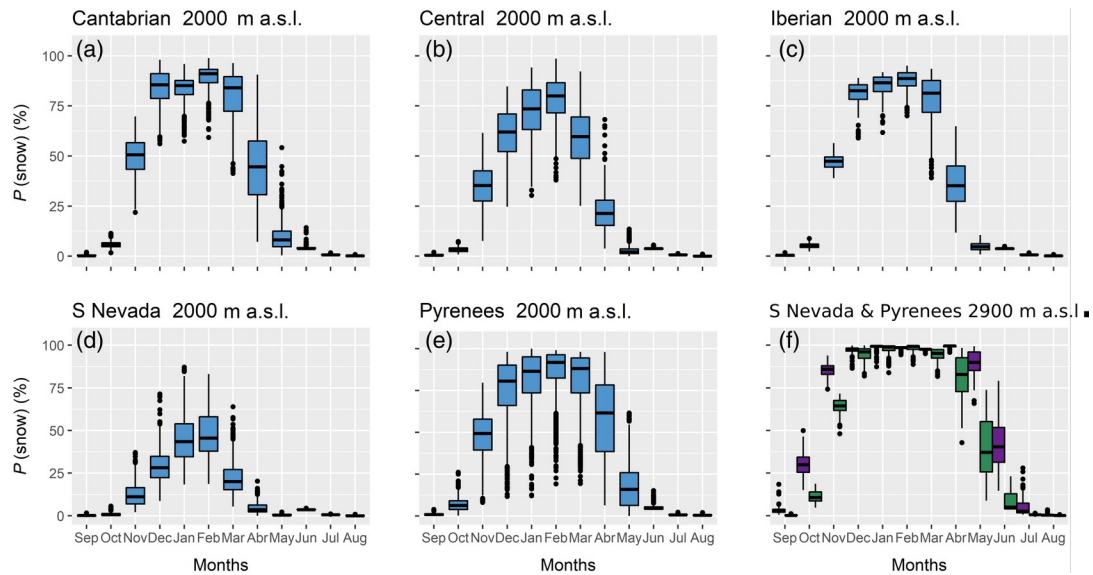


Figure 4: (a-e) Monthly distribution of values of P (Snow) from MODIS products for mountain ranges at 2,000 m a.s.l.; (f) distribution of values of P (Snow) from MODIS products for the Pyrenees and the Sierra Nevada at 2900 m a.s.l. (Pyrenees in purple and Sierra Nevada in green).

There is a general trend in all mountain ranges toward lower CV (interannual variability) as elevation increases (Figure 5). This is particularly evident around 1,000 m a.s.l., related to the occurrence of frequent snowfall but also to the ephemeral nature of the snowpack (Grünewald et al., 2014). As shown for P_{Snow} , the Pyrenees, Cantabrian and Iberian range show similar distribution and mean CV values, with a noticeable increase in the variability for the Central range that becomes similar to the other ranges at 2,000 m a.s.l. The Sierra Nevada is the mountain range that shows the greatest values of CV at all elevations above 1,500 m a.s.l. (i.e., ~16% more than in the Pyrenees at 2,000 m a.s.l.). Indeed, at the highest elevations in the Sierra Nevada, CV is still higher than that observed in the other mountains at 2,000 m a.s.l., indicating that the interannual variability of $P(\text{Snow})$ is related to the climatic dynamics of each mountain range. In the particular case of the Sierra Nevada, the very strong dependency of winter precipitation on the occurrence of negative phases of NAO (López-Moreno et al., 2011c) explains the very large interannual variability found at this mountain range. Although the effect of NAO has obvious implications in the variability of different snow indexes, its complexity exceeds the objectives of this work, making necessary further research in this topic.

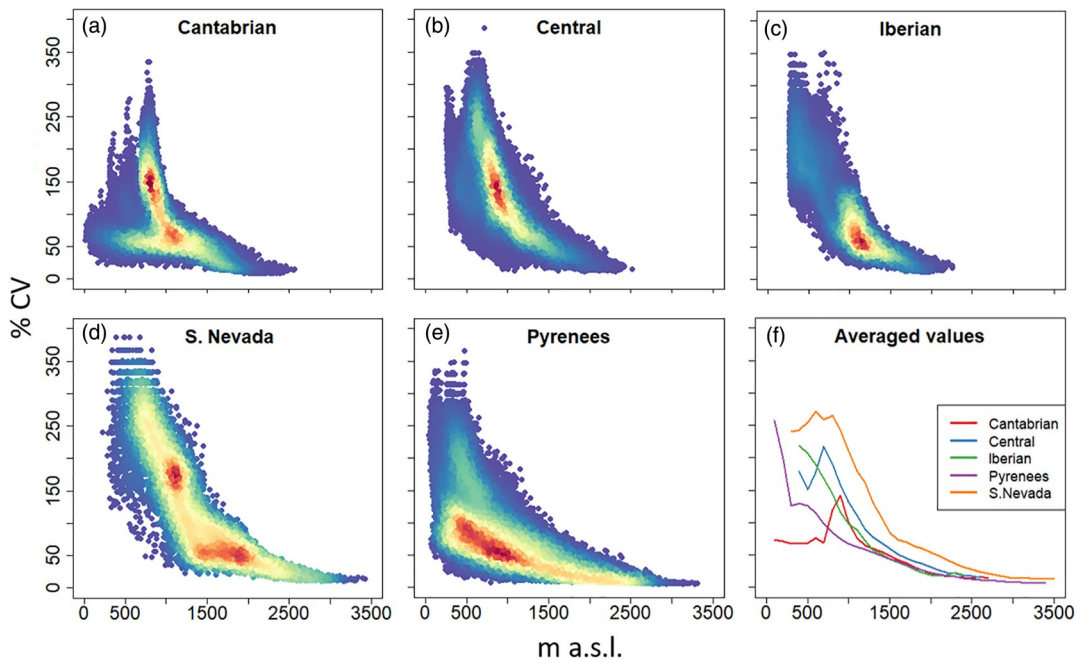


Figure 5: (a-e) Distribution of values of CV per elevations over the main mountain ranges of Iberia from MODIS data; (f) Intercomparison of mean values of CV for each mountain range. The colours of the scatterplots indicates the relative density of points, ranging from blue (lower density) to red (higher density).

4.2 Simulated snow SD and SWE

There is a general trend in all the mountain ranges of delay in the peak SWE date with elevation (Table 3), due to delay in the onset of melt and spring precipitation falling as snow in the highest portions of the mountain ranges (Navarro-Serrano et al., 2018). Peak SWE shows the highest values in the Cantabrian Range for the maximum comparable elevation band (2,400 m a.s.l.) with 1,687 mm, followed by the Pyrenees with 713 mm. The Central range shows values of 475 mm and the Sierra Nevada shows only 164 mm. At the highest elevations (over 2,900 m a.s.l.), the Pyrenees and the Sierra Nevada show noticeable differences in SWE peak values, with 1,313 and 656 mm, respectively.

Table 3: Average peak SWE and average date of maximum SWE, for different representative elevation bands for the main mountain ranges of the Iberian Peninsula.

	Elevation	Pyrenees	S. Nevada	Cantabrian	Central	Iberian
Avg. Max. SWE (mm)	1400	99.4	~0	77.5	~0	~0
	1900	347.5	8.3	471.5	119.9	150.1
	2400	713.2	184.7	1686.9	*	*
	2900	1313.4	655.0	*	*	*
Date max (date)	1400	08-Mar	0	01-Mar	0	0
	1900	08-Mar	30-Jan	01-Mar	22-Feb	23-Feb
	2400	18-Apr	01-Mar	Apr-26	06-Mar	*
	2900	14-Apr	13-Apr	*	*	*

To properly interpret the results in terms of snow abundance at each mountain range, it is important to consider the hypsography of the ranges (see Section 2. Study area, Figure 1 and Table 1). As an example, the Cantabrian range shows the highest values for average SWE peak (Figure 6), but it has 143 km² lying between 2,000 and 2,500 m a.s.l., compared with 3,543 km² for the Pyrenees. This means that even though there are certain areas in the Cantabrian range with maximum values of SWE peak for the whole Iberian Peninsula, the total amount of snow is much larger in the Pyrenees. As a consequence of the extension and climatological variability of the Pyrenees at 2400 m a.s.l., this value of averaged SWE peak (713.2 mm) hides a great dispersion over the mountain range (from a maximum of 1895.9 mm to a minimum 94.54 mm).

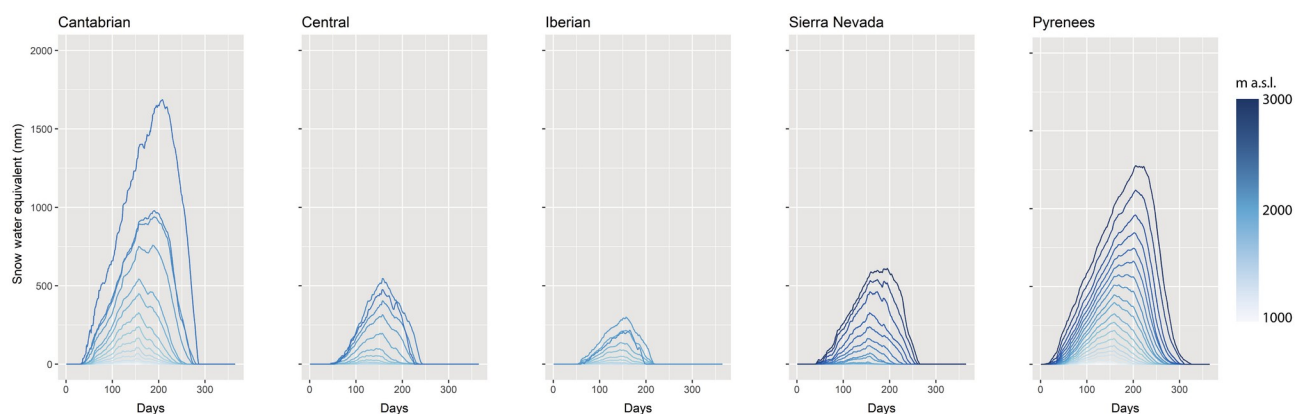


Figure 6: Averaged SWE series at different elevation bands for each mountain range of the Iberian Peninsula in the hydrological year (from 1 October to 30 September) based on FSM simulations.

From the k-means cluster analysis, four different snow-pack behaviours over Iberian Peninsula were found with different averaged values of elevation (Z), mean snow season duration (Duration), mean maximum SD (Maximum), and maximum SD coefficient of variability (SDCV) (Table 4). These four behaviours can be summarized as:

Cluster 1: No snow is detected.

Cluster 2: Transition mid-mountain areas where insignificant amounts of snow can be found. The slightly higher values of peak SD and Duration in conjunction with a high value of SDCV, suggests that occasional snowfalls can occur.

Cluster 3: Mountain environments with significant amounts of snow most seasons. The SDCV added to the peak SD values suggests that years with shallow snowpacks can occur.

Cluster 4: High mountain environments where greats amount of snow can be found every year. The SDCV is lower than previous clusters, which means that, together with a much higher Maximum SD, we found important amounts of snow lying in these areas in every season.

The cluster groups show geographical consistency along the Iberian Peninsula (Figure 7) but with significant differences in the distribution of P(Snow) values above 1,000 m a.s.l. (Figure 8). Cluster 1 is restricted to the low elevated portions of the most Mediterranean areas, with the exception of the western limits of the Central range Cluster 2 contains most of the areas below 1,000 m a.s.l. of the Iberian Peninsula, with the exception of the Sierra Nevada, where cluster 1 is dominant at the same elevations, and in the southwestern Pyrenees and northeastern Central range. The distribution of cluster 3 shows an evident decline with latitude. The Cantabrian range and the Pyrenees show significant percentages belonging to this cluster (25 and 32% of its area over 1,000 m a.s.l.), at an average elevation lower than other mountain ranges (~1,550 m a.s.l.).

Table 4: Averaged values of elevation, snow probability, maximum SD and CV for each cluster group.

Cluster group	Z m.a.s.l.	Duration (%)	Maximum (m)	SDCV (%)
1	1111	0.1	0.1	162.4
2	1281	21.0	0.2	81.2
3	1667	24.3	1.1	49.7
4	2197	54.1	3.0	35.3

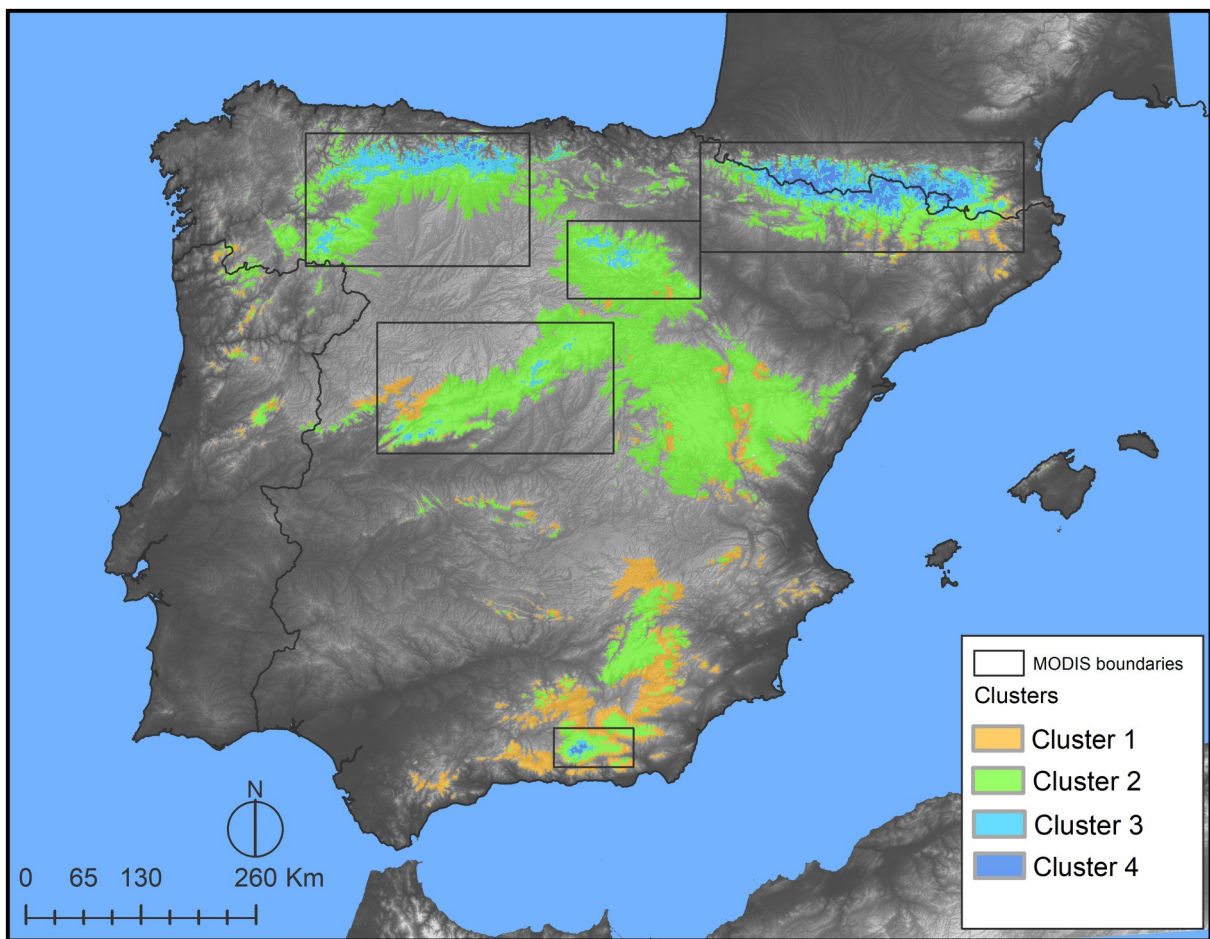


Figure 7: Spatial distribution of cluster groups over 1,000 m a.s.l.

The 4 cluster is found mostly in the highest elevations in the Iberian Peninsula, namely in the Pyrenees and the Sierra Nevada. In the Iberian range, it is not possible to find this cluster at any elevation. In the Central range, it is possible to find it only in small areas at the highest elevations in the southwest (Figure 7). In the Cantabrian range, it is possible to find areas associated with the 4th cluster at the lowest elevation of the Iberian Peninsula. Thus, in the northern areas of the Cantabrian range, it is possible to find cluster 4 from 1,450 m a.s.l. to the maximum elevation (Torre Cerredo peak 2,648 m a.s.l.) (Figure 8). The reason for this small percentage of surface (2.2%) covered by cluster 4 in the Cantabrian range is the hypsography of the range (Figure 1), as the southern part of the range shows a great surface over 1,000 m a.s.l. Cluster 4 is only found at the highest elevations of the Sierra Nevada (above 2,500 m a.s.l.) with little variability in the values of elevation. The Pyrenees show the highest percentage of area associated with cluster 4 (17.27%). This cluster is

found above 1,300 m a.s.l. in the northwestern sectors, increasing to 2,900 m a.s.l. in the southeastern sectors.

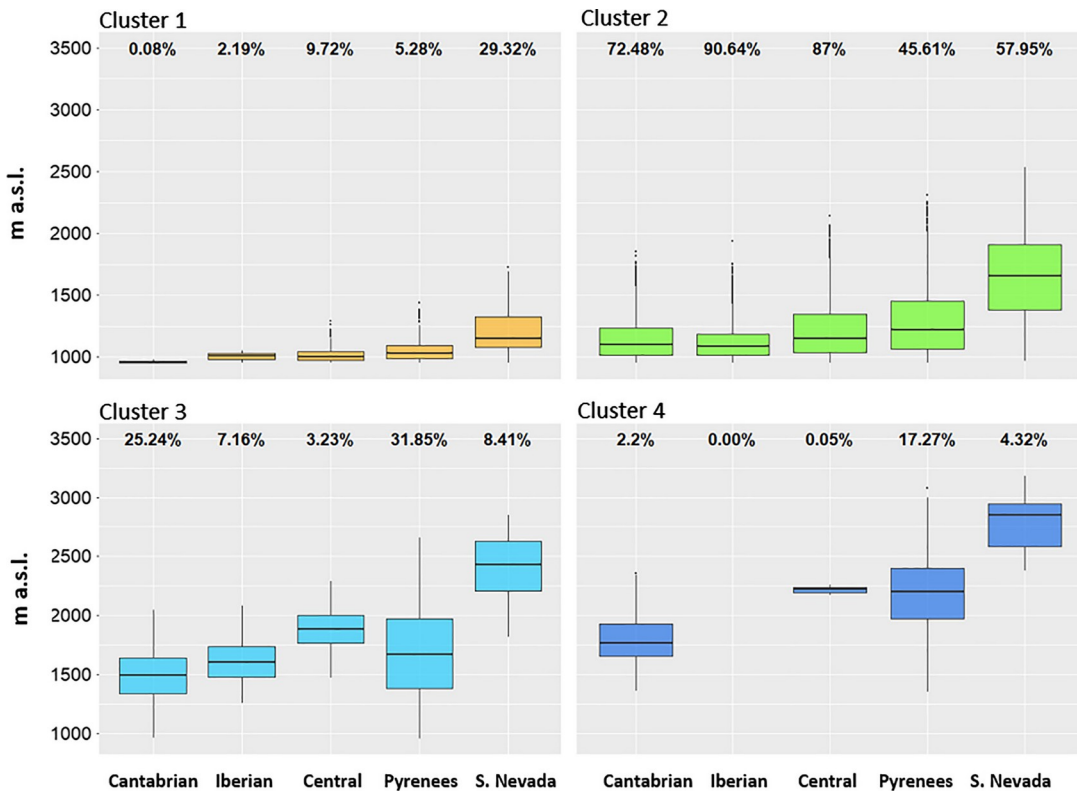


Figure 8: Distribution of elevation values (over 1,000 m a.s.l.) for each mountain range per cluster group. The values at the top of the boxplots show percentage of the surface of the range included in each cluster.

The different distribution of elevation values at each cluster for each mountain range highlights the complexity of snowpack characteristics over Iberia. This distribution is strongly related with latitude but also with other effects as north to south precipitation patterns that have strong implications even in the Central range that is relatively far from the sea (Durán et al., 2013). The Pyrenees shows the highest scatter of elevation values for each cluster group, due to the high spatial variability in the precipitation patterns (Lemus-Canovas et al., 2019), that varies along the longitudinal axe (see Section 4.3). The higher influence of the Atlantic winds in the Cantabrian range (as in the north-western part of the Pyrenees), explains the lower values of elevation at each cluster compared with other mountain ranges (Navarro-Serrano and López-Moreno, 2017). The

Sierra Nevada shows the higher values of elevation for each cluster (Figure 8), likely due to its more southerly latitude.

4.3 Intra-range variability from simulated snow data

The snowpack behaviour inside each mountain range differs over the Iberian Peninsula (Figure 9). The Cantabrian range shows less variability than the Pyrenees but with a noticeable north-to-south gradient, from its northern part with higher P(Snow) values to the southern part with lower P(Snow) values. This gradient is the result of the strong rain shadow effect that occurs in the lee side of this range (south face) (Ortega Villazán and Morales Rodríguez, 2015).

In the Pyrenees, the longitudinal and latitudinal P(Snow) gradients are much larger; despite the existence of a north (higher values) to south (lower values) transition. This is consistent with the results of other analysis in this study, as a consequence of the large climatological differences found in this sector of the Iberian Peninsula (Buisan et al., 2015; Navarro-Serrano and López-Moreno, 2017). The strongest gradient can be found in an oblique line from the southeast, where the snow probability values are much lower, to the northwest, which is affected by the Mediterranean-Atlantic gradient (east to west). There were strong north–south precipitation differences induced by the blocking effect of the range to the very common advections from the north and northwest during winter months (Navarro-Serrano and López-Moreno, 2017).

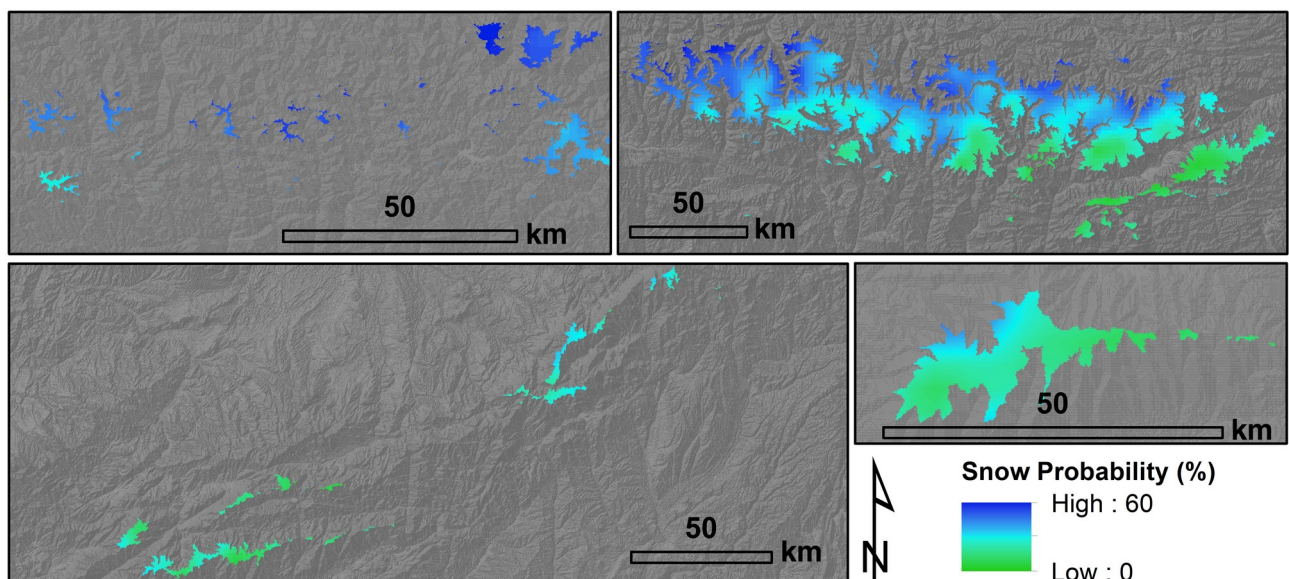


Figure 9: Spatial patterns of mean $P(\text{snow})$ based on FSM simulations for Cantabrian range (a), Pyrenees (b), central range (c) at 2,000 m a.s.l. and for Sierra Nevada (d) at 2500 m a.s.l.

Over the Central range and the Sierra Nevada, the gradients are lower than in the Pyrenees or even the Cantabrian range. The main reason for this is their reduced size and lack of high values of $P_{(Snow)}$. For the Central range, it is possible to find a longitudinal gradient from the northeast, with the highest values in the southwest. The latter is one of the wettest spots in the Iberian Peninsula (García et al., 2017). Despite the reduced size of the Sierra Nevada, $P_{(Snow)}$ values are higher in the northern part of the range due to the precipitation and incoming radiation gradients (Huete-Morales et al., 2018).

4.4 Implications of the presented results

Numerical modelling techniques and remote sensing data have some uncertainties that should be considered for proper interpretation of the presented results. MODIS products have limitations in snow and cloud detection (Wang et al., 2016). Forest existence below the subalpine belts are another source of uncertainty for snow detection (Simic et al., 2003). Furthermore, gap-filling products used here could introduce uncertainties, as the process makes some necessary assumptions and a regression tree in its last step (Gascoin et al., 2015).

The estimation of uncertainty on the distribution of precipitation over complex terrain in numerical mesoatmospheric models as WRF is still an active research topic (i.e., Jing et al., 2017; Gerber et al., 2018). Moreover, the methodology proposed by Alonso-González et al. (2018) makes some assumptions, such as constant temperature lapse-rates, which is a common practice in the distribution of meteorological data (Liston and Elder, 2006). As a consequence of the high computational cost of numerical weather simulations (Gutmann et al., 2016), final resolution of the outputs was not enough to resolve the local particularities of the meteorological variables involved in the energy and mass balance of the snowpack. The subpixel snowpack redistribution due to topographic factors such as slope, curvature or wind sheltering (López-Moreno et al., 2017b) was not considered in this study. The smoothing of the topography can also cause some problems in accurately reproducing interactions between precipitation and terrain complexity due to the constant precipitation along the elevation assumption, as noted by Alonso-González et al. (2018). Despite these uncertainties, the same study illustrates the consistency of the database with in situ observations for both reproducing thickness and duration of the snowpack, but especially for accurately reproducing the temporal (seasonal and interannual) patterns of the snowpack, which gives the data set reliability for developing regional scale studies (Alonso-González et al., 2018).

5 Conclusions

This work has shown the high variability of snowpack characteristics over the different mountain ranges of Iberia. Pyrenees and Cantabrian range store the deepest and long lasting snowpack in the Iberian Peninsula having similar averaged snowpack behaviours. Nevertheless, Pyrenees has the greatest snowpack spatial variability of all the Iberian ranges. This is as a consequence of the high climatological variability induced by the long longitudinal axis and the strong climatological gradients from Atlantic to Mediterranean conditions and north–south slopes. On the contrary Sierra Nevada reveals the shallowest and ephemeral snow-pack, where the accumulation and duration is similar to the Pyrenees and Cantabrian ranges with a downward offset of at least 500 m a.s.l. The Iberian and Central ranges have shown intermediate accumulation and duration patterns but their snowpack tend to be closer to the observed in the Pyrenees and Cantabrian ranges compared to Sierra Nevada. Specifically compared to Cantabrian and Pyrenees, Iberian range shows similar duration values whit lower values of accumulation and Central range shows lower values of accumulation and duration. The differences between mountain ranges cannot be only explained by the latitudinal gradient, other drivers as continentality and precipitation patterns play also an important role.

Acknowledgements. Esteban Alonso-González is granted with a pre-doctoral FPI grant by the Spanish Ministry of Economy and Competitive-ness (BES-2015-071466). This study was funded by the Spanish Ministry of Economy and Competitiveness projects CGL2014-52599-P 10 (“Estudio del manto de nieve en la montaña española y su respuesta a la variabilidad y cambio climatico) and CGL2017-82216-R (HIDROIBERNIEVE). Navarro-Serrano, F. and Sanmiguel-Vallelado, A. are granted with a pre-doctoral FPU grant (Spanish Ministry of Education, Culture and Sports). J. Revuelto benefited from a grant within the above-cited PAPI project and is now supported by a Post-doctoral Fellowship of the AXA research fund (le Post-Doctorant Jesús Revuelto est bénéficiaire d'une bourse postdoctorale du Fonds AXA pour la Recherchem Ref: CNRM 3.2.01/17). All the snow simu-lated and remote sensing data is freely downloadable at <https://zenodo.org/record/854619>.

References

- Alonso-González, E., Ignacio López-Moreno, J., Gascoin, S., García-Valdecasas Ojeda, M., Sanmiguel-Vallelado, A., Navarro-Serrano, F., Revuelto, J., Ceballos, A., Esteban-Parra, M.J. and Essery, R. (2018) Daily gridded datasets of snow depth and snow water equivalent for the Iberian Peninsula from 1980 to 2014. *Earth System Science Data*, 10(1), 303–315. <https://doi.org/10.5194/essd-10-303-2018>.
- Aran M, Rigo T, Bech J, Brucet C, Vilaclara E. (2010) Analysis of the hazardous low-altitude snowfall, 8th March 2010, in Catalonia. 12th Plinius Conference on Mediterranean Storms, held September 1-4, 2010 in Corfu Island, Greece. <http://meetings.copernicus.org/plinius12>, id.Plinius12-77.
- Arndt, D.S., Baringer, M.O. and Johnson, M.R. (2010) State of the Climate in 2009. *Bulletin of the American Meteorological Society*, 91, s1–s222. <https://doi.org/10.1175/BAMS-91-7-StateoftheClimate>.
- Bech, J., Pineda, N., Rigo, T. and Aran, M. (2013) Remote sensing analysis of a Mediterranean thundersnow and low-altitude heavy snowfall event. *Atmospheric Research*, 123, 305–322. <https://doi.org/10.1016/j.atmosres.2012.06.021>.
- Berrisford P, Dee DP, Poli P, Brugge R, Fielding K, Fuentes M, Kallberg PW, Kobayashi S, Uppala S, Simmons A. (2011) The ERA-Interim archive Version 2.0. ERA Report Series. ECMWF: Shinfield Park, Reading, 23.
- Buisan, S.T., Saz, M.A. and López-Moreno, J.I. (2015) Spatial and temporal variability of winter snow and precipitation days in the western and central Spanish Pyrenees. *International Journal of Climatology*, 35(2), 259–274. <https://doi.org/10.1002/joc.3978>.
- Carrera-Gómez, P. and Valcárcel, M. (2018) The geomorphological role of snow since the little ice age in the sierra de Ancares(NW Spain). *Cuadernos de Investigación Geográfica*, 44(1), 171. <https://doi.org/10.18172/cig.3379>.
- Casas-Sainz, A.M. and de Vicente, G. (2009) On the tectonic origin of Iberian topography. *Tectonophysics*, 474(1–2), 214–235. <https://doi.org/10.1016/J.TECTO.2009.01.030>.

Ceballos-Barbancho A, Llorente-Pinto JM, Alonso-González E, López-Moreno JI. (2018) Dinámica del manto de nieve en una pequeña cuenca de montaña mediterránea: el caso del río Tormes (Cuenca del Duero, España). Norte Grande 71.

Charrad, M., Ghazzali, N., Boiteau, V. and Niknafs, A. (2014) NbClust an R package for determining the relevant number of clusters in a data set. *Journal of Statistical Software*, 61(6), 1–36. <https://doi.org/10.18637/jss.v061.i06>.

Chueca Cía, J., Andrés, A.J. and Montañés Magallón, A. (2014) A pro-posal for avalanche susceptibility mapping in the Pyrenees using GIS: the Formigal-Peyreget area (sheet 145-I; scale 1:25.000). *Journal of Maps*, 10(2), 203–210. <https://doi.org/10.1080/17445647.2013.870501>.

Durán, L., Sánchez, E. and Yagüe, C. (2013) Climatology of precipitation over the Iberian central system mountain range. *International Journal of Climatology*, 33(9), 2260–2273. <https://doi.org/10.1002/joc.3602>.

Elsasser, H. and Bürki, R. (2002) Climate change as a threat to tourism in the Alps. *Climate Research*, 20, 253–257. <https://doi.org/10.3354/cr020253>.

Essery, R. (2015) A factorial snowpack model (FSM 1.0). *Geoscientific model development. Geoscientific Model Development*, 8(12), 3867–3876. <https://doi.org/10.5194/gmd-8-3867-2015>.

Fayad, A., Gascoin, S., Faour, G., López-Moreno, J.I., Drapeau, L., Le Page, M. and Escadafal, R. (2017) Snow hydrology in Mediterranean mountain regions: a review. *Journal of Hydrology*, 551, 374–396. <https://doi.org/10.1016/j.jhydrol.2017.05.063>.

García, C., Martí, G., Oller, P., Moner, I., Gavaldà, J., Martínez, P. and Carlos, P.J. (2009) Major avalanches occurrence at regional scale and related atmospheric circulation patterns in the eastern Pyrenees. *Cold Regions Science and Technology*, 59, 106–118.

García, M.M., Martín, J.R., Sánchez Llorente, J.M., Soriano, L.R. and de Pablo Dávila, F. (2017) Intense precipitation events in the central range of the Iberian Peninsula. *Natural Hazards and Earth System Sciences*, 17(12), 2289–2300. <https://doi.org/10.5194/nhess-17-2289-2017>.

García-Hernández, C., Ruiz Fernández, J. and Gallinar, D. (2016) Los efectos de las grandes nevadas históricas sobre la fauna en Asturias, a través de la prensa. In *Avances en Biogeografía. Áreas de distribución: entre puentes y barreras*. Editorial Universidad de Granada, Granada pp. 418–427.

García-Hernández, C., Ruiz-Fernández, J., Sánchez-Posada, C., Pereira, S. and Oliva, M. (2018) An extreme event between the little ice age and the 20th century: the snow avalanche cycle of 1888 in the asturian massif (northern Spain) | un evento extremo entre la pequeña edad de hielo y el siglo xx: El ciclo de avalanchas de 1888 en el macizo asturi. Cuadernos de Investigacion Geografica, 44(1), 187–212. <https://doi.org/10.18172/cig.3386>.

García-Ruiz, J.M., López-Moreno, J.I., Vicente-Serrano, S.M., Lasanta-Martínez, T. and Beguería, S. (2011) Mediterranean water resources in a global change scenario. Earth-Science Reviews, 105(3), 121–139. <https://doi.org/10.1016/j.earscirev.2011.01.006>. García-Valdecasas Ojeda, M., Gámiz-Fortis, S.R., Castro-Díez, Y. and

Esteban-Parra, M.J. (2017) Evaluation of WRF capability to detect dry and wet periods in Spain using drought indices. Journal of Geo-physical Research: Atmospheres, 122(3), 1569–1594. <https://doi.org/10.1002/2016JD025683>.

Garvelmann, J., Pohl, S. and Weiler, M. (2015) Spatio-temporal controls of snowmelt and runoff generation during rain-on-snow events in a mid-latitude mountain catchment. Hydrological Processes, 29 (17), 3649–3664. <https://doi.org/10.1002/hyp.10460>.

Gascoin, S., Hagolle, O., Huc, M., Jarlan, L., Dejoux, J.-F., Szczypta, C., Marti, R. and Sánchez, R. (2015) A snow cover climatology for the Pyrenees from MODIS snow products. Hydrology and Earth System Sciences, 19(5), 2337–2351. <https://doi.org/10.5194/hess-19-2337-2015>.

Gerber, F., Besic, N., Sharma, V., Mott, R., Daniels, M., Gabella, M., Berne, A., Germann, U. and Lehning, M. (2018) Spatial variability in snow precipitation and accumulation in COSMO–WRF simulations and radar estimations over complex terrain. The Cryosphere, 12, 3137–3160. <https://doi.org/10.5194/tc-12-3137-2018>.

Gilaberte-Búrdalo, M., López-Martín, F., Pino-Otín, M.R. and López-Moreno, J.I. (2014) Impacts of climate change on ski industry. Environmental Science & Policy, 44, 51–61. <https://doi.org/10.1016/j.envsci.2014.07.003>.

Gilaberte-Búrdalo, M., López-Moreno, J.I., Morán-Tejeda, E., Jerez, S., Alonso-González, E., López-Martín, F. and Pino-Otín, M. R. (2017) Assessment of ski condition reliability in the Spanish and Andorran Pyrenees for the second half of the 20th century. Applied Geography, 79, 127–142. <https://doi.org/10.1016/j.apgeog.2016.12.013>.

González Trueba, J.J. and Serrano, E. (2010) La nieve en los Picos de Europa: implicaciones geomorfológicas y ambientales. Cuadernos de investigación geográfica, ISSN 0211–6820, 36(2), 61–84.

Grünewald, T., Bühler, Y. and Lehning, M. (2014) Elevation dependency of mountain snow depth. The Cryosphere, 8(6), 2381–2394. <https://doi.org/10.5194/tc-8-2381-2014>.

Gutmann, E., Barstad, I., Clark, M., Arnold, J. and Rasmussen, R. (2016) The intermediate complexity atmospheric research model (ICAR). Journal of Hydrometeorology, 17(3), 957–973. <https://doi.org/10.1175/JHM-D-15-0155.1>.

Hall, K.D., Riggs, G.A. and Salomonson, V.V. (2006) MODIS/Terra Snow Cover Daily L3 Global 500m Grid V005. National Snow and Ice Data Center. Boulder, Colorado: Digital Media.

Harder, P. and Pomeroy, J. (2013) Estimating precipitation phase using a psychrometric energy balance method. Hydrological Processes, 27(13), 1901–1914. <https://doi.org/10.1002/hyp.9799>.

Hartigan, J.A. and Wong, M.A. (1979) Algorithm AS 136: a K-means clustering algorithm. Applied Statistics, 28(1), 100. <https://doi.org/10.2307/2346830>.

Herrero, J., Polo, M.J. and Losada, M.A. (2011) Snow evolution in Sierra Nevada (Spain) from an energy balance model validated with Landsat TM data. In Proceedings of SPIE 8174, Remote Sensing for Agriculture, Ecosystems, and Hydrology XIII, 06 October 2011. Prague, Czech Republic: SPIE Remote Sensing, pp. 817403– 817403. <https://doi.org/10.1117/12.898270>.

Höller, P. (2007) Avalanche hazards and mitigation in Austria: a review. Natural Hazards, 43(1), 81–101. <https://doi.org/10.1007/s11069-007-9109-2>.

Huete-Morales, M.D., Quesada-Rubio, J.-M., Rosales-Moreno, M.-J., Navarrete-Alvarez, E. and Del-Moral-Avila, M.-J. (2018) Environmental differences between two neighboring regions of southern Spain. Polish Journal of Environmental Studies, 27(5), 2071–2080. <https://doi.org/10.1524/pjoes.78625>.

Izimomon, M.G., Mayer, H. and Matzarakis, A. (2003) Downward atmospheric longwave irradiance under clear and cloudy skies: measurement and parameterization. Journal of Atmospheric and Solar-Terrestrial Physics, 65, 1107–1116. <https://doi.org/10.1016/j.jastp.2003.07.007>.

Jing, X., Geerts, B., Wang, Y. and Liu, C. (2017) Evaluating seasonal orographic precipitation in the interior Western United States using gauge data, gridded precipitation estimates, and a regional

climate simulation. *Journal of Hydrometeorology*, 18(9), 2541–2558. <https://doi.org/10.1175/JHM-D-17-0056.1>.

Jones, H.G. (1999) The ecology of snow-covered systems: a brief over-view of nutrient cycling and life in the cold. *Hydrological Pro-cesses*, 13(14–15), 2135–2147. [https://doi.org/10.1002/\(SICI\)1099-1085\(199910\)13:14/15<2135::AID-HYP862>3.0.CO;2-Y](https://doi.org/10.1002/(SICI)1099-1085(199910)13:14/15<2135::AID-HYP862>3.0.CO;2-Y).

Lemus-Canovas, M., Lopez-Bustins, J.A., Trapero, L. and Martin-Vide, J. (2019) Combining circulation weather types and daily pre-cipitation modelling to derive climatic precipitation regions in the Pyrenees. *Atmospheric Research*, 220, 181–193. <https://doi.org/10.1016/J.ATMOSRES.2019.01.018>.

Liston, G.E. and Elder, K. (2006) A meteorological distribution system for high-resolution terrestrial modeling (MicroMet). *Journal of Hydrometeorology*, 7(2), 217–234. <https://doi.org/10.1175/JHM 486.1>.

López, R. and Justribó, C. (2010) The hydrological significance of mountains in the Ebro River basin. *Hydrological Sciences Journal*, 55(2), 223–233. <https://doi.org/10.1080/02626660903546126>.

Lopez-Bustins, J.-A., Martin-Vide, J. and Sanchez-Lorenzo, A. (2008) Iberia winter rainfall trends based upon changes in teleconnection and circulation patterns. *Global and Planetary Change*, 63(2–3), 171–176. <https://doi.org/10.1016/J.GLOPLACHA.2007.09.002>.

López-Moreno, J.I., Fassnacht, S.R., Beguería, S. and Latron, J.B.P. (2011a) Variability of snow depth at the plot scale: implications for mean depth estimation and sampling strategies. *The Cryosphere*, 5(3), 617–629. <https://doi.org/10.5194/tc-5-617-2011>.

López-Moreno, J.I., Fassnacht, S.R., Heath, J.T., Musselman, K.N., Revuelto, J., Latron, J., Morán-Tejeda, E. and Jonas, T. (2013) Small scale spatial variability of snow density and depth over complex alpine terrain: implications for estimating snow water equiva-lent. *Advances in Water Resources*, 55, 40–52. <https://doi.org/10.1016/J.ADVWATRES.2012.08.010>.

López-Moreno, J.I., Gascoin, S., Herrero, J., Sproles, E.A., Pons, M., Alonso-González, E., Hanich, L., Boudhar, A., Musselman, K.N., Molotch, N.P., Sickman, J. and Pomeroy, J. (2017a) Different sen-sitivities of snowpacks to warming in Mediterranean climate moun-tain areas. *Environmental Research Letters*, 12(7), 074006. <https://doi.org/10.1088/1748-9326/aa70cb>.

López-Moreno, J.I., Goyette, S. and Beniston, M. (2009) Impact of climate change on snowpack in the Pyrenees: horizontal spatial variability and vertical gradients. *Journal of Hydrology*, 374(3), 384–396. <https://doi.org/10.1016/j.jhydrol.2009.06.049>.

López-Moreno, J.I. and Nogués-Bravo, D. (2005) A generalized additive model for the spatial distribution of snowpack in the Spanish Pyrenees. *Hydrological Processes*, 19(16), 3167–3176. <https://doi.org/10.1002/hyp.5840>.

López-Moreno, J.I., Revuelto, J., Alonso-González, E., Sanmiguel-Vallelado, A., Fassnacht, S.R., Deems, J. and Morán-Tejeda, E. (2017b) Using very long-range terrestrial laser scanner to analyze the temporal consistency of the snowpack distribution in a high mountain environment. *Journal of Mountain Science*, 14(5), 823–842. <https://doi.org/10.1007/s11629-016-4086-0>.

López-Moreno, J.I., Revuelto, J., Fassnacht, S.R., Azorín-Molina, C., Vicente-Serrano, S.M., Morán-Tejeda, E. and Sexstone, G.A. (2015) Snowpack variability across various spatio-temporal resolutions. *Hydrological Processes*, 29(6), 1213–1224. <https://doi.org/10.1002/hyp.10245>.

López-Moreno, J.I., Vicente-Serrano, S.M., Morán-Tejeda, E., Lorenzo-Lacruz, J., Kenawy, A. and Beniston, M. (2011c) Effects of the North Atlantic oscillation (NAO) on combined temperature and precipitation winter modes in the Mediterranean mountains: observed relationships and projections for the 21st century. *Global and Planetary Change*, 77(1–2), 62–76. <https://doi.org/10.1016/j.gloplacha.2011.03.003>.

Lund, M., Stiegler, C., Abermann, J., Citterio, M., Hansen, B.U. and van As, D. (2017) Spatiotemporal variability in surface energy balance across tundra, snow and ice in Greenland. *Ambio*, 46(S1), 81–93. <https://doi.org/10.1007/s13280-016-0867-5>.

Merino, A., Fernández, S., Hermida, L., López, L., Sánchez, J.L., García-Ortega, E. and Gascón, E. (2014) Snowfall in the Northwest Iberian Peninsula: synoptic circulation patterns and their influence on snow day trends. *The Scientific World Journal*, 2014, 1–14. <https://doi.org/10.1155/2014/480275>.

Mora, J.A.N., Martín, J.R., García, M.M., de Pablo Davila, F. and Rivas Soriano, L. (2016) Climatological characteristics and synoptic patterns of snowfall episodes in the central Spanish Mediterranean area. *International Journal of Climatology*, 36(14), 4488–4496. <https://doi.org/10.1002/joc.4645>.

Morán-Tejeda, E., Lorenzo-Lacruz, J., López-Moreno, J.I., Rahman, K. and Beniston, M. (2014) Streamflow timing of mountain rivers in Spain: recent changes and future projections. *Journal of Hydrology*, 517, 1114–1127. <https://doi.org/10.1016/j.jhydrol.2014.06.053>.

Navarro-Serrano, F. and López-Moreno, J.I. (2017) Spatio-temporal analysis of snowfall events in the Spanish pyrenees and their relationship to atmospheric circulation | Análisis espacio-temporal de los eventos de nevadas en el pirineo Español y su relación con la circulación atmosférica. *Cuadernos de Investigacion Geografica*, 43(1), 233–254. <https://doi.org/10.18172/cig.3042>.

Navarro-Serrano, F., López-Moreno, J.I., Azorin-Molina, C., Alonso-González, E., Tomás-Burguera, M., Sanmiguel-Vallelado, A., Revuelto, J. and Vicente-Serrano, S.M. (2018) Estimation of near-surface air temperature lapse rates over continental Spain and its mountain areas. *International Journal of Climatology*, 38, 3233–3249. <https://doi.org/10.1002/joc.5497>.

Ortega Villazán, M.T. and Morales Rodríguez, C.G. (2015) El clima de la Cordillera Cantábrica castellano-leonesa: diversidad, contrastes y cambios. *Investigaciones Geográficas*, 0(63), 45–67. <https://doi.org/10.14198/INGEO2015.63.04>.

Palacios, D., de Andrés, N. and Luengo, E. (2003) Distribution and effectiveness of nivation in Mediterranean mountains: Peñalara (Spain). *Geomorphology*, 54(3–4), 157–178. [https://doi.org/10.1016/S0169-555X\(02\)00340-9](https://doi.org/10.1016/S0169-555X(02)00340-9).

Pfeifer, C., Höller, P. and Zeileis, A. (2018) Spatial and temporal analysis of fatal off-piste and backcountry avalanche accidents in Austria with a comparison of results in Switzerland, France, Italy and the US. *Natural Hazards and Earth System Sciences*, 185194, 571–582. <https://doi.org/10.5194/nhess-18-571-2018>.

Quéno, L., Vionnet, V., Dombrowski-Etchevers, I., Lafaysse, M., Dumont, M. and Karbou, F. (2016) Snowpack modelling in the Pyrenees driven by kilometric-resolution meteorological forecasts. *The Cryosphere*, 10(4), 1571–1589. <https://doi.org/10.5194/tc-10-1571-2016>.

Revuelto, J., Azorin-Molina, C., Alonso-González, E., Sanmiguel-Vallelado, A., Navarro-Serrano, F., Rico, I. and Ignacio López-Moreno, J. (2017) Meteorological and snow distribution data in the Izas experimental catchment (Spanish Pyrenees) from 2011 to 2017. *Earth System Science Data*, 9(2), 993–1005. <https://doi.org/10.5194/essd-9-993-2017>.

Reuelto, J., Lecourt, G., Lafaysse, M., Zin, I., Charrois, L., Vionnet, V., Dumont, M., Rabatel, A., Six, D., Condom, T., Morin, S., Viani, A. and Sirguey, P. (2018) Multi-criteria evaluation of

snowpack simulations in complex alpine terrain using satel-lite and in situ observations. *Remote Sensing*, 10(8), 1171. <https://doi.org/10.3390/rs10081171>.

Revuelto, J., López-Moreno, J.I., Azorin-Molina, C. and Vicente-Serrano, S.M. (2014) Topographic control of snowpack distribution in a small catchment in the central Spanish Pyrenees: intra- and inter-annual persistence. *Copernicus*, 8(5), 1989–2006. <https://doi.org/10.5194/tc-8-1989-2014>.

Sanmiguel-Vallelado, A., Morán-Tejeda, E., Alonso-González, E. and López-Moreno, J.I. (2017) Effect of snow on mountain river regimes: an example from the Pyrenees. *Frontiers of earth Science*, 11, 515–530. <https://doi.org/10.1007/s11707-016-0630-z>.

Serrano Cañas, E., Gómez Lende, M. and Pisabarro Pérez, A. (2016) Nieve y riesgo de aludes en la montaña cantábrica: el alud de car-daño de arriba, alto carrión (Palencia). *Polígonos. Revista de Geografía*, 0(28), 239. <https://doi.org/10.18002/pol.v0i28.4295>.

Simic A, Fernandes R, Brown R, Romanov P, Park W, Hall DK. (2003) Validation of MODIS, VEGETATION, and GOES+SSM/I snow cover products over Canada based on surface snow depth observations. *IGARSS 2003. 2003 IEEE International Geoscience and Remote Sensing Symposium. Proceedings (IEEE Cat. No.03CH37477)*. IEEE, 836–838. <https://doi.org/10.1109/IGARSS.2003.1293936>.

Skamarock WC, Klemp JB, Dudhia J, Gill DO, Barker DM, Dudha MG, Huang X, Wang W, Powers Y. (2008) A Description of the Advanced Research WRF Version 3. NCAR Technical Note NCAR/TN-475+STR. <https://doi.org/10.5065/D68S4MVH>.

Slatyer, R.A., Nash, M.A. and Hoffmann, A.A. (2017) Measuring the effects of reduced snow cover on Australia's alpine arthropods. *Austral Ecology*, 42(7), 844–857. <https://doi.org/10.1111/aec.12507>.

Soteres García, R.L., Pedraza Gilsanz, J. and Carrasco González, R.M. (2016) Cartografía de susceptibilidad y estimación del máximo alcance de aludes en el circo de gredos (sistema central ibérico). *Polígonos. Revista de Geografía*, 0(28), 265. <https://doi.org/10.18002/pol.v0i28.4296>.

Stethem, C., Jamieson, B., Schaerer, P., Liverman, D., Germain, D. and Walker, S. (2003) Snow avalanche Hazard in Canada – a review. *Natural Hazards*, 28(2/3), 487–515. <https://doi.org/10.1023/A:1022998512227>.

van Pelt, W.J.J., Kohler, J., Liston, G.E., Hagen, J.O., Luks, B., Reijmer, C.H. and Pohjola, V.A. (2016) Multidecadal climate and seasonal snow conditions in Svalbard. *Journal of Geophysical Research: Earth Surface*, 121(11), 2100–2117. <https://doi.org/10.1002/2016JF003999>.

Vicente-Serrano, S.M., Lopez-Moreno, J.-I., Beguería, S., Lorenzo-Lacruz, J., Sanchez-Lorenzo, A., García-Ruiz, J.M., Azorin-Molina, C., Morán-Tejeda, E., Revuelto, J., Trigo, R., Coelho, F. and Espejo, F. (2014) Evidence of increasing drought severity caused by temperature rise in southern Europe. *Environmental Research Letters*, 9(4), 044001. <https://doi.org/10.1088/1748-9326/9/4/044001>.

Viviroli, D., Archer, D.R., Buytaert, W., Fowler, H.J., Greenwood, G. B., Hamlet, A.F., Huang, Y., Koboltschnig, G., Litaor, M.I., López-Moreno, J.I., Lorentz, S., Schädler, B., Schreier, H., Schwaiger, K., Vuille, M. and Woods, R. (2011) Climate change and mountain water resources: overview and recommendations for research, management and policy. *Hydrology and Earth System Sciences*, 15(2), 471–504. <https://doi.org/10.5194/hess-15-471-2011>.

Viviroli, D., Dürr, H.H., Messerli, B., Meybeck, M. and Weingartner, R. (2007) Mountains of the world, water towers for humanity: typology, mapping, and global significance. *Water Resources Research*, 43(7), W07447. <https://doi.org/10.1029/2006WR005653>.

Wang, T., Fetzer, E.J., Wong, S., Kahn, B.H. and Yue, Q. (2016) Validation of MODIS cloud mask and multilayer flag using CloudSat-CALIPSO cloud profiles and a cross-reference of their cloud classifications. *Journal of Geophysical Research: Atmospheres*, 121(19), 11,620–11,635. <https://doi.org/10.1002/2016JD025239>.

Wrzesien, M.L., Durand, M.T., Pavelsky, T.M., Howat, I.M., Margulis, S.A., Huning, L.S., Wrzesien, M.L., Durand, M.T., Pavelsky, T.M., Howat, I.M., Margulis, S.A. and Huning, L.S. (2017) Comparison of methods to estimate snow water equivalent at the mountain range scale: a case study of the California Sierra Nevada. *Journal of Hydrometeorology*, 18(4), 1101–1119. <https://doi.org/10.1175/JHM-D-16-0246.1>.

Wrzesien, M.L., Durand, M.T., Pavelsky, T.M., Kapnick, S.B., Zhang, Y., Guo, J. and Shum, C.K. (2018) A new estimate of north American Mountain snow accumulation from regional climate model simulations. *Geophysical Research Letters*, 45(3), 1423–1432. <https://doi.org/10.1002/2017GL076664>.

Wu, X., Shen, Y., Wang, N., Pan, X., Zhang, W., He, J. and Wang, G. (2016) Coupling the WRF model with a temperature index model based on remote sensing for snowmelt simulations in a river basin in the Altay Mountains, north-West China. *Hydrological Processes*, 30(21), 3967–3977. <https://doi.org/10.1002/hyp.10924>.

Würzer, S. and Jonas, T. (2018) Spatio-temporal aspects of snowpack runoff formation during rain on snow. *Hydrological Processes*, 32 (23), 3434–3445. <https://doi.org/10.1002/hyp.13240>.

Capítulo 4: Impacto de la Oscilación del Atlántico Norte en el manto de nieve de las montañas de la Península Ibérica

Resumen: La Oscilación del Atlántico Norte (NAO) es considerada el principal factor atmosférico que explica el clima invernal y la evolución de la nieve en gran parte del hemisferio norte. Sin embargo, la ausencia series largas del manto de nieve en las regiones montañosas de la península Ibérica ha impedido una evaluación completa del impacto de la NAO a escala regional en esta zona. En este estudio, evaluamos la relación entre la NAO de los meses de invierno (DJFM-NAO) y el manto de nieve de la Península Ibérica. Para ello, hemos simulado la temperatura, precipitación y nieve para el período 1979-2014 mediante reducción dinámica de la resolución de los datos del reanálisis ERA-Interim, correlacionando nuestras simulaciones con el índice DJFM-NAO en las cinco principales cadenas montañosas de la Península Ibérica (Cordillera Cantábrica, Sistema Central, Sistema Ibérico, Pirineos y Sierra Nevada). Los resultados confirmaron que los valores negativos del DJFM-NAO generalmente ocurren durante condiciones húmedas y templadas en la mayor parte de la Península Ibérica. Debido a la dirección de las masas de aire húmedo inducidas por las fases negativas de la NAO, esta tiene una gran influencia en la duración de la nieve y en el máximo anual de SWE en la mayoría de las cordilleras del estudio, sobre todo en las laderas al sur del eje principal de las cordilleras. En cambio, el impacto de la variabilidad de la NAO es limitado en las laderas orientadas al norte. Los valores negativos (positivos) de DJFM-NAO se asociaron a una duración más larga (más corta) y a picos más altos (más bajos) de SWE en todas las montañas analizadas en el estudio. Encontramos una marcada variabilidad en las correlaciones del índice DJFM-NAO con los índices de nieve dentro de cada cadena montañosa, incluso cuando sólo se consideraron las laderas orientadas al sur. Las correlaciones encontradas fueron más elevadas en las mayores elevaciones de las cordilleras, pero la longitud geográfica también explicaba la variabilidad dentro de las cordilleras en la mayoría de las montañas estudiadas.

Cita completa:

Alonso-González, E.; López-Moreno, J.I.; Navarro-Serrano, F.M.; Revuelto, J. Impact of North Atlantic Oscillation on the Snowpack in Iberian Peninsula Mountains. *Water* **2020**, *12*(1), 105; <https://doi.org/10.3390/w12010105>

Impact of North Atlantic Oscillation on the Snowpack in Iberian Peninsula Mountains

Esteban Alonso-González , Juan I. López-Moreno, Francisco M. Navarro-Serrano and Jesús Revuelto

Instituto Pirenaico de Ecología, CSIC. Campus de Aula Dei, Av. Montaña 1005, 50059 Zaragoza,

Correspondence: Esteban Alonso-González (e.alonso@ipe.csic.com)

Received: 11 November 2019

Accepted: 20 December 2019

Abstract: The North Atlantic Oscillation (NAO) is considered to be the main atmospheric factor explaining the winter climate and snow evolution over much of the Northern Hemisphere. However, the absence of long-term snow data in mountain regions has prevented full assessment of the impact of the NAO at the regional scales, where data are limited. In this study, we assessed the relationship between the NAO of the winter months (DJFM-NAO) and the snowpack of the Iberian Peninsula. We simulated temperature, precipitation, and snow data for the period 1979–2014 by dynamic downscaling of ERA-Interim reanalysis data, and correlated this with the DJFM-NAO for the five main mountain ranges of the Iberian Peninsula (Cantabrian Range, Central Range, Iberian Range, the Pyrenees, and the Sierra Nevada). The results confirmed that negative DJFM-NAO values generally occur during wet and mild conditions over most of the Iberian Peninsula. Due to the direction of the wet air masses, the NAO has a large influence on snow duration and the annual peak snow water equivalent (peak SWE) in most of the mountain ranges in the study, mostly on the slopes south of the main axis of the ranges. In contrast, the impact of NAO variability is limited on north-facing slopes. Negative (positive) DJFM-NAO values were associated with longer (shorter) duration and higher (lower) peak SWEs in all mountains analyzed in the study. We found marked variability in correlations of the DJFM-NAO with snow indices within each mountain range, even when only the south-facing slopes were considered. The correlations were stronger for higher elevations in the mountain ranges, but geographical longitude also explained the intrarange variability in the majority of the studied mountains.

1. Introduction

The North Atlantic Oscillation (NAO) is a mode of atmospheric circulation, and its index value is calculated as the difference in atmospheric pressure for the dipole centered on Iceland and the Azores Islands (Hurrell, 1995). The NAO is considered to be the main pattern of climate variability in the Northern Hemisphere (Hurrell and Deser, 2010; Kjellström, 2016), especially during winter. Negative (positive) NAO phases generally are related to weak (strong) westerly winds to Europe, leading to positive (negative) anomalies of temperature and precipitation in Southern (Northern) Europe (Sánchez-López et al., 2015; Trigo et al., 2002; Wanner et al., 2001). It is also clear that NAO anomalies are more related with the winter precipitation variability than with the interannual winter temperature fluctuations (Durán et al., 2015; J. I. López-Moreno et al., 2011).

As NAO fluctuations are related with the winter temperature and precipitation over much of the Northern Hemisphere, it is unsurprising that many studies have reported that the NAO is a good indicator of the duration and depth of the snowpack. This is the case for Mediterranean mountains (J. I. López-Moreno et al., 2011), the Pyrenees (López-Moreno and Vicente-Serrano, 2007; Revuelto et al., 2013), the Alps (Beniston, 1997; Scherrer and Appenzeller, 2006; Schöner et al., 2019), Nordland (Theakstone, 2013), Western Poland (Bednorz, 2002), Bulgaria (Brown and Petkova, 2007), and the Russian Arctic (Bednorz and Wibig, 2016). At wider spatial scales, Henderson and Leathers (2010) associated negative (positive) phases of the NAO with expansion (reduction) of the snow cover in Europe. Keylock 2003, Jomelli et al. (2007) and García et al. (2009) also found significant relationships between NAO phases and the frequency of avalanches in Iceland, the French Alps, and the Pyrenees, respectively. The main value of understanding the relationship between snow and interannual fluctuations of the snowpack is that, despite the stochastic nature of the NAO, the statistic and dynamic seasonal forecasting of this phenomenon has been very promising, to the point of achieving useful levels of predictability (Cohen and Fletcher, 2007; Scaife et al., 2014; Wang et al., 2017). Improving predictions of snowpack anomalies has a clear applied importance because of the direct impact of the snowpack on water availability, plant and animal phenology, and a wide range of economic activities in mountain and downstream areas (Beniston, 2003; Fayad et al., 2017). In addition, a good understanding of the relationship between the NAO and the snowpack is necessary to accurately interpret the reported trends in the snowpack over recent decades, as a strong correlation has been observed between trends in the snowpack and the duration of dominant NAO anomalies (Buisan et al., 2016).

Although studies have provided clear insights into how the NAO is related with the snowpack in many mountains and cold regions of Europe, at the local scale, many uncertainties about its effects remain. This is because mountain ranges present a topographical barrier to main wind flows, causing shadow effects in the main atmospheric circulation patterns(Navarro-Serrano and López-Moreno, 2017; Riaz et al., 2017). In addition, elevation also affects the impact relationship of NAO with snow in mountain areas because of its greater relationship with precipitation relative to temperature. Thus, at high elevations, interannual variability of the snowpack is mainly driven by precipitation, so such areas are expected to exhibit a stronger response to the NAO than lower elevation sites, where temperature has a major role in snow variability (Morán-Tejeda et al., 2013). López-Moreno and Vicente-Serrano (López-Moreno and Vicente-Serrano, 2007) suggested that this phenomenon is the main explanation for the control of NAO on the snowpack in areas above 2000 m a.s.l. in the Spanish Pyrenees. The spatial variability in the relationship between the NAO and snow cover makes it difficult to assess NAO effects in many areas, because of the limited data on snowpacks, especially in mountain areas at the highest elevations.

The aim of this study is to extend knowledge of the NAO and snowpack relationship in the main mountainous regions of the Iberian Peninsula. This is one of the highest elevation regions of Europe, where the accumulation of snow is of major importance to water resource availability (Lorenzo-Lacruz et al., 2011; Morán-Tejeda et al., 2014), and on which many economically important activities, including agriculture, forestry, and winter tourism, depend (Gilaberte-Búrdalo et al., 2014; López-Moreno et al., 2008). Because of the limited data on snowpacks in the Iberian Peninsula, we used a recently developed database on snow water equivalent (SWE) and snow depth (SD) for the main mountain areas of the Iberian Peninsula (Alonso-González et al., 2018), to enable us to undertake the first detailed assessment of the relationship between the winter (December, January, February, and March) NAO (DJFM-NAO) on the interannual variability in the peak SWE and the duration of snow on the ground.

2. Study Area

The Iberian Peninsula is located at the southwest edge of Europe, between latitudes 36 N and 44 N. It is an area of contrasting climate, as a consequence of Atlantic and Mediterranean influences. The topography is characterized by two main plateaus surrounded by mountainous areas and comprises five main mountain ranges that have seasonal snow cover, including the Cantabrian Range, the Central Range, the Iberian Range, the Pyrenees, and the Sierra Nevada. The highest elevation (3478

m a.s.l.) is Mulhacén Peak in the Sierra Nevada, followed by Aneto Peak in the Pyrenees (3404 m a.s.l.). The other mountainranges exceed 2000 m a.s.l., reaching 2648 m a.s.l. (Torrecerredo Peak) in the Cantabrian Range, 2596 m a.s.l. (Almanzor Peak) in the Central Range, and 2314 m a.s.l. in the Iberian Range.

The spatial distribution of these mountain ranges (Figure 1), which extend within Spain from west to east at different latitudes and distances to the sea, results in wide snowpack variability at similar elevations, even within the same mountain range (Alonso-González et al., 2020)



Figure 1: Geographical locations of the main mountain ranges of the Iberian Peninsula.

3. Methods

3.1. NAO Index and Temperature and Precipitation Patterns

The NAO index, which is defined as the normalized sea surface pressure (SLP) difference between the Icelandic low pressure and the Azores high pressure regions (Hurrell, 1995), is a widely used indicator of the atmospheric situation over the North Atlantic. In this study the NAO index was calculated from the SLP difference between the positions 65° N 20° W (near Reykjavik, Iceland) and 35° N 5° W (near Gibraltar Straight), following the procedure and recommendations of Osborn et al. (1999), Trigo et al. (2005) and Fernández-González et al. (2012) among others. The SLP data were downloaded from the NCAR SLP reanalysis dataset (<https://climatedataguide.ucar.edu/climate-data/ncar-sea-level-pressure>; last accessed 20 October 2019). The normalization was performed in relation to normal values for the study period 1979–2015.

The accumulated winter precipitation and the minimum and maximum averaged daily temperatures were linearly correlated with the DJFM-NAO index. The temperature and precipitation meteorological variables were obtained from the regional atmospheric simulation described below. In this study the winter period was considered to encompass the months December, January, February, and March.

3.2. Snowpack Database and Statistical Analysis

The SWE and SD database used in this study was developed using the weather research and forecast (WRF) model (Skamarock et al., 2008), forced using the ERA-Interim reanalysis (Berrisford et al., 2009; Dee et al., 2011). The spatial resolution of the atmospheric simulations was ~10 km, and the simulations covered the period 1979–2014 (García-Valdecasas Ojeda et al., 2017). The surface meteorological outputs of the simulations were subsequently projected to various elevation bands that differed by 100 m, using an array of psychrometric and radiative formulae and lapse rates (Alonso-González et al., 2018). The new meteorological data were used as forcing data for the physically based energy and mass balance snowpack factorial snow model (FSM) (Essery, 2015). The final product was a semi-distributed daily SWE and SD database. Alonso-González et al. (Alonso-González et al., 2018) validated the database, using in situ observations and remote

sensing information, and were able to reproduce the spatial and temporal patterns of the snowpack over the entire Iberian Peninsula.

We computed the annual peak SWE and the annual snowpack duration for each elevation band from the snowpack database. These values were linearly correlated with the averaged DJFM-NAO, along with the Pearson's R value. To identify different responses of the snowpack on the windward and leeward sides of each mountain range, we separated the correlation values for each mountain range along the principal longitudinal axis, which runs generally from west to east. The Wilcoxon–Mann–Whitney test (Salkind, 2012) was used to identify statistical differences between the groupings of north- and south-facing slopes.

Following calculation of the Pearson's R values between the DJFM-NAO and the snow indices, we correlated the value with the elevation and geographical longitude, to investigate the spatial patterns of DJFM-NAO influence on the snowpack within each mountain range.

Finally, to highlight the spatial patterns of the correlation between the DJFM-NAO and the snow indices, 500 random samples of 100 values of the Pearson's R values were calculated. We performed partial correlations between snow indices and longitude (removing the effect of the elevation), and elevation (removing the effect of the longitude). This recursive resampling of the dataset was performed to avoid using excessively big samples, which can lead to overestimation of statistically significant correlations and has associated problems caused by spatial autocorrelation (Koenig, 1999; Revuelto et al., 2014).

4. Results and Discussion

4.1. Relationship between the DJFM-NAO and Temperature and Precipitation

Except for small areas on the Mediterranean coast, most of the Iberian Peninsula showed positive correlations between the NAO and the maximum temperature (Figure 2), being consistent with previous studies in the Mediterranean mountain ranges (Juan I. López-Moreno et al., 2011). A clear difference was evident between the north- and south-facing slopes along the main longitudinal axis of the mountain ranges, including in the Central Range (north approximately 0.5, south approximately 0.8) and Cantabrian Range (north approximately 0.4, south approximately 0.8). This result is consistent with previous studies based on meteorological observations (Sáenz et al., 2001),

and can be explained by the Foehn effect on the northern slopes during negative NAO phases (Lorente-Plazas et al., 2015). This phenomenon is very common in the Cantabrian and Pyrenean ranges during DJFM-NAO negative phases.

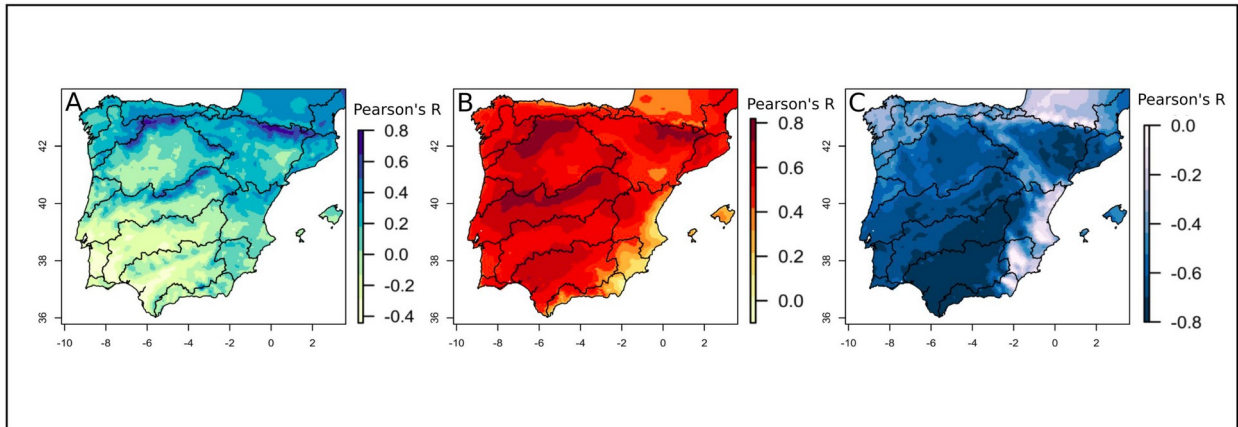


Figure 2: Pearson's R values between the DJFM-NAO and minimum temperatures(A), maximum temperatures (B), and precipitation (C). The lines represent the boundaries of the main catchments in the Iberian Peninsula

4.2. Relationship between the Winter NAO and Temperature and Precipitation

High elevation areas generally showed strong positive correlations, which we attribute to the fact that mountain climates are strongly related to the movement of air masses (Stefanicki et al., 1998). Thus, during positive NAO phases, the maximum air temperature on the slopes and summits increase, and during negative NAO phases, the lapse rates increase and the summits cool, although the existence of southern fluxes (Navarro-Serrano and López-Moreno, 2017).

The correlations between the DJFM-NAO and minimum temperatures tended to be positive, but showed a progressive decrease towards the southwest and lower areas of the main hydrological basins. In the valley bottoms the correlations became negative, as reported by del Río et al. (2007) for the Duero basin. This progressive change is because of the increased cloudiness during negative NAO phases in this Atlantic southwest area, related to the associated southern and western cyclonic flows. The cloudiness slows the nighttime reduction in the air temperature (Esteban-Parra et al., 2003), but this effect does not penetrate fully inland to the north, making the signal less obvious.

The DJFM-NAO and temperature were generally positively correlated. During negative DJFM-NAO phases the occurrence of more frequent cyclonic circulations brings lower temperatures than during anticyclonic periods, but the most frequent wind directions during negative DJFM-NAO phases has a clear Atlantic influence, which generally brings mild temperatures during snowfall events. This causes a marked increase of the elevation where precipitation changes from liquid to solid phase compared to other synoptic situations over Iberia (López-Moreno, 2005; Navarro-Serrano and López-Moreno, 2017).

The correlation between monthly accumulated precipitation and the NAO index was negative for the entire Iberian Peninsula, as previously reported by other authors over central Portugal (Trigo et al., 2005) or in the northwestern part of Spain (Fernández-González et al., 2012), as well as in the main mountain ranges of the Iberian Peninsula (Juan I. López-Moreno et al., 2011)(Figure 2); although, for small Mediterranean and Cantabrian areas, the correlations were negligible (Ríos-Cornejo et al., 2015; Rodrigo et al., 2000). Southwest areas showed the greatest negative correlations (values of approximately 0.8), which is consistent with the findings of Munoz-Díaz and Rodrigo (2004), where they found different areas of correlation of the precipitation with the NAO index over the Iberian Peninsula and, more specifically, Queralt et al. (2009) about extreme precipitation events associated with DJFM-NAO phases.

There was differentiation between the highly correlated southern slopes and the less correlated northern slopes, as previously reported for the Spanish Pyrenees by Vada et al. (2013) and Buisan et al. (2015), and for the Alps by Stefanicki et al. (1998). This differentiation was especially evident for the mountain ranges located at higher elevations (i.e., the Cantabrian Range and the Pyrenees).

The differences between the southward and northward slopes of the mountain ranges were clear for the Pyrenees (north approximately 0.1; south approximately 0.7), the Cantabrian Range (north approximately 0.3; south approximately 0.6), and the Iberian Range (north approximately 0.2; south approximately 0.6). The differences were less marked for the Central Range (north approximately 0.4; south approximately 0.5), and for the Sierra Nevada were almost negligible. This effect is caused likely by the geographical position of Sierra Nevada and Central Range, and its limited potential to be an effective topographical barrier against the westerly and southwesterly wind directions associated to negative DJFM-NAO phases.

4.3. NAO Spatial Influence on Peak SWE and Snow Season Duration

Figure 3 shows that the DJFM-NAO has a clear correlation with the interannual variability of the snow duration on the southern slopes of the Pyrenees and the Cantabrian, Central, and Iberian ranges. The correlation of the DJFM-NAO with snow duration was high and statistically significant at the highest elevations of the Sierra Nevada, but with no statistically significant differences between the north- and south-facing slopes. However, the other mountain areas showed statistical significance (p -value < 0.05 ; Wilcoxon–Mann–Whitney test) between north- and south-facing slopes. This finding is consistent with the spatial patterns shown in Section 3.2, between the NAO and the interannual variability of winter temperature and precipitation.

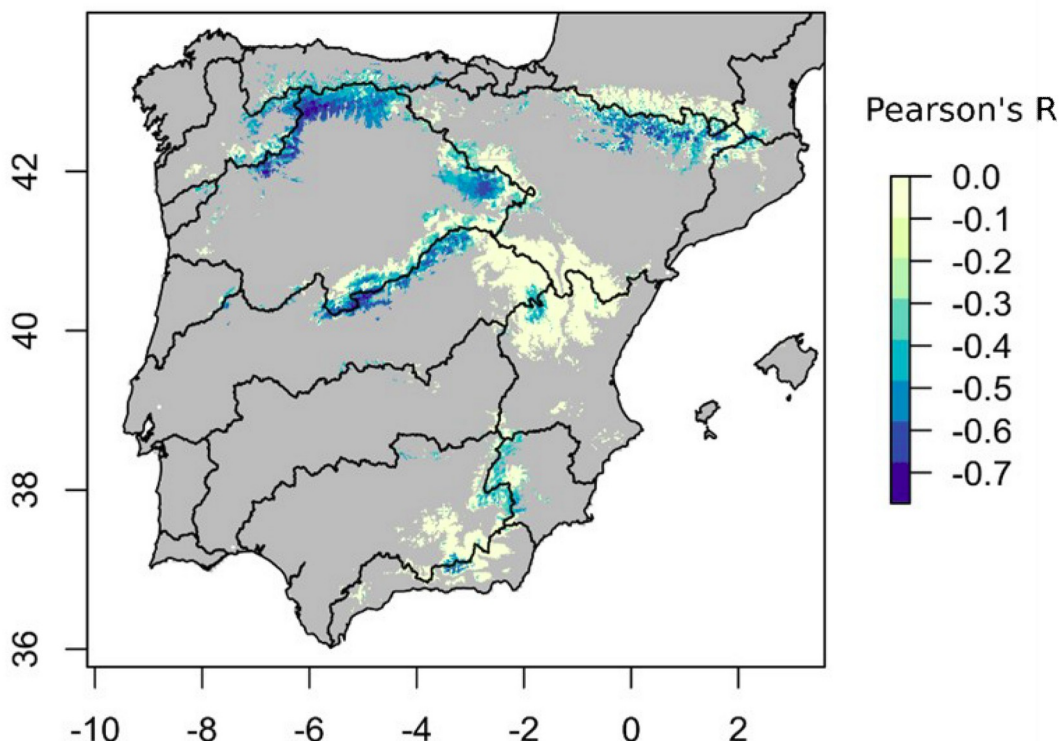


Figure 3: Pearson's R values between de DJFM-NAO and the snowpack duration. The lines represent the boundaties of the main catchments in the Iberian Peninsula.

The spatial patterns and magnitude of the correlations for peak SWE were very similar to those for snow duration (Supplementary Figure S1). However, there were differences between these snow variables. Figure 4 shows the absolute difference in the Pearson's correlation coefficients of the DJFM-NAO with the snow duration and the peak SWE for each pixel for the south-facing slopes,

where high correlation values were found (except for the Sierra Nevada, for which all pixels were considered). The greatest differences were found for the higher elevations in the Pyrenees and the Sierra Nevada, where the correlations for peak SWE were higher than those for snow duration. These two mountain ranges exhibit large areas above 2000 m a.s.l., in contrast with the other mountain ranges. We hypothesize that, at high elevations, the correlation of the DJFM-NAO with the temperature and precipitation leads to high levels of snow accumulation during the DJFM-NAO phases, as a consequence of the driving mechanism that controls the DJFM-NAO; however, this is not reflected in the duration of the snow cover. This is mainly because snow duration also depends on solid precipitation occurring during April and May, which is not related to the DJFM-NAO. In addition, the very late and rapid melting that occurs in these high elevation areas (Musselman et al., 2017) is mostly due to the marked increase of the incoming solar radiation at the end of the snow season period.

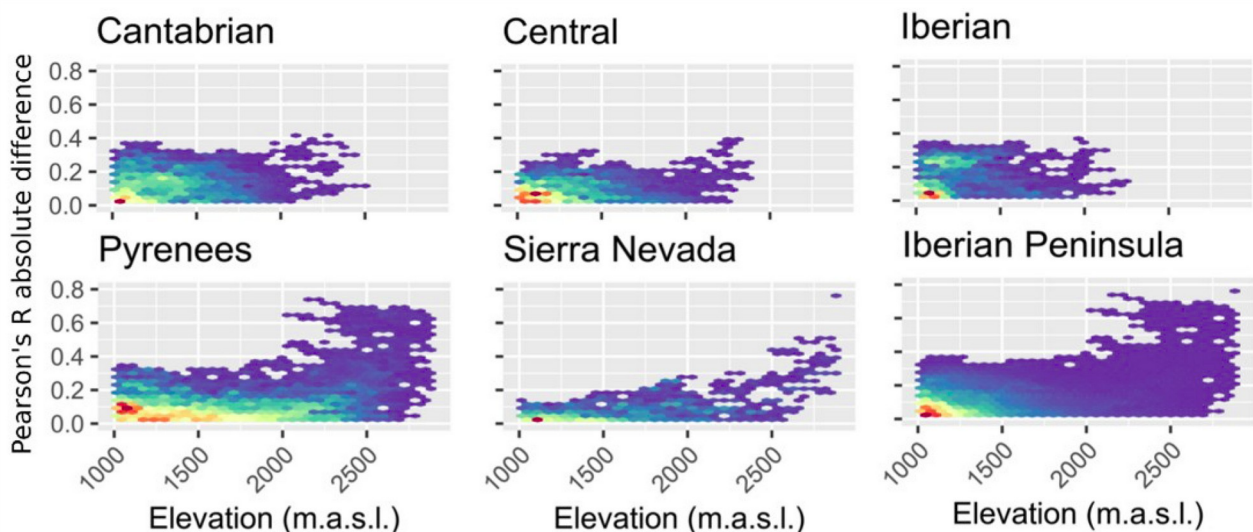


Figure 4: Absolute differences in the Pearson's R statistic for correlations of the DJFM-NAO with the snow duration and the peak SWE. The colors in the scatterplots indicate the relative density of points, ranging from blue (lower relative density) to red (higher relative density).

Figure 4 shows that there was large spatial variability in the correlation coefficients between the DJFM-NAO and the snow indices within each of the analyzed mountain ranges. The influence of elevation on the distribution of the DJFM-NAO correlation values between snow duration and the peak SWE (on south-facing slopes, except in the Sierra Nevada, where both slopes were

considered) is shown in Figure 5, and the comparable influence of geographical longitude is shown in Figure 6.

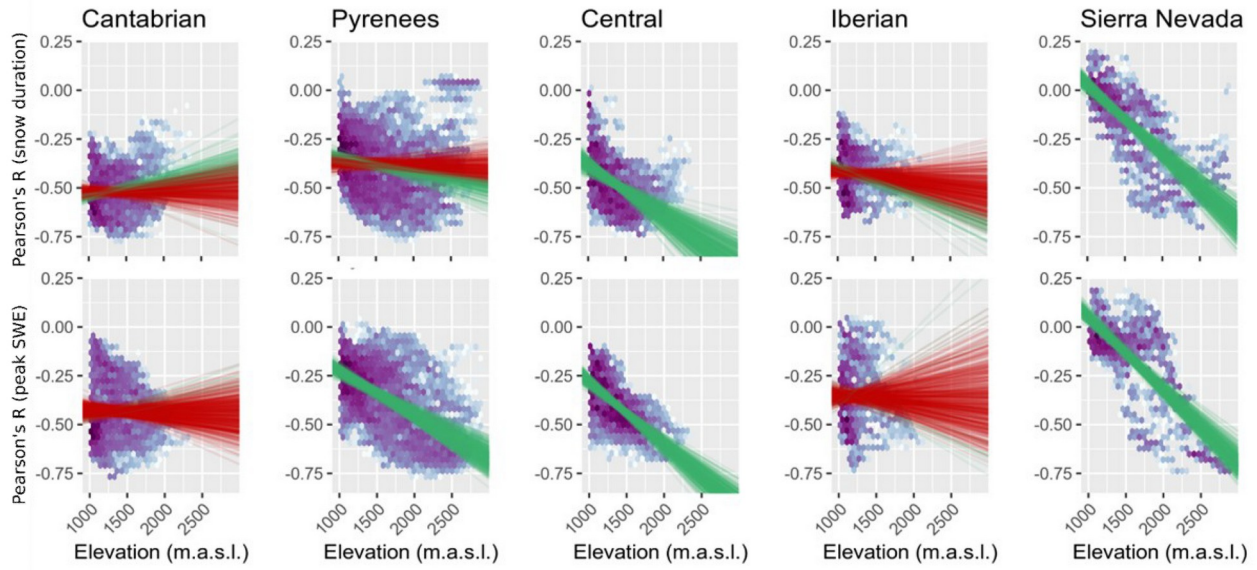


Figure 5: Influence of elevation on the correlation of the DJFM-NAO with snow duration and the peak SWE. Red lines indicate no statistical significance of the correlations of the random samples (p -value > 0.05), while green lines show the statistically significant correlation).

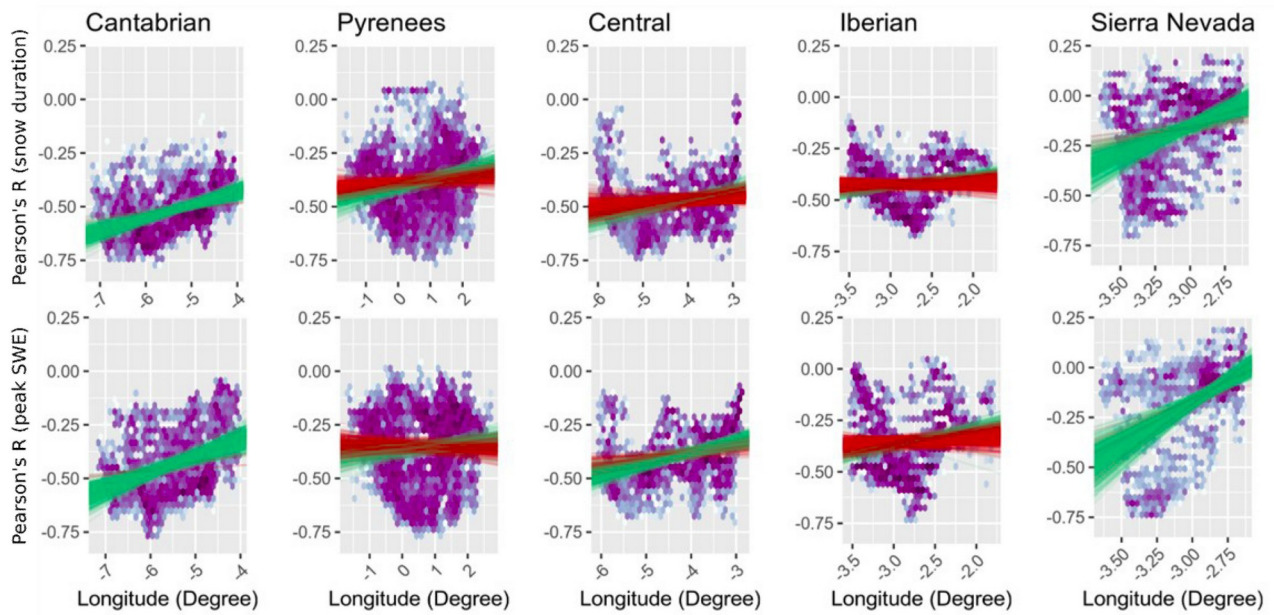


Figure 6: Influence of geographical longitude on the correlation of the DJFM-NAO with snow duration and the peak SWE. Red lines indicate no statistical significance of the correlations of the random samples (p -value > 0.05), while green lines show the statistically significance correlation).

For the Cantabrian Range, most of the correlations of the DJFM-NAO with snow duration ranged from 0.25 to 0.75, and with peak SWE ranged from 0 to 0.75. This variability showed no relationship to elevation, but a clear link with longitude was evident, with an increase in correlation westward. For the Pyrenees, most correlations ranged from 0 to 0.75 for snow duration and peak SWE. While the response of snow duration to elevation was unclear, there was a strong negative relationship for peak SWE. The increase in the correlation of the DJFM-NAO on snow magnitude at high elevations has previously been reported by López-Moreno and Vicente-Serrano (2007), where they found statistically significant correlations of the DJFM-NAO with snowpack observations above 1700 m a.s.l., being consistent with our results. These findings suggest that the frequent westerly and southwesterly air fluxes during negative DJFM-NAO years bring mild temperatures during snowfall events, which may cause rain precipitation at low and mid elevations, but heavy snowfalls over 1800–2000 m a.s.l. The absence of a vertical gradient on the relationship of the DJFM-NAO on snow duration is explained by the presence of snow cover and snowfalls until late spring (end of May to early June); these are also highly dependent on spring precipitation, which is unrelated to the DJFM-NAO. Figure 6 does not show statistically significant correlations with longitude but reveals a clear pattern for both indices, characterized by the highest correlations

(values reaching 0.75) for the Central Pyrenees, and a decrease westward and eastward. This effect is likely a consequence of the small surface with elevation above 1800 m a.s.l. in the western part compared to the Central Pyrenees, causing low correlation between DJFM-NAO and snow indices (Figure 5). The also-low correlations at the easternmost part are explained because southwestern air fluxes, which are frequent during negative DJFM-NAO phases and generally affect only the Western and Central Pyrenees. Thus, DJFM-NAO are not clearly related with both temperature and precipitation in this sector (Figure 2). In the Central Range, the correlation with the DJFM-NAO ranged from 0 to 0.75 for snow duration and 0.1 to 0.6 for peak SWE. This variability showed a clear negative trend with elevation for both indices. There was no strong relationship with longitude for the correlations between the snow indices and the DJFM-NAO for the Central Range. For the Iberian Range, most of the correlations with the DJFM-NAO ranged from 0.1 to 0.6 for snow duration, and 0 to 0.75 for peak SWE. The reduced area at high elevations and their limited geographical extent made it difficult to distinguish clear spatial patterns in the relationship of the DJFM-NAO and the snow indices. The Sierra Nevada showed the largest variability in the correlation values for both indices, ranging from slightly positive values to 0.75. For both indices the impact of the DJFM-NAO was clearer at higher elevations and eastward in this southern mountain range.

This study shows that the relationship of the DJFM-NAO and the snowpack can be seen in long-term trends of snow cover over wide areas of the Iberian Peninsula. Thus, very different trends in snow accumulation have been found in the Pyrenees when different periods have been analyzed. López-Moreno (2005) found a statistically significant decrease in snow accumulation in the central Spanish Pyrenees for the period 1950–1999, but Buisan et al. (2015) found no significant trends for the period 1985–2014. Such disagreements were explained by strong decadal fluctuations in the snow data, which correlated with the DJFM-NAO. The marked spatial differences observed in the correlation between the DJFM-NAO and snow indices may explain the marked contrast in snow trends over very short distances, as has been observed in the Pyrenees (Morán-Tejeda et al., 2017; Revuelto et al., 2013). The presence of areas showing strong correlations between the snowpack and the DJFM-NAO, independent of the study period (as demonstrated by Buisan et al. 2015 for the Pyrenees), provides the promise of improving the seasonal forecasting of snowpack based on short- and medium-term projections for the DJFM-NAO from climate models (Dunstone et al., 2016). This could improve optimization of water management and benefit the skiing industry, both of

which are highly affected by interannual fluctuations in snow accumulation and the duration of the snowpack.

5. Conclusions

The DJFM-NAO is related to the atmospheric circulation patterns over the Iberian Peninsula during the snow-accumulation period. The NAO is related to contrasts in precipitation and temperature over the Iberian Peninsula, and hence related to the snow-accumulation and melting processes.

The mountain ranges analyzed in this study are topographic barriers to the main westerly and southwesterly air fluxes related to the DJFM-NAO and explain their variable impacts on the snowpack. Thus, the snowpack on north-facing slopes along the main mountain range axes did not show statistically significant correlations in most of its surface, but there were significant correlations in south-facing slopes. The Sierra Nevada was the only mountain range where this north south difference was not observed. For all Iberian mountain areas, the statistically significant correlations between the DJFM-NAO and snow indices were negative, and, in some cases, R values exceeded 0.7. Marked spatial differences were found, even for those slopes where the DJFM-NAO generally affects the temporal evolution of the snow. In most of the mountain areas, the strength of the relationship between the DJFM-NAO and peak SWE increased with elevation. This also occurred for snow duration, except in the Pyrenees, where spring snowfall can have a strong influence on the snow duration at high elevations, and snowmelt occurs later and more rapidly. This explains why the snowpack duration and peak SWE are not always related, and explains the weaker correlations between the DJFM-NAO and snow duration compared with peak SWE.

In several mountain areas, we found spatial differences that were related to geographical longitude. This was evident for the Cantabrian Range and the Sierra Nevada, where the correlation values decreased from west to east. For the Pyrenees, the maximum correlations were found for the central valleys and decreased toward its western and eastern edges. The results of this study have clear implications for understanding the effect of the length of the study period on the detection of robust long-term trends in snow data, and also spatial differences in trend analyses over short distances.

Supplementary Materials. The following are available online at <https://www.mdpi.com/2073-4441/12/1/105/s1>, Figure S1: Pearson's R values between the DJFM-NAO and the peak SWE. The lines represent the boundaries of the main catchments in the Iberian Peninsula.

Acknowledgements. Esteban Alonso-González is the recipient of a pre-doctoral FPI grant by the Spanish Ministry of Economy and Competitiveness (BES-2015-071466). This study was funded by the Spanish Ministry of Economy and Competitiveness project CGL2017-82216-R (HIDROIBERNIEVE). Francisco Navarro-Serrano is the recipient of a pre-doctoral FPU grant (Spanish Ministry of Education, Culture and Sports). All the simulation data are freely downloadable at <https://zenodo.org/record/854619>.

References

- Alonso-González, E., Ignacio López-Moreno, J., Gascoin, S., García-Valdecasas Ojeda, M., Sanmiguel-Vallelado, A., Navarro-Serrano, F., Revuelto, J., Ceballos, A., Esteban-Parra, M.J., Essery, R., 2018. Daily gridded datasets of snow depth and snow water equivalent for the Iberian Peninsula from 1980 to 2014. *Earth Syst. Sci. Data* 10, 303–315. <https://doi.org/10.5194/essd-10-303-2018>
- Alonso-González, E., López-Moreno, J.I., Navarro-Serrano, F., Sanmiguel-Vallelado, A., Revuelto, J., Domínguez-Castro, F., Ceballos, A., 2020. Snow climatology for the mountains in the Iberian Peninsula using satellite imagery and simulations with dynamically downscaled reanalysis data. *Int. J. Climatol.* 40, 477–491. <https://doi.org/10.1002/joc.6223>
- Bednorz, E., 2002. Snow cover in western Poland and macro-scale circulation conditions. *Int. J. Climatol.* 22, 533–541. <https://doi.org/10.1002/joc.752>
- Bednorz, E., Wibig, J., 2016. Spatial distribution and synoptic conditions of snow accumulation in the Russian Arctic. *Polar Res.* 35, 25916. <https://doi.org/10.3402/polar.v35.25916>
- Beniston, M., 2003. Climatic change in mountain regions: A review of possible impacts. *Clim. Change* 59, 5–31. <https://doi.org/10.1023/A:1024458411589>
- Beniston, M., 1997. Variations of snow depth and duration in the Swiss Alps over the last 50 years: Links to changes in large-scale climatic forcings, in: *Climatic Change*. Springer, pp. 281–300. https://doi.org/10.1007/978-94-015-8905-5_3
- Berrisford, P., Dee, D., Poli, P., Brugge, R., Fielding, K., Fuentes, M., Kallberg, P., Kobayashi, S., Uppala, S., Simmons, A., 2009. The ERA-Interim Archive Version 2.0. *ERA Rep. Ser.*
- Brown, R.D., Petkova, N., 2007. Snow cover variability in Bulgarian mountainous regions, 1931–2000. *Int. J. Climatol.* 27, 1215–1229. <https://doi.org/10.1002/joc.1468>
- Buisan, S.T., López-Moreno, J.I., Saz, M.A., Kochendorfer, J., 2016. Impact of weather type variability on winter precipitation, temperature and annual snowpack in the Spanish Pyrenees. *Clim. Res.* 69, 79–92. <https://doi.org/10.3354/cr01391>

Buisan, S.T., Saz, M.A., López-Moreno, J.I., 2015. Spatial and temporal variability of winter snow and precipitation days in the western and central Spanish Pyrenees. *Int. J. Climatol.* 35, 259–274. <https://doi.org/10.1002/joc.3978>

Cohen, J., Fletcher, C., 2007. Improved skill of northern hemisphere winter surface temperature predictions based on land-atmosphere fall anomalies. *J. Clim.* 20, 4118–4132. <https://doi.org/10.1175/JCLI4241.1>

Dee, D.P., Uppala, S.M., Simmons, A.J., Berrisford, P., Poli, P., Kobayashi, S., Andrae, U., Balmaseda, M.A., Balsamo, G., Bauer, P., Bechtold, P., Beljaars, A.C.M., van de Berg, L., Bidlot, J., Bormann, N., Delsol, C., Dragani, R., Fuentes, M., Geer, A.J., Haimberger, L., Healy, S.B., Hersbach, H., Hólm, E. V., Isaksen, L., Kållberg, P., Köhler, M., Matricardi, M., McNally, A.P., Monge-Sanz, B.M., Morcrette, J.J., Park, B.K., Peubey, C., de Rosnay, P., Tavolato, C., Thépaut, J.N., Vitart, F., 2011. The ERA-Interim reanalysis: Configuration and performance of the data assimilation system. *Q. J. R. Meteorol. Soc.* 137, 553–597. <https://doi.org/10.1002/qj.828>

del Río, S., Fraile, R., Herrero, L., Penas, A., 2007. Analysis of recent trends in mean maximum and minimum temperatures in a region of the NW of Spain (Castilla y León). *Theor. Appl. Climatol.* 90, 1–12. <https://doi.org/10.1007/s00704-006-0278-9>

Dunstone, N., Smith, D., Scaife, A., Hermanson, L., Eade, R., Robinson, N., Andrews, M., Knight, J., 2016. Skilful predictions of the winter North Atlantic Oscillation one year ahead. *Nat. Geosci.* 9, 809–814. <https://doi.org/10.1038/ngeo2824>

Durán, L., Rodríguez-Fonseca, B., Yagüe, C., Sánchez, E., 2015. Water vapour flux patterns and precipitation at Sierra de Guadarrama mountain range (Spain). *Int. J. Climatol.* 35, 1593–1610. <https://doi.org/10.1002/joc.4079>

Essery, R., 2015. A factorial snowpack model (FSM 1.0). *Geosci. Model Dev.* 8, 3867–3876. <https://doi.org/10.5194/gmd-8-3867-2015>

Esteban-Parra, M.J., Pozo-Vázquez, D., Rodrigo, F.S., Castro-Díez, Y., 2003. Temperature and Precipitation Variability and Trends in Northern Spain in the Context of the Iberian Peninsula Climate, in: *Mediterranean Climate*. Springer Berlin Heidelberg, Berlin, Heidelberg, pp. 259–276. https://doi.org/10.1007/978-3-642-55657-9_15

- Fayad, A., Gascoin, S., Faour, G., López-Moreno, J.I., Drapeau, L., Page, M. Le, Escadafal, R., 2017. Snow hydrology in Mediterranean mountain regions: A review. *J. Hydrol.* 551, 374–396. <https://doi.org/10.1016/j.jhydrol.2017.05.063>
- Fernández-González, S., Del Río, S., Castro, A., Penas, A., Fernández-Raga, M., Calvo, A.I., Fraile, R., 2012. Connection between NAO, weather types and precipitation in León, Spain (1948-2008). *Int. J. Climatol.* 32, 2181–2196. <https://doi.org/10.1002/joc.2431>
- García-Valdecasas Ojeda, M., Gámiz-Fortis, S.R., Castro-Díez, Y., Esteban-Parra, M.J., 2017. Evaluation of WRF capability to detect dry and wet periods in Spain using drought indices. *J. Geophys. Res.* 122, 1569–1594. <https://doi.org/10.1002/2016JD025683>
- García, C., Martí, G., Oller, P., Moner, I., Gavaldà, J., Martínez, P., Peña, J.C., 2009. Major avalanches occurrence at regional scale and related atmospheric circulation patterns in the Eastern Pyrenees. *Cold Reg. Sci. Technol.* 59, 106–118. <https://doi.org/10.1016/j.coldregions.2009.07.009>
- Gilaberte-Búrdalo, M., López-Martín, F., Pino-Otín, M.R., López-Moreno, J.I., 2014. Impacts of climate change on ski industry. *Environ. Sci. Policy* 44, 51–61. <https://doi.org/10.1016/j.envsci.2014.07.003>
- Henderson, G.R., Leathers, D.J., 2010. European snow cover extent variability and associations with atmospheric forcings. *Int. J. Climatol.* 30, 1440–1451. <https://doi.org/10.1002/joc.1990>
- Hurrell, J.W., 1995. Decadal trends in the North Atlantic oscillation: Regional temperatures and precipitation. *Science* (80-.). 269, 676–679. <https://doi.org/10.1126/science.269.5224.676>
- Hurrell, J.W., Deser, C., 2010. North Atlantic climate variability: The role of the North Atlantic Oscillation. *J. Mar. Syst.* <https://doi.org/10.1016/j.jmarsys.2009.11.002>
- Jomelli, V., Delval, C., Grancher, D., Escande, S., Brunstein, D., Hetu, B., Filion, L., Pech, P., 2007. Probabilistic analysis of recent snow avalanche activity and weather in the French Alps. *Cold Reg. Sci. Technol.* 47, 180–192. <https://doi.org/10.1016/j.coldregions.2006.08.003>
- Keylock, C.J., 2003. The North Atlantic Oscillation and snow avalanching in Iceland. *Geophys. Res. Lett.* 30, n/a-n/a. <https://doi.org/10.1029/2002gl016272>
- Kjellström, E., 2016. North atlantic oscillation (Nao), in: Encyclopedia of Earth Sciences Series. p. 540. https://doi.org/10.1007/978-94-007-6644-0_192-1

- Koenig, W.D., 1999. Spatial autocorrelation of ecological phenomena. *Trends Ecol. Evol.* 14, 22–26. [https://doi.org/10.1016/S0169-5347\(98\)01533-X](https://doi.org/10.1016/S0169-5347(98)01533-X)
- López-Moreno, J.I., 2005. Recent variations of snowpack depth in the central Spanish Pyrenees. *Arctic, Antarct. Alp. Res.* 37, 253–260. [https://doi.org/10.1657/1523-0430\(2005\)037\[0253:RVOSDI\]2.0.CO;2](https://doi.org/10.1657/1523-0430(2005)037[0253:RVOSDI]2.0.CO;2)
- López-Moreno, J.I., Beniston, M., García-Ruiz, J.M., 2008. Environmental change and water management in the Pyrenees: Facts and future perspectives for Mediterranean mountains. *Glob. Planet. Change* 61, 300–312. <https://doi.org/10.1016/j.gloplacha.2007.10.004>
- López-Moreno, J.I., Vicente-Serrano, S.M., 2007. Atmospheric circulation influence on the interannual variability of snow pack in the Spanish Pyrenees during the second half of the 20th century. *Nord. Hydrol.* 38, 33–44. <https://doi.org/10.2166/nh.2007.030>
- López-Moreno, J. I., Vicente-Serrano, S.M., Morán-Tejeda, E., Lorenzo-Lacruz, J., Kenawy, A., Beniston, M., 2011. Effects of the North Atlantic Oscillation (NAO) on combined temperature and precipitation winter modes in the Mediterranean mountains: Observed relationships and projections for the 21st century. *Glob. Planet. Change* 77, 62–76. <https://doi.org/10.1016/j.gloplacha.2011.03.003>
- López-Moreno, Juan I., Vicente-Serrano, S.M., Morán-Tejeda, E., Lorenzo-Lacruz, J., Zabalza, J., Kenawy, A. El, Beniston, M., 2011. Influence of Winter North Atlantic Oscillation Index (NAO) on Climate and Snow Accumulation in the Mediterranean Mountains, in: *Advances in Global Change Research*. Springer, Dordrecht, pp. 73–89. https://doi.org/10.1007/978-94-007-1372-7_6
- Lorente-Plazas, R., Montávez, J.P., Jimenez, P.A., Jerez, S., Gómez-Navarro, J.J., García-Valero, J.A., Jimenez-Guerrero, P., 2015. Characterization of surface winds over the Iberian Peninsula. *Int. J. Climatol.* 35, 1007–1026. <https://doi.org/10.1002/joc.4034>
- Lorenzo-Lacruz, J., Vicente-Serrano, S.M., López-Moreno, J.I., González-Hidalgo, J.C., Morán-Tejeda, E., 2011. The response of Iberian rivers to the North Atlantic Oscillation. *Hydrol. Earth Syst. Sci.* 15, 2581–2597. <https://doi.org/10.5194/hess-15-2581-2011>
- Morán-Tejeda, E., López-Moreno, J.I., Beniston, M., 2013. The changing roles of temperature and precipitation on snowpack variability in Switzerland as a function of altitude. *Geophys. Res. Lett.* 40, 2131–2136. <https://doi.org/10.1002/grl.50463>

Morán-Tejeda, E., López-Moreno, J.I., Sanmiguel-Vallelado, A., 2017. Changes in Climate, Snow and Water Resources in the Spanish Pyrenees: Observations and Projections in a Warming Climate, in: Advances in Global Change Research. Springer, Cham, pp. 305–323. https://doi.org/10.1007/978-3-319-55982-7_13

Morán-Tejeda, E., Lorenzo-Lacruz, J., López-Moreno, J.I., Rahman, K., Beniston, M., 2014. Streamflow timing of mountain rivers in Spain: Recent changes and future projections. *J. Hydrol.* 517, 1114–1127. <https://doi.org/10.1016/j.jhydrol.2014.06.053>

Munoz-Díaz, D., Rodrigo, F.S., 2004. Impacts of the North Atlantic Oscillation on the probability of dry and wet winters in Spain. *Clim. Res.* 27, 33–43. <https://doi.org/10.3354/cr027033>

Musselman, K.N., Clark, M.P., Liu, C., Ikeda, K., Rasmussen, R., 2017. Slower snowmelt in a warmer world. *Nat. Clim. Chang.* 7, 214–219. <https://doi.org/10.1038/nclimate3225>

Navarro-Serrano, F., López-Moreno, J.I., 2017. Análisis espacio-temporal de los eventos de nevadas en el pirineo Español y su relación con la circulación atmosférica. *Cuad. Investig. Geogr.* 43, 233–254. <https://doi.org/10.18172/cig.3042>

Osborn, T.J., Briffa, K.R., Tett, S.F.B., Jones, P.D., Trigo, R.M., 1999. Evaluation of the North Atlantic Oscillation as simulated by a coupled climate model. *Clim. Dyn.* 15, 685–702. <https://doi.org/10.1007/s003820050310>

Queralt, S., Hernández, E., Barriopedro, D., Gallego, D., Ribera, P., Casanova, C., 2009. North Atlantic Oscillation influence and weather types associated with winter total and extreme precipitation events in Spain. *Atmos. Res.* 94, 675–683. <https://doi.org/10.1016/j.atmosres.2009.09.005>

Revuelto, J., López-Moreno, J.I., Azorin-Molina, C., Vicente-Serrano, S.M., 2014. Topographic control of snowpack distribution in a small catchment in the central Spanish Pyrenees: Intra- and inter-annual persistence. *Cryosphere* 8, 1989–2006. <https://doi.org/10.5194/tc-8-1989-2014>

Revuelto, J., López-Moreno, J.I., Morán-Tejeda, E., Fassnacht, S.R., Vicente Serrano, S.M., 2013. Variabilidad interanual del manto de nieve en el Pirineo: tendencias observadas y su relación con índices de teleconexión durante el periodo 1985-2011. <https://doi.org/978-84-695-4331-3>

Riaz, S.M.F., Iqbal, M.J., Hameed, S., 2017. Impact of the North Atlantic Oscillation on winter climate of Germany. *Tellus, Ser. A Dyn. Meteorol. Oceanogr.* 69, 1406263. <https://doi.org/10.1080/16000870.2017.1406263>

Ríos-Cornejo, D., Peñas, Á., Álvarez-Esteban, R., del Río, S., 2015. Links between teleconnection patterns and precipitation in Spain. *Atmos. Res.* 156, 14–28. <https://doi.org/10.1016/j.atmosres.2014.12.012>

Rodrigo, F.S., Esteban-Parra, M.J., Pozo-Vázquez, D., Castro-Díez, Y., 2000. Rainfall variability in southern Spain on decadal to centennial time scales. *Int. J. Climatol.* 20, 721–732. [https://doi.org/10.1002/1097-0088\(20000615\)20:7<721::AID-JOC520>3.0.CO;2-Q](https://doi.org/10.1002/1097-0088(20000615)20:7<721::AID-JOC520>3.0.CO;2-Q)

Sáenz, J., Zubillaga, J., Rodríguez-Puebla, C., 2001. Interannual winter temperature variability in the north of the Iberian Peninsula. *Clim. Res.* 16, 169–179. <https://doi.org/10.3354/cr016169>

Salkind, N., 2012. Nonparametric Statistics for the Behavioral Sciences, Encyclopedia of Research Design. McGraw-Hill. <https://doi.org/10.4135/9781412961288.n273>

Sánchez-López, G., Hernández, A., Pla-Rabes, S., Toro, M., Granados, I., Sigró, J., Trigo, R.M., Rubio-Inglés, M.J., Camarero, L., Valero-Garcés, B., Giralt, S., 2015. The effects of the NAO on the ice phenology of Spanish alpine lakes. *Clim. Change* 130, 101–113. <https://doi.org/10.1007/s10584-015-1353-y>

Scaife, A.A., Arribas, A., Blockley, E., Brookshaw, A., Clark, R.T., Dunstone, N., Eade, R., Fereday, D., Folland, C.K., Gordon, M., Hermanson, L., Knight, J.R., Lea, D.J., MacLachlan, C., Maidens, A., Martin, M., Peterson, A.K., Smith, D., Vellinga, M., Wallace, E., Waters, J., Williams, A., 2014. Skillful long-range prediction of European and North American winters. *Geophys. Res. Lett.* 41, 2514–2519. <https://doi.org/10.1002/2014GL059637>

Scherrer, S.C., Appenzeller, C., 2006. Swiss Alpine snow pack variability: *Clim. Res.* 32, 187–199.

Schöner, W., Koch, R., Matulla, C., Marty, C., Tilg, A.M., 2019. Spatiotemporal patterns of snow depth within the Swiss-Austrian Alps for the past half century (1961 to 2012) and linkages to climate change. *Int. J. Climatol.* 39, 1589–1603. <https://doi.org/10.1002/joc.5902>

Skamarock, W.C., Klemp, J.B., Dudhia, J.B., Gill, D.O., Barker, D.M., Duda, M.G., Huang, X.-Y., Wang, W., Powers, J.G., 2008. A description of the Advanced Research WRF Version 3, NCAR Technical Note TN-475+STR. Tech. Rep. 113. <https://doi.org/10.5065/D68S4MVH>

Stefanicki, G., Talkner, P., Weber, R.O., 1998. Frequency changes of weather types in the Alpine region since 1945. *Theor. Appl. Climatol.* 60, 47–61. <https://doi.org/10.1007/s007040050033>

Theakstone, W.H., 2013. Long-term variations of the seasonal snow cover in Nordland, Norway: The influence of the North Atlantic Oscillation. *Ann. Glaciol.* 54, 25–34. <https://doi.org/10.3189/2013AoG62A300>

Trigo, R.M., Osborn, T.J., Corte-Real, J.M., 2002. The North Atlantic Oscillation influence on Europe: Climate impacts and associated physical mechanisms. *Clim. Res.* 20, 9–17. <https://doi.org/10.3354/cr020009>

Trigo, R.M., Zêzere, J.L., Rodrigues, M.L., Trigo, I.F., 2005. The Influence of the North Atlantic Oscillation on rainfall triggering of landslides near Lisbon. *Nat. Hazards* 36, 331–354. <https://doi.org/10.1007/s11069-005-1709-0>

Vada, J.A., Rodríguez-Marcos, J., Buisán, S., Ambrosio, I.S., 2013. Climatological Comparison of 2011-2012 and 2012-2013 Snow Seasons in Central and Western Spanish Pyrenees and its Relationship With the North Atlantic Oscillation (NAO), International Snow Science Workshop Grenoble – Chamonix Mont-Blanc - October 07-11, 2013.

Wang, L., Ting, M., Kushner, P.J., 2017. A robust empirical seasonal prediction of winter NAO and surface climate. *Sci. Rep.* 7, 279. <https://doi.org/10.1038/s41598-017-00353-y>

Wanner, H., Brönnimann, S., Casty, C., Gyalistras, D., Luterbacher, J., Schmutz, C., Stephenson, D.B., Xoplaki, E., 2001. North Atlantic oscillation - Concepts and studies. *Surv. Geophys.* 22, 321–381. <https://doi.org/10.1023/A:1014217317898>

Capítulo 5: Sensibilidad del manto de nieve a la variabilidad de la temperatura, precipitación y radiación solar en un gradiente altitudinal en la Península Ibérica

Resumen: En el siguiente trabajo se ha investigado la sensibilidad del manto de nieve al aumento de la temperatura y a la radiación de onda corta, y al cambio de las precipitaciones a lo largo de un gradiente altitudinal (1500 - 2500 m s.n.m.) sobre las principales cadenas montañosas de la Península Ibérica (Cordillera Cantábrica, Sistema Central, Sistema Ibérico, Pirineos y Sierra Nevada). Hemos utilizado la salida de un modelo mesoatmosférico (WRF) como forzamiento en un modelo de base física de balance de masa y energía de la nieve (FSM2). Se aplicó un algoritmo de agrupamiento a los datos de entrada del modelo FSM2 para identificar un total de 12 celdas que resumen la variabilidad climática de las cadenas montañosas. Las salidas de WRF se proyectaron a diferentes bandas altitudinales utilizando una serie de fórmulas psicrométricas y radiativas así como gradientes de temperatura del aire. Con estos datos, hemos realizado un experimento factorial generando series meteorológicas sintéticas que implicaban una alteración gradual de la temperatura (aumentos de 0 - 4 °C), radiación de onda corta (aumentos de 0-40 Wm⁻²) y precipitaciones (variaciones de ± 20%) en todas sus posibles combinaciones y usando estas series como forzamiento de FSM2. Los resultados muestran diferentes sensibilidades del manto de nieve en las diversas zonas montañosas como consecuencia de las diferentes particiones de los balances de masa y energía. Los resultados mostraron un impacto generalmente negativo del calentamiento climático en la magnitud, duración y tasas de fusión de la capa de nieve en todas las bandas de elevación, incluso bajo los escenarios de mayor precipitación. El efecto medio del calentamiento sobre la duración del manto de nieve osciló entre -23% por °C a 1500 m s.n.m. y -13% por °C a 2500 m s.n.m., sobre el máximo SWE acumulado osciló entre -20% por °C a 1500 m s.n.m. y -15% por °C a 2500 m s.n.m., y sobre las tasas de fusión osciló entre -9% y -6% por °C. El efecto del aumento de la radiación de onda corta sobre el manto de nieve varió desde aproximadamente -2% por 10 Wm⁻² a 1500 m a.s.l. hasta -1% por 10 Wm⁻² a 2500 m a.s.l. tanto para la duración del manto de nieve como para los máximos de SWE. El efecto sobre el manto de nieve causado por los cambios en

la precipitación se redujo gradualmente con el aumento de la elevación, especialmente en las zonas más frías. La respuesta de las tasas de fusión al calentamiento fue negativa en la mayoría de las áreas en todas las elevaciones, lo que sugiere períodos de fusión menos intensos pero más largos.

Cita completa:

Alonso-González, E., López-Moreno, J. I., Navarro-Serrano, F., Sanmiguel-Vallelado, A., Aznárez-Balta, M., Revuelto, J., Ceballos, A.(2020). Snowpack sensitivity to temperature, precipitation, and solar radiation variability over an elevational gradient in the Iberian mountains. *Atmospheric Research*. Pp: 104973. <https://doi.org/10.1016/j.atmosres.2020.104973>

Snowpack sensitivity to temperature, precipitation, and solar radiation variability over an elevational gradient in the Iberian mountains

Esteban Alonso-González¹, Juan Ignacio López-Moreno¹, Francisco Navarro-Serrano¹, Alba Sanmiguel-Vallelado^{1,M}, M. Aznárez-Balta¹, Jesús Revuelto², Fernando Domínguez-Castro¹, Ceballos, A².

1. Instituto Pirenaico de Ecología, Consejo Superior de Investigaciones Científicas (IPE-CSIC), Zaragoza, Spain
2. Dept. Geografía, Universidad de Salamanca, Salamanca, Spain

Correspondence: Esteban Alonso-González (e.alonso@ipe.csic.com)

Received: 16 January 2020

Accepted: 26 March 2019

Abstract. In this study we investigated the sensitivity of the snowpack to increased temperature and short-wave radiation, and precipitation change along an elevation gradient (1500 - 2500 m a.s.l.) over the main mountain ranges of the Iberian Peninsula (Cantabrian Range, Central Range, Iberian Range, Pyrenees, and the Sierra Nevada). The output of a meso-atmospheric model (WRF) was used as forcing data in a physically-based energy and mass balance snowpack model (FSM2). A cluster analyses was applied to the input data of the FSM2 model to identify a total of 12 cells that summarized the climatic variability of the mountain ranges. The WRF output was then rescaled to various elevation bands using an array of psychrometric and radiative formulae and air temperature lapse rates. A factorial experiment was performed to generate synthetic meteorological series involving gradual alteration of the temperature (0 – 4 °C increases), short-wave radiation (0-40 Wm⁻² increases), and precipitation (variations of ± 20%) to force the FSM2. We found differing sensitivities across the various mountainous areas as a consequence of differences in their energy and mass balances. The results showed a generally negative impact of climate warming on the magnitude, duration, and melt rates of the snowpack over all elevation bands, even under scenarios of greater precipitation. The average effect of warming on the duration of the snowpack ranged from -23% per °C at 1500 m a.s.l. to -13% per °C at 2500 m a.s.l., on the peak snow water equivalent ranged from -20% per °C at 1500 m a.s.l. to -15% per °C at 2500 m a.s.l., and on melt rates ranged from -9% to -6% per °C. The effect of increasing short-wave radiation on the snowpack ranged from approximately -2% per 5 Wm⁻² at 1500 m a.s.l. to -1% per 5 Wm⁻² at 2500 m a.s.l. for both the snowpack duration and peak SWE indices. The effect on the snowpack caused by

precipitation changes reduced gradually with increasing elevation, especially in the colder areas. The response of the melt rates to warming was negative in most of the areas at all elevations, suggesting less intense but longer melt seasons.

1 Introducción

As a consequence of its physical properties (low thermal conductivity, high water storage capacity, and high albedo), the snowpack is a key element in many ecological, hydrological, and atmospheric processes in cold and mountainous areas.

As in other Mediterranean areas (Fayad et al., 2017), in the Iberian Peninsula a large amount of the total annual precipitation falls during winter (López-Moreno et al., 2011, 2008), resulting in extensive snow-covered areas each year (Alonso-González et al., 2019a). Thus, the snowpack has a major influence on seasonal river flows (García-Ruiz et al. 2011), and enables water availability to be matched with the high demand during the warm and dry season (López-Moreno and García-Ruiz, 2004; Sanmiguel-Vallelado et al., 2017). Furthermore, winter tourism represents a key economic resource for mountainous areas of the Iberian Peninsula, where there are 64 ski resorts including in Spain (31), France (29), Andorra (3), and Portugal (1). However, various scenarios suggest that the snowpack and winter tourism are very vulnerable to climate change (Gilaberte-Búrdalo et al., 2017, 2014; Pons et al., 2015).

The magnitude and duration of the snowpack responds rapidly to changes in temperature and other climate parameters (Barnett et al., 2005; Connolly et al., 2019), with deep implications over such processes. However, the response of the seasonal snowpack to climate variability is complex. Beyond the obvious implications for reduction in the magnitude and duration of the snowpack, recent studies have shown the potential for warming to decelerate melting rates (Musselman et al., 2017), and also the influence of humidity in controlling melting events (Harpold and Brooks, 2018). These indicate very contrasting sensitivities to warming processes, even among mountainous areas identified as Mediterranean (López-Moreno et al., 2017). Furthermore, potentially large within-range variability in the response of the snowpack to climate change can occur because of elevation differences and local climatological variability, as has been reported for the Pyrenees (López-Moreno et al., 2009) or the Cascades (Sproles et al., 2013). Differing energy and mass balances in the snowpack, caused by different climatological characteristics, explain this contrasting response. Thus, physically-based models are commonly used to study and reproduce the heat and mass fluxes

of the snowpack under varying conditions. Accurate meteorological forcing data are essential to correctly represent the snow processes in physically-based snowpack models (Côté et al., 2017; Raleigh et al., 2016; Slater et al., 2013). Unfortunately, there is a generalized lack of meteorological observational data for the mountainous areas of Iberia, and the available series are too short, sparse, or incomplete. Although data from meteorological observations are available for some mountain locations (Polo et al., 2019; Revuelto et al., 2017), meso-atmospheric simulations are the only available tool for obtaining long-term forcing data over the Iberian mountains.

In addition to future warmer conditions, the Iberian Peninsula shows a significant positive trend in downward shortwave radiation, caused by the combined effect of a decrease in cloudiness and atmospheric aerosols (Vicente-Serrano et al., 2017). Radiative heat flux is an important factor in the energetic flux of the snowpack (Marsh et al., 2012), but how its variability affects the snowpack has been little investigated, even though it is known that this flux can control the spatiotemporal sensitivity of the snowpack, depending on slope and aspect (López-Moreno et al., 2013). Furthermore, there is large uncertainty in the projections for future precipitation over the Iberian Peninsula (Monjo et al., 2016), which has clear implications for predicting the evolution of the snowpack under changing climate conditions.

Because of the dependence of the Iberian Peninsula on water stored as snow in mountain areas (López-Moreno and García-Ruiz, 2004), it is important to take into account the effect of elevation in investigating the sensitivity of the snowpack, as this will markedly affect the susceptibility of the snowpack to increasing temperature (López-Moreno et al., 2009; Marty et al., 2017; Sospedra-Alfonso et al., 2015). These uncertainties can be considered from a factorial point of view (Rasouli et al., 2015) by studying how variability in various factors influences the snowpack response, either independently or jointly..

In this study we investigated the sensitivity of the snowpack in various Iberian mountain ranges to changing temperature, incoming solar radiation, and precipitation. We used a pre-existing meso-atmospheric simulation as forcing data in a physically-based energy and mass balance snowpack model. Altering the forcing meteorological variables enabled us to simulate the snowpack under different climatological scenarios across an elevational gradient.

2 Study Area

The Iberian Peninsula is located in the south-western part of Europe between latitudes 36 °N and 43.5 °N, and covers an area of 596,740 km². It is characterized by high topographical complexity, and includes five main mountain ranges (the Cantabrian, Iberian, and Central ranges, and the Pyrenees and Sierra Nevada). These are each aligned roughly east-west, with maximum elevations of approximately 2500 m a.s.l. in the Cantabrian, Iberian, and Central ranges, and exceeding 3000 m a.s.l. in the Pyrenees and Sierra Nevada (Fig. 1).

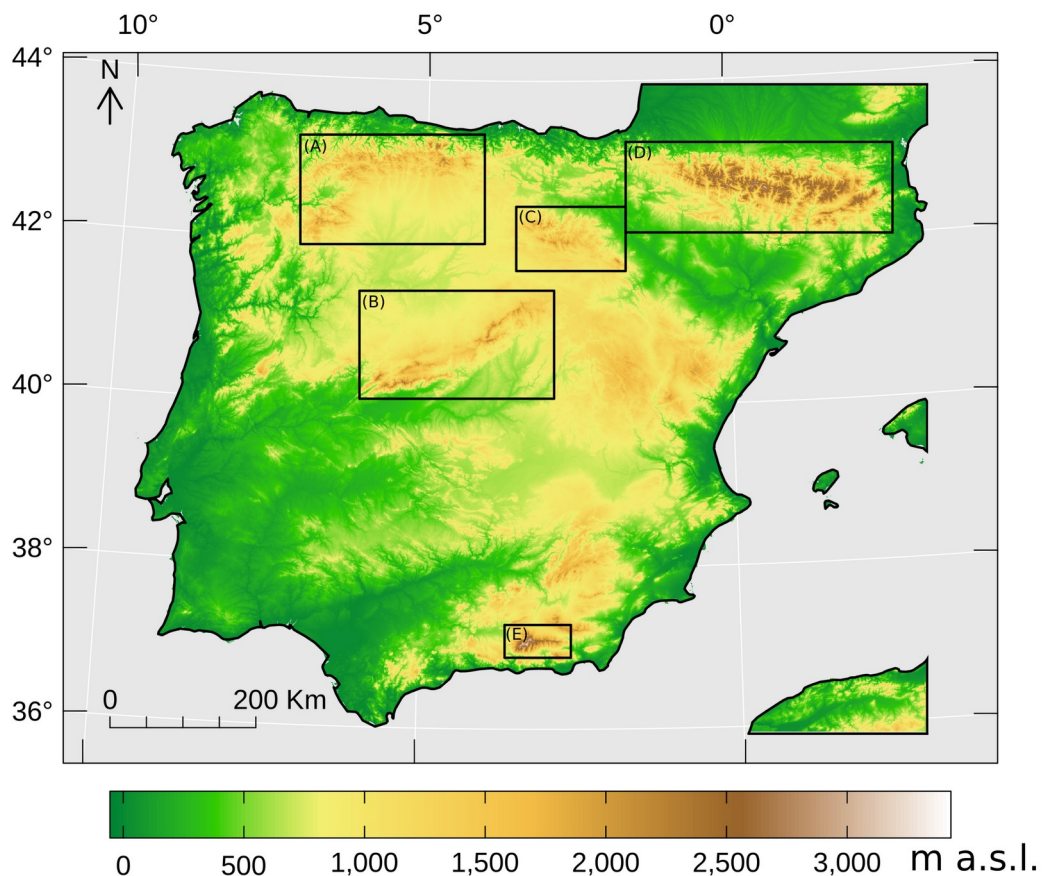


Figure 1: Main mountain ranges of the Iberian Peninsula; (A) Cantabrian range, (B) Central range, (C) Iberian range, (D) Pyrenees, (E) Sierra Nevada. Digital Elevation Model provided by the Spanish Geographical Survey.

Most of the mainland areas of Iberia are on the Central Plateau, which is crossed by the Central Range, with the Cantabrian Range to the north, the Iberian Range to the east, and the Sierra Nevada

to the south, in addition to many other secondary middle mountain ranges. The Pyrenees is the largest mountain range, in the north-eastern part of Iberian Peninsula, and is separated from the Central Plateau by the Ebro basin. As a consequence of this topographical complexity, the wide latitudinal range, and differing exposures to Atlantic and Mediterranean air masses, the Iberian Peninsula exhibits large climatological variability. This is reflected in the rich diversity of snowpack behaviors at different elevations in each mountain area, and within each mountain range (Alonso-González et al., 2019a).

3 Data and methods

We used a pre-existing meso-atmospheric simulation for Iberia (García-Valdecasas Ojeda et al., 2017) as meteorological forcing data in a physically-based snowpack model, the Flexible Snow Model (FSM2) which is the second version of the Factorial Snow Model (Essery, 2015). The FSM model can be freely downloadable from <https://github.com/RichardEssery/FSM2>. The meso-atmospheric simulation was developed using the Weather Research and Forecast model (WRF) (Skamarock et al., 2008), driven by the ERA-Interim reanalysis dataset (Berrisford et al., 2011; Dee et al., 2011). The simulation spans the period 1980-2014 using a spatial resolution of 0.088° (~10 km at the latitude of the Iberian Peninsula). Previously, the meteorological surface data was rescaled to the common elevation band of 2000 m a.s.l. to make all the cells comparable independently of its elevation, using the methodology described by Alonso-González et al. (2018). Reescaling was performed using an array of psychrometric, barometric, and radiative formulae (Harder and Pomeroy, 2014; Liston and Elder, 2006). The 2000 m a.s.l. band was selected as it is a representative elevation band in all the involved mountain ranges (Alonso-González et al., 2019a). Thus, 2-m temperature, atmospheric pressure, longwave radiation, relative humidity and precipitation phase is corrected while wind speed, total precipitation, and shortwave radiation were not adjusted with the elevation difference.

To reduce the computational cost of using all the cells of the simulation, we computed a spatial cluster analysis using the K-means algorithm (Hartigan and Wong, 1979) over the rescaled meteorological fields to enable selection of those pixels for each mountain range representing the most contrasting climatic characteristics. Firstly, we extracted those cells from the 3-hourly WRF simulation representing the main mountains of the Iberian Peninsula at 2000 m a.s.l., and obtained the temporally averaged values for the main variables involved in the snow energy and mass balance (2-m surface temperature, precipitation, short-wave radiation, and long-wave radiation) for

winter (December, January, February) and spring (March, April, May). We then computed a principal components analysis (PCA) for the calculated variables, to reduce the number of dimensions. The cluster analysis was computed for the PCA components that overall explained > 85% of the variability of the meteorological data for each range independently. To determine the most appropriated cluster partitioning schema we computed an array of 30 indices for determining the number of clusters of each mountain range. We follow the majority criteria, where the most appropriate number of clusters is the most common number among the 30 indices (Charrad et al., 2014). The meteorological forcing data used in this study were extracted from the cell nearest to each cluster centroid, previously rescaled to the common elevation bands of 1500, 2000 and 2500 m a.s.l. using the same methodology explained before.

The 2-m surface temperature, short-wave incoming radiation, and precipitation variables for each centroid were altered independently and in all possible combinations over the selected ranges to simulate differing climatological scenarios. Temperature was progressively increased by 0 to +4 °C using 0.5 °C incremental steps, while short-wave incoming radiation was increased over the range 0-40 Wm⁻², using 5 Wm⁻² steps. The selected ranges fall within the range of expected changes at the end of the 21st century, estimated from the observed trends for the period 1985-2010 (Sanchez-Lorenzo et al., 2013; Vicente-Serrano et al., 2017). Changes in precipitation were simulated incrementally by 5% steps over the range ± 20%, which encompassed the uncertainty projected by climatological models for the Mediterranean area (Knutti and Sedláček, 2013). These meteorological fields were altered using the framework proposed by Alonso-González et al. (2018), where the forcing meteorological fields are interrelated. For this study a constant relative humidity was maintained inside the framework, independently of the warming scenario (López-Moreno et al., 2017; Rasouli et al., 2014). All the new synthetic forcing series summarize a total of 1215 forcing datasets per centroid considering the three elevation bands. The topographical effects like slope or aspect are not considered in this study.

We used the newly synthetically generated meteorological data as forcing in the FSM2 (Essery, 2015), for simulating daily snow water equivalent (SWE) series. We estimated the mean peak SWE and mean snow season duration by averaging the long-term values of annual maximum SWE values, and the annual number of days with SWE exceeding 10 mm. The mean melt rates were calculated by averaging the long-term annual ratio between peak SWE and the length of the melting season . We then calculated the sensitivity of each snow index, from the averaged change in each index influenced by the forcing variability. As a consequence of the generalized lack of

observational snow data available to calibrate FSM2, we chose the model configuration with more physically based parametrizations, as the alternative configurations of the FSM were mostly a simplification of the snowpack processes like constant density or the estimation of the albedo as function of the surface temperature. This configuration has proved to be consistent with high mountain observations in previous studies in the Iberian Peninsula, and reproduced the inter- and intra-annual snowpack patterns (Alonso-González et al., 2018). Thus, albedo decreased as snow aged with time, and increased with snowfall. The compaction rate was calculated based on the overburden and thermal metamorphism. The turbulent exchange coefficient was corrected based on the bulk Richardson number. The thermal conductivity was calculated based on snow density. Finally, FSM2 configuration accounted for retention and refreezing of water inside the snowpack. We estimated the average peak SWE, snow season duration, and melt rates from the generated SWE series. The sensitivity of the snowpack duration, peak SWE, and snow melt rate was calculated for each forcing perturbation. The sensitivity was calculated as the average of the relative changes for each snow index to each forcing perturbation step (Fig. 2).

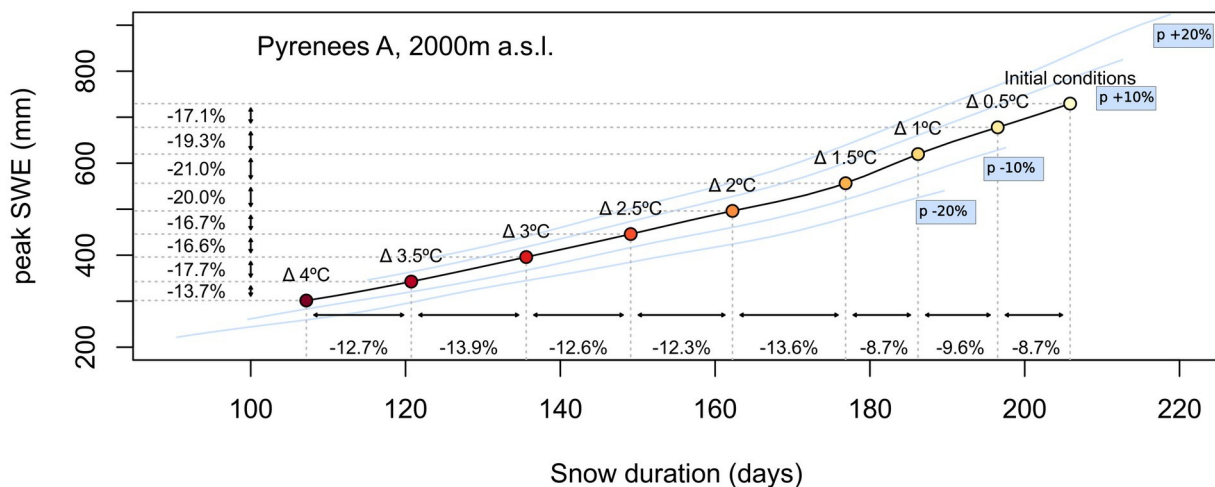


Figure 2: Example showing the relative sensitivities of snow duration and peak SWE for one of the centroids. The blue lines represent the variability caused uncertainty caused by a ± 20% perturbation in precipitation (at 10% intervals).

4 Results

4.1 Selection of representative areas

The number of clusters selected for each mountain range from the majority of the various cluster tests applied varied from two (the Cantabrian and Iberian ranges and the Sierra Nevada) to three (the Pyrenees and Central Range) (Fig. 3). The distribution of the clusters mainly followed the longitudinal axes of the ranges. There was a clear division in the Cantabrian Range between southwestern areas and the northern part. For the Pyrenees there was a clear division between the northern and southern parts, which are affected differently by the Atlantic and Mediterranean air masses, and are separated by a transitional region. For the Iberian Range, areas exposed to the Atlantic air masses were in the same cluster, while the exposed to the Mediterranean air masses formed a second cluster. The Central Range was divided along its longitudinal axis, and showed a third cluster in the western part, where most of the precipitation in the mountain range occurs (Fig. 4). The Sierra Nevada had two clusters, separated along its longitudinal axis, that mainly differed in precipitation levels (Fig. 4). The western cluster centroid of the Sierra Nevada was the warmest in both winter (maximum of 1.9°C) and spring (maximum of 6.9 °C). In contrast, the northern and central centroids of the Pyrenees were the coldest (minima of -5.9 °C and -0.4 °C, respectively). The centroid for the eastern cluster of the Sierra Nevada represented the lower limit of the precipitation range (154.9 mm in winter and 166.9 mm in spring). The upper limits of the precipitation range were in the western Central Range in winter (752.3 mm) and in the central cluster of the Pyrenees in spring (614.8 mm). The highest levels of short-wave radiation occurred in the two Sierra Nevada cluster centroids (in the western and eastern parts), which showed maxima of 158.31 and 149.23 Wm⁻² in winter and 296.4 and 287.1 Wm⁻² in spring, respectively. The lowest mean short-wave radiation level was in the centroid in the northern cluster of the Cantabrian Range (107.21 W and 249.2 W in winter and spring, respectively). The precipitation, temperature, and radiation values of the other cluster centroids were distributed within these extremes (Fig. 4). The set of cluster centroids was highly variable with respect to the averages for the meteorological variables (Fig. 4). Thus, the selected areas were representative of the average mountain climate patterns in the Iberian Peninsula.

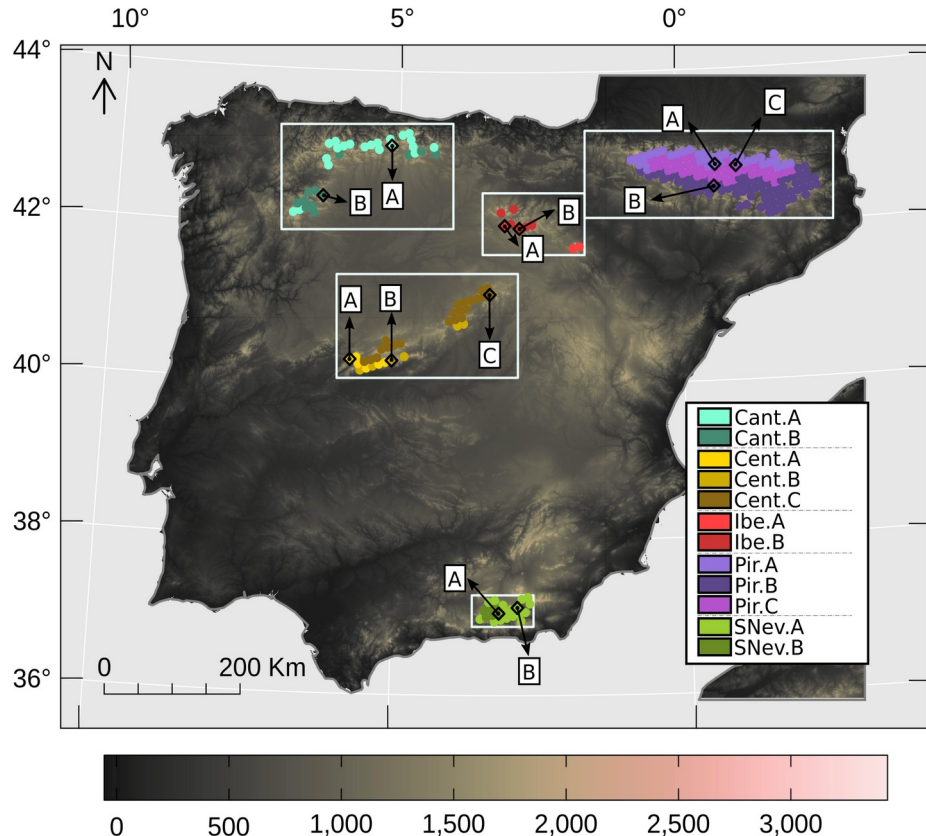


Figure 3: Distribution of the clusters for each mountain range. The diamond symbols indicate the cell nearest to the centroid of each cluster.

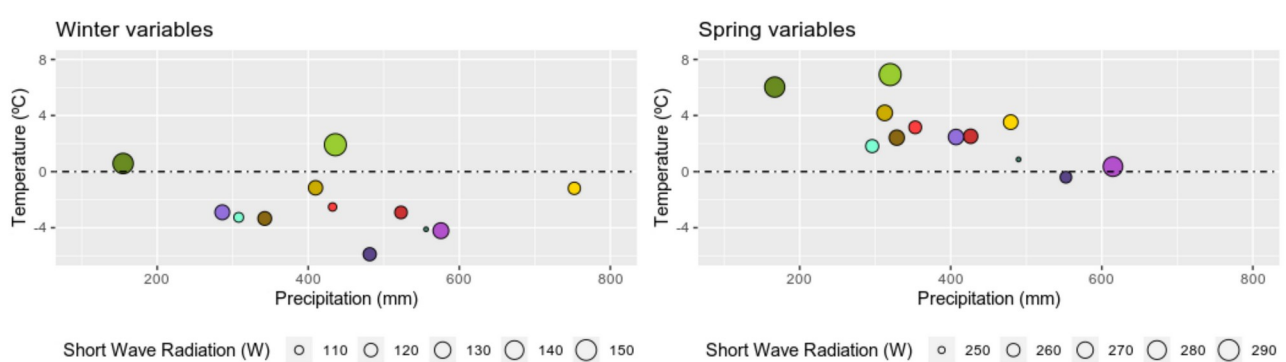


Figure 4: Mean values for accumulated precipitation, mean daily temperature, and mean daily short-wave radiation for each cluster centroid in winter and spring. The colors indicate the clusters for the mountain ranges shown in Figure 3.

The contrasting initial climatological conditions of the cluster centroids explain their different snowpack energy balances. Figure 5 shows the average heat fluxes for the selected areas under non perturbed climatic conditions (over the time steps when the snowpack was present), obtained from the outputs of the FSM2 simulation. In general, under colder conditions (mountain areas having lower temperature or at higher elevations) the values for incoming and outgoing heat fluxes were lower than for warmer areas. Figure 5 shows there was considerable variety of partitions of the snowpack energy balance, which potentially will lead to contrasted sensitivities of snowpack when temperature, short-wave incoming radiation and precipitation will be perturbed.

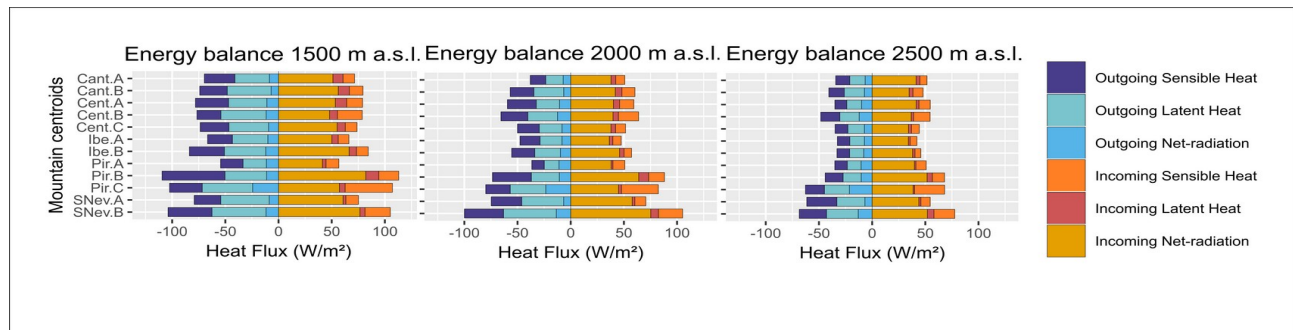


Figure 5: Average energy fluxes for each centroid at various elevations.

4.2 Sensitivity of the snowpack duration and peak SWE to precipitation, short wave radiation, and temperature change

Remarkable differences were found in the sensitivity of the duration of the snowpack to temperature increase over the study areas (Fig. 6: Upper panels). In general, there was a clear decrease in the sensitivity of the duration of the snowpack to temperature increase with increasing elevation, particularly in colder areas (see Section 4.1). For most of the mountain ranges the sensitivity of the duration of the snowpack ranged from -20 to -25% per °C at elevations of 1500 m a.s.l. and 2000 m a.s.l. The exceptions were the Pyrenees A and B and the Cantabrian Range A, which showed values ranging from -11 to -18% per °C. At the 2500 m a.s.l. elevation band, most of the values decreased from -5 to -15% per °C, except in the Sierra Nevada, where the values remained approximately -20 % per °C.

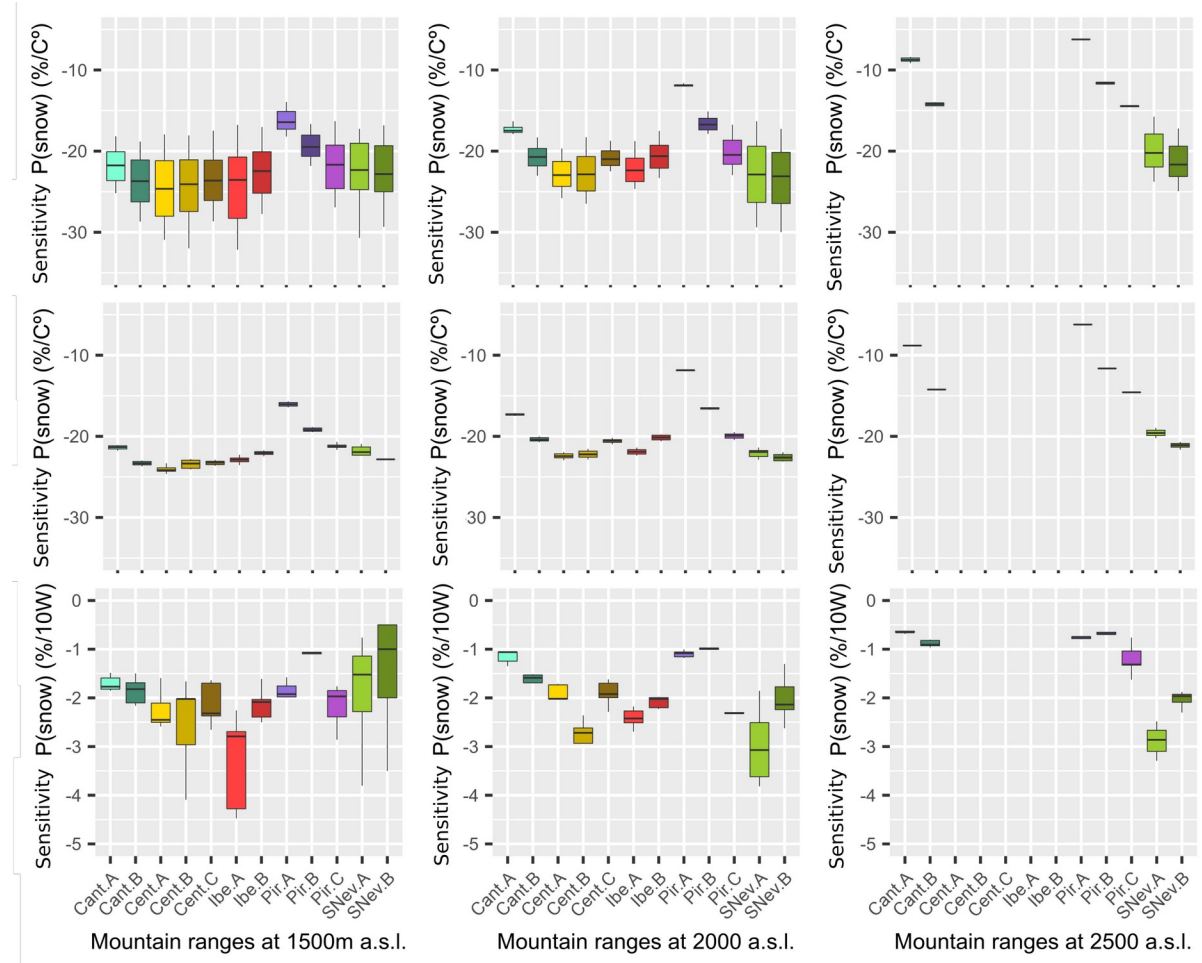


Figure 6: Sensitivity of snow duration to climate perturbations at 1500 (left), 2000 (center) and 2500 (right) m a.s.l. elevation bands. Upper panels) Average sensitivity per $^{\circ}\text{C}$ warming: the boxplots represent the uncertainty caused by a $\pm 20\%$ perturbation in precipitation. Central panels) Average sensitivity per $^{\circ}\text{C}$ warming: the boxplots represent the uncertainty caused by a $+0-40 \text{ Wm}^{-2}$ of perturbation in short-wave radiation increase. Bottom panels) Average sensitivity per 10 Wm^{-2} short-wave radiation increase: the boxplots represents the uncertainty caused by a $\pm 20\%$ perturbation in precipitation. The colors of the boxplots correspond to the selected areas in figures 3 and 4.

The effects of variation in precipitation on the sensitivity of the duration of the snowpack decreased markedly with increasing elevation of the centroids (Fig. 6: Upper panels); the exception was the Sierra Nevada, which was the warmest among the study mountain ranges (i.e. warmer initial

conditions). The effect of short-wave radiation variability on the duration of the snowpack was less than that caused by variations in temperature, with little effect induced by variation in the precipitations(Fig. 6: Central panels). The effect of solar radiation on the snowpack tended to be less at higher elevations, with values for the majority of centroids ranging from -1 to -3% per 10 Wm⁻² at 1500 m a.s.l., and 0.5–1.5 % per 10 Wm⁻² at 2500 m a.s.l (Fig. 6: Bottom panels)..

The effect of short-wave radiation on the peak SWE was similar to, but less than, its effect on the duration of the snowpack (Fig. 7: Bottom panels), ranging from -1 to -2% per 10 Wm⁻². With increasing elevation its effect on the peak SWE decreased, but to a lesser extent compared with its effect on snowpack duration. Thus, variability in the sensitivity of peak SWE to precipitation variability was similar over all elevation bands, for both increasing temperature (Fig. 7: Upper panels) and short-wave radiation (Fig. 7: Central panels). Nevertheless, the effect of temperature increases on the duration of the snowpack and peak SWE was negative for all centroids, and for all elevation bands over the simulation ranges for precipitation and short-wave radiation. These results suggest a generalized reduction in the magnitude and duration of the snowpack at all the elevation bands, even under higher precipitation conditions.

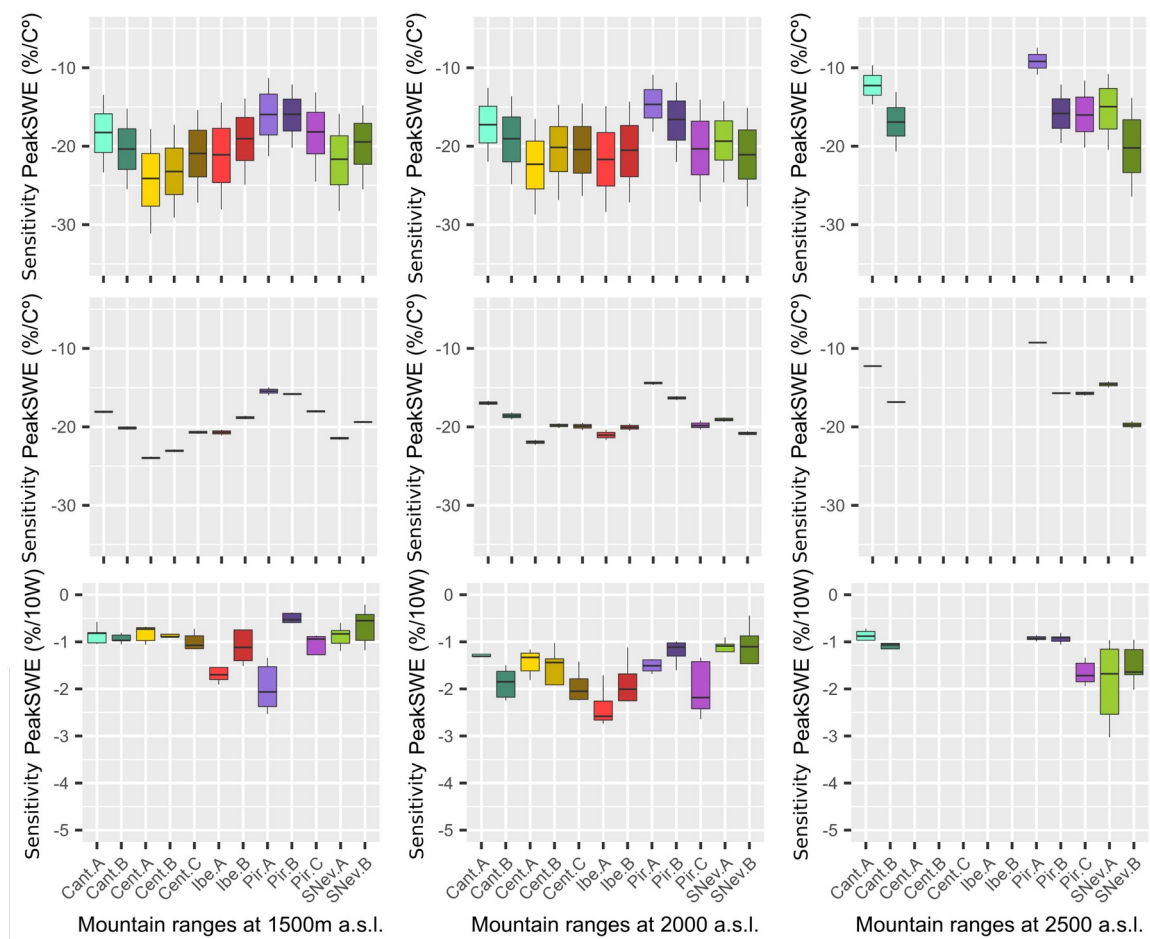


Figure 7: Sensitivity of peak SWE to climate perturbations at 1500 (left), 2000 (center) and 2500 (right) m a.s.l. elevation bands. Upper panels) Average sensitivity per °C warming: the boxplots represent the uncertainty caused by a ± 20% perturbation in precipitation. Central panels) Average sensitivity per °C warming: the boxplots represent the uncertainty caused by a +0-40 Wm⁻² of perturbation in short-wave radiation increase. Bottom panels) Average sensitivity per 10 Wm⁻² short-wave radiation increase: the boxplots represents the uncertainty caused by a ± 20% perturbation in precipitation. The colors of the boxplots correspond to the selected areas in figures 3 and 4.

The mean initial temperature conditions, before the perturbations, explained most of the variability in the sensitivity of the duration of the snowpack and the peak SWE (Table 1). Thus, the correlation values between the mean temperature at 2000 m a.s.l. and the snow indices were $R = -0.67$ and $R = -0.57$ for the snow duration and peak SWE sensitivity, respectively. The correlation sign suggest that at warmer initial conditions, higher negative sensitivities are expected. The other main

meteorological variables involved in the energy and mass balance of the snowpack had lower and non-significant correlation values.

Table 1: Pearson's R values between the initial conditions of the meteorological variables and the snow indices. The asterisk marks the significant correlations ($pvalue < 0.05$).

	Snow duration sensitivity	Peak SWE sensitivity
Mean temperature	-0.67	-0.57
Accumulated precipitation	-0.27	0.10
Mean short-wave radiation	-0.3	-0.24

4.3 Effect of temperature variability on the snowmelt rate

The average sensitivity of the melt rates per °C of warming was negative for all elevation bands in most mountain ranges, but there was wide variability (Fig. 8). Thus, a generalized decrease in the melt rate of snowmelt is expected under future warmer conditions. At the 1500 m a.s.l. elevation band the melt rates ranged from a minimum of -22% per °C in the Central Range A to a maximum of 7% per °C in the Cantabrian Range A. At the 2000 m a.s.l. band the values ranged from -21% per °C in the Sierra Nevada B to 4% per °C in the Pyrenees B and the Central Range B. At the 2500 m a.s.l. elevation band the values ranged from -16% per °C in the Pyrenees A to 6% per °C in the Sierra Nevada A. The results suggest a decrease in variability among the various mountain areas at the highest elevation.

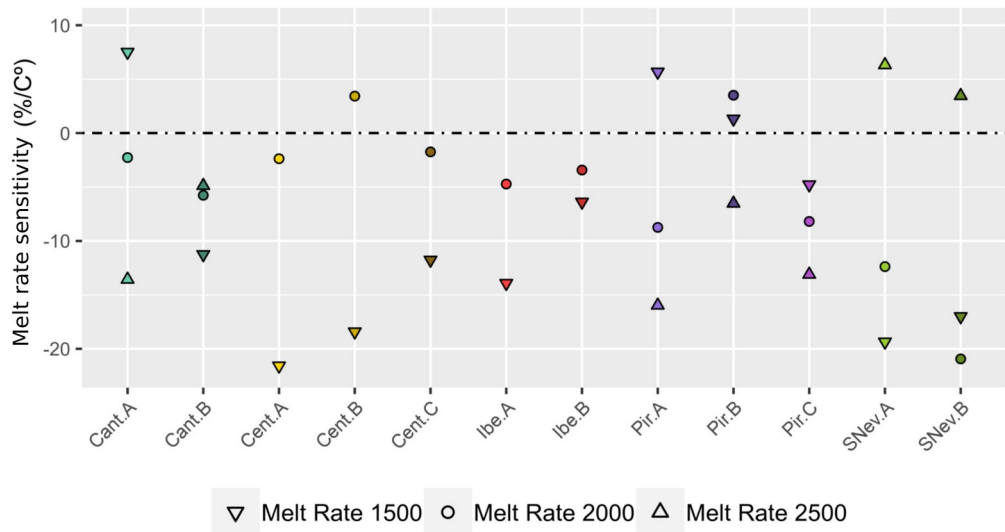


Figure 8: Effect of 1 °C temperature increase on the melt rates.

Figure 9 shows the linear and partial correlations between the melt rates and the peak SWE and the day on which the peak SWE occurred. The partial correlation values decreased with increasing elevation, from $R = 0.79$ for peak SWE and $R = 0.69$ for the date of occurrence of peak SWE at 1500 m a.s.l., to $R = -0.31$ and $R = 0.2$, respectively, at 2500 m a.s.l. Thus, at lower elevations the melt rate was lower for higher (later) peak SWE values, but this was not the case at higher elevations.

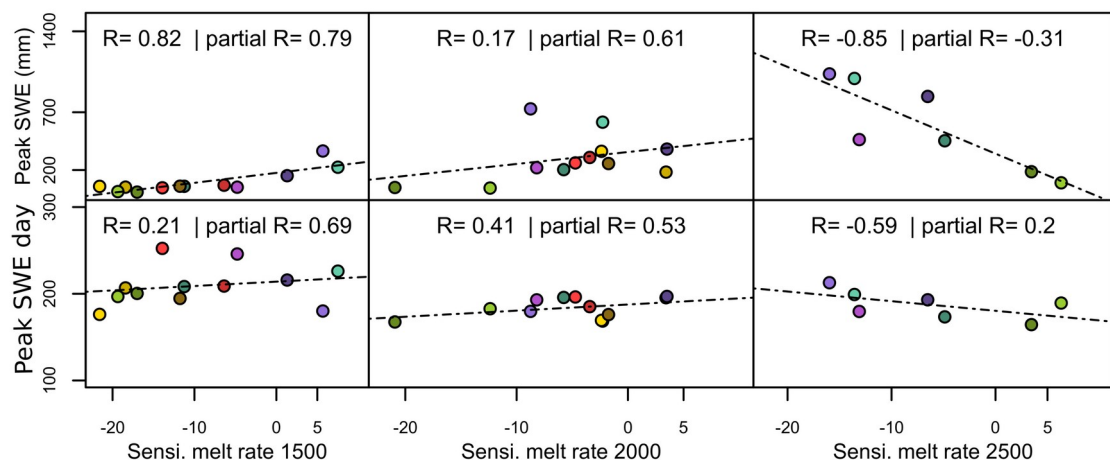


Figure 9: Linear and partial correlations between the melt rate and the magnitude of the peak SWE and the hydrological Julian day on which the peak SWE occurred at 1500 (left), 2000 (center) and 2500 m a.s.l.

5 Discussion

The effect of temperature warming, increased short-wave radiation, and precipitation change on the snowpack was analyzed for mountains of the Iberian Peninsula. Meso-atmospheric simulations have been shown to be useful in situations such as this, where there is a generalized lack of in situ observations. The high resolution of the meso-atmospheric simulation used in this study combined with the methodology proposed by Alonso-González et al. (2018) provided a complete database of physically consistent meteorological data. We classified the mountain areas into climatologically similar zones to reduce computational cost and simplify the presentation of results. The approach of combining a reduction of dimensions using a PCA with the automatic classification of the k-means cluster algorithm has been previously applied to the regionalization of homogeneous climatological areas in various places worldwide (Baeriswyl and Rebetez, 1997; Fovell and Fovell, 1993). Moreover, K-means clustering has also been used to detect homogeneous climatology regions from atmospheric model outputs (Carvalho et al., 2016). This combination of techniques has previously been successfully applied to the Iberian Peninsula in tests of its potential to automatically detect similar climatological areas (Muñoz-Díaz and Rodrigo, 2004). We applied the PCA/K-means methodology to separate the main climatological regions in each mountain range. The selection of centroids of clusters as representative of the entire cluster has obvious implications, as the cluster cells that fall far from the centroid are not represented. However, the aim of this study was to describe the sensitivity of the snowpack at a regional scale in the Iberian Peninsula; this was achieved as the averaged climatologies for the identified centroids covered a wide range of variability (Fig. 4), encompassing most of the climatological variability of the mountains of the Iberian Peninsula.

Despite the obvious uncertainties in meso-atmospheric simulations, the representative areas found in this study (Figs. 3 and 4) using the PCA/K-means have also been identified in previous studies. For instance, for the Cantabrian Range there were marked differences in the amounts and variability of precipitation between the two sides along its main longitudinal axis, as a consequence of the Atlantic Ocean influence, which mainly affect the northern part (Marzol Jaén et al., 1996; Ortega Villazán and Morales Rodríguez, 2015). Similarly, for the Central Range there were major differences between the northern and southern areas (Durán et al., 2015, 2013). We found a differentiated climatological area in the south-western part of the Central Range, which has been reported to be one of the wettest areas of the Iberian Peninsula, and this contrasted with the other

areas of the mountain range (Ceballos-Barbancho et al., 2018; Palacios and De Marcos, 1998). We also differentiated two climatological areas in the Iberian Range, which reflect the blocking of the Atlantic air masses (Jiménez et al., 2009). Our findings are consistent with earlier studies of the climate of the Pyrenees that identified a north-western part having a strong Atlantic influence and a south-eastern part having a strong Mediterranean influence (Buisan et al., 2016; Gascoin et al., 2015; López-Moreno et al., 2017). This was represented in our analyses by three areas, one generally aggregating the Mediterranean area, a second the Atlantic area, and a third the transitional zone. Despite the small size of the Sierra Nevada, marked differences between its north-western and south-eastern slopes have been reported, and these have clear similarities with our results. Thus, the clusters found in this study cover the climatological patterns of the main ranges of the Iberian Peninsula.

The sensitivity of the duration of the snowpack and the peak SWE to temperature increase showed marked differences. More specifically, the results suggest a slightly higher variability in the sensitivity of peak SWE compared with snow duration, although both tended to be more sensitive in the warmer mountain areas, as previously reported for the western USA(Pierce et al., 2013). This was particularly evident in the comparison between the Pyrenees A (north-western region, one of the coldest zones) and the much warmer two zones of the Sierra Nevada (Figs. 6 and 7). This decrease in sensitivity was also observed with change in elevation within each of the zones, as has previously been observed in earlier studies of the maritime mountainous areas of the Cascades Range (Jefferson, 2011; Sproles et al., 2013) and the Alps (Marty et al., 2017). The sensitivity of the snowpack to increased temperature caused by changes in precipitation depended on the elevation. Thus, the effect on the snow duration decreased with increasing elevation in all the study areas. This finding is consistent with that of López-Moreno et al. (2017) for a set of mountains having a Mediterranean climate, using forcing data previously rescaled to an elevation band where the mean temperature from December to March is -2 °C; this showed little change in the sensitivity of the snowpack for all precipitation variability tested. The sensitivity of the peak SWE caused by precipitation variability was less obvious, as precipitation changes have a major role over the entire elevation gradient. However, despite the variability found, the effect on both the peak SWE and snowpack duration was negative even under the higher precipitation scenarios, with an increase in precipitation up to +20% unable to counteract the effect of temperature increase.

The sensitivity of the snowpack duration and peak SWE to increasing short-wave radiation was less than that for temperature increase. This is because, despite the consistent positive trends on the

observed downward short-wave radiation (Sanchez-Lorenzo et al., 2013; Vicente-Serrano et al., 2017), the increase in short-wave radiation represented a minor addition to the current level of short-wave radiation. However, the effect of short-wave radiation needs to be considered, as it can reduce the snow duration by 2% for every 10 Wm⁻² at low elevations, even though its effect is reduced at higher elevations. Radiation has clear repercussions for the peak SWE and duration of the snowpack if the current trends continue. Peak SWE was less sensitive to increasing short-wave radiation than was the snowpack duration. This is probably because of the date of occurrence of the peak SWE, which occurred when the total short-wave radiation was low relative to the end of the snow season, and the snowpack has high albedo as a consequence of fresh snow cover (Baker et al., 1990). The effect of short-wave radiation on melting of the snowpack is strongly controlled by the characteristics of the terrain (DeBeer and Pomeroy, 2017). Thus, the values obtained suggest increasing heterogeneity of the melt rates, with greater increases in the most exposed areas.

The effect of temperature on the melt rates was negative in most cases. This suggests a generalized increase in the length of the melt season, and shorter periods of snow accumulation. The decrease in the melt rates suggest uncharted questions on mountain hydrology, with many downstream hydrological implications that future works should investigate in depth. For example the snowpack controls the streamflow of the Pyrenees (López-Moreno and García-Ruiz, 2004), which will be likely influenced by the decrease of the melt rates. This scenario could have implications in many key strategic fields as the hydropower production that has been proved to be sensitive to the snowpack in the Pyrenees (Gascoin et al., 2015). The extension of the melt periods will have unknown implications on other topics too, such as spring floods, soil moisture or water resources availability. This finding is consistent with other studies that have found slower melt rates under warmer conditions (Musselman et al., 2017). Nevertheless, wide variability in the effect on melt rates was also found. Some areas showed a positive effect on melt rates, suggesting an acceleration of the melt rates in a warmer climate. We found that this effect was partially explained at the lowest and mid elevations by the peak SWE and the date of occurrence of the peak SWE, with higher negative values in places having a lower snowpack elevation and an earlier date of peak SWE occurrence. A similar hypothesis was proposed by Trujillo and Molotch (2014) for the western USA.

The present study involved uncertainties that need to be considered. Meso-atmospheric simulations have limitations arising from the parameterization and errors in the forcing data. Furthermore, the methodology proposed by Alonso-González et al. (2018) involves a number of assumptions, as

explained above. Nevertheless, this methodology has proven to be a computationally affordable and appropriate tool for regional and local scale studies in locations where there is a generalized lack of data (Alonso-González et al., 2019a, 2019b; Ceballos-Barbancho et al., 2018; Sanmiguel-Vallelado et al., 2019). The results indicate the regional sensitivity of the snowpack of the main mountain ranges of the Iberian Peninsula. The findings are useful in understanding the potential evolution of the snowpack over the Iberian Peninsula, and suggest how the snowpack will respond under the various climate projections and different proposed scenarios. The results also have clear implications for the potential impacts of climate change on land and water management.

6 Conclusions

The output of a meso-atmospheric model (WRF) was used as forcing data in a physically-based energy and mass balance snow model (FSM2) to study the sensitivity of the snowpack to increasing temperature and short-wave radiation at various elevations under differing precipitation scenarios. The sensitivity of the snowpack to climate warming was considerable, with estimated reductions ranging on average from -23% per °C at 1500 m a.s.l. to -13% per °C at 2500 m a.s.l. for the duration of the snowpack, and -20% per °C at 1500 m a.s.l. to -15% per °C at 2500 m a.s.l. for the peak snow water equivalent, and -9% per °C to -6% per °C for the melt rates. The major distinction among the mountain areas was closely related to initial climatic conditions, with the warmer areas being more sensitive than the colder areas. This was also the case within each mountain range, with decreasing sensitivity with increasing elevation. Although precipitation variability introduced marked variability in the response of snowpack to increasing temperature and solar radiation, the snow duration and peak SWE decreased even under the wettest scenarios. The sensitivity of the snowpack to increased short-wave radiation was less than that in response to temperature increase across the ranges tested. However, the effect of short-wave radiation should not be neglected. Melt rates are expected to decrease in most of the study areas if temperature increases, but there are particular sites where an opposite response may occur, including sites having a deeper snow pack.

Acknowledgments. Esteban Alonso-González is the recipient of a pre-doctoral FPI grant from the Spanish Ministry of Economy and Competitiveness (BES-2015-071466). This study was funded by the Spanish Ministry of Economy and Competitiveness project CGL2017-82216-R (HIDROIBERNIEVE). F. Navarro-Serano and A. Sanmiguel-Vallelado are recipients of pre-doctoral FPU grants (Spanish Ministry of Education, Culture and Sports).

References

- Alonso-González, E., López-Moreno, J.I., Gascoin, S., García-Valdecasas Ojeda, M., Sanmiguel-Vallelado, A., Navarro-Serrano, F., Revuelto, J., Ceballos, A., Esteban-Parra, M.J., Essery, R., 2018. Daily gridded datasets of snow depth and snow water equivalent for the Iberian Peninsula from 1980 to 2014. *Earth Syst. Sci. Data* 10, 303–315. <https://doi.org/10.5194/essd-10-303-2018>
- Alonso-González, E., López-Moreno, J.I., Navarro-Serrano, F.M., Revuelto, J., 2019b. Impact of North Atlantic Oscillation on the Snowpack in Iberian Peninsula Mountains. *Water* 12, 105. <https://doi.org/10.3390/w12010105>
- Alonso-González, E., López-Moreno, J.I., Navarro-Serrano, F., Sanmiguel-Vallelado, A., Revuelto, J., Domínguez-Castro, F., Ceballos, A., 2019a. Snow climatology for the mountains in the Iberian Peninsula using satellite imagery and simulations with dynamically downscaled reanalysis data. *Int. J. Climatol.* joc.6223. <https://doi.org/10.1002/joc.6223>
- Baeriswyl, P.A., Rebetez, M., 1997. Regionalization of precipitation in Switzerland by means of principal component analysis. *Theor. Appl. Climatol.* 58, 31–41. <https://doi.org/10.1007/BF00867430>
- Baker, D.G., Ruschy, D.L., Wall, D.B., 1990. The Albedo Decay of Prairie Snows. *J. Appl. Meteorol.* 29, 179–187. [https://doi.org/10.1175/1520-0450\(1990\)029<0179:TADOPS>2.0.CO;2](https://doi.org/10.1175/1520-0450(1990)029<0179:TADOPS>2.0.CO;2)
- Barnett, T.P., Adam, J.C., Lettenmaier, D.P., 2005. Potential impacts of a warming climate on water availability in snow-dominated regions. *Nature* 438, 303–309. <https://doi.org/10.1038/nature04141>
- Berrisford, P., Dee, D.P., Poli, P., Brugge, R., Fielding, K., Fuentes, M., Kållberg, P.W., Kobayashi, S., Uppala, S., Simmons, A., 2011. The ERA-Interim archive Version 2.0. *ERA Rep. Ser.*
- Buisan, S.T., López-Moreno, J.I., Saz, M.A., Kochendorfer, J., 2016. Impact of weather type variability on winter precipitation, temperature and annual snowpack in the Spanish Pyrenees. *Clim. Res.* 69. <https://doi.org/10.3354/cr01391>
- Carvalho, M.J., Melo-Gonçalves, P., Teixeira, J.C., Rocha, A., 2016. Regionalization of Europe based on a K-Means Cluster Analysis of the climate change of temperatures and precipitation. *Phys. Chem. Earth, Parts A/B/C* 94, 22–28. <https://doi.org/10.1016/J.PCE.2016.05.001>

Ceballos-Barbancho, A., Llorente-Pinto, J.M., Alonso-González, E., López-Moreno, J.I., 2018. Dinámica del manto de nieve en una pequeña cuenca de montaña mediterránea: el caso del río Tormes (Cuenca del Duero, España). Norte Gd. 71.

Charrad, M., Ghazzali, N., Boiteau, V., Niknafs, A., 2014. NbClust : An R Package for Determining the Relevant Number of Clusters in a Data Set. *J. Stat. Softw.* 61, 1–36. <https://doi.org/10.18637/jss.v061.i06>

Connolly, R., Connolly, M., Soon, W., Legates, D.R., Cionco, R.G., Herrera, V.M.V., 2019. Northern Hemisphere Snow-Cover Trends (1967–2018): A Comparison between Climate Models and Observations. *Geosciences* 9, 135. <https://doi.org/10.3390/geosciences9030135>

Côté, K., Madore, J.-B., Langlois, A., 2017. Uncertainties in the SNOWPACK multilayer snow model for a Canadian avalanche context: sensitivity to climatic forcing data. *Phys. Geogr.* 38, 124–142. <https://doi.org/10.1080/02723646.2016.1277935>

DeBeer, C.M., Pomeroy, J.W., 2017. Influence of snowpack and melt energy heterogeneity on snow cover depletion and snowmelt runoff simulation in a cold mountain environment. *J. Hydrol.* 553. <https://doi.org/10.1016/j.jhydrol.2017.07.051>

Dee, D.P., Uppala, S.M., Simmons, A.J., Berrisford, P., Poli, P., Kobayashi, S., Andrae, U., Balmaseda, M.A., Balsamo, G., Bauer, P., Bechtold, P., Beljaars, A.C.M., van de Berg, L., Bidlot, J., Bormann, N., Delsol, C., Dragani, R., Fuentes, M., Geer, A.J., Haimberger, L., Healy, S.B., Hersbach, H., Hólm, E. V., Isaksen, L., Kållberg, P., Köhler, M., Matricardi, M., McNally, A.P., Monge-Sanz, B.M., Morcrette, J.-J., Park, B.-K., Peubey, C., de Rosnay, P., Tavolato, C., Thépaut, J.-N., Vitart, F., 2011. The ERA-Interim reanalysis: configuration and performance of the data assimilation system. *Q. J. R. Meteorol. Soc.* 137, 553–597. <https://doi.org/10.1002/qj.828>

Durán, L., Rodríguez-Fonseca, B., Yagüe, C., Sánchez, E., 2015. Water vapour flux patterns and precipitation at Sierra de Guadarrama mountain range (Spain). *Int. J. Climatol.* 35, 1593–1610. <https://doi.org/10.1002/joc.4079>

Durán, L., Sánchez, E., Yagüe, C., 2013. Climatology of precipitation over the Iberian Central System mountain range. *Int. J. Climatol.* 33, 2260–2273. <https://doi.org/10.1002/joc.3602>

Essery, R., 2015. A factorial snowpack model (FSM 1.0). *Geosci. Model Dev.* 8, 3867–3876. <https://doi.org/10.5194/gmd-8-3867-2015>

- Fayad, A., Gascoin, S., Faour, G., López-Moreno, J.I., Drapeau, L., Page, M. Le, Escadafal, R., 2017. Snow hydrology in Mediterranean mountain regions: A review. *J. Hydrol.* 551, 374–396. <https://doi.org/10.1016/j.jhydrol.2017.05.063>
- Fovell, R.G., Fovell, M.Y.C., 1993. Climate zones of the conterminous United States defined using cluster analysis. *J. Clim.* 6, 2103–2135. [https://doi.org/10.1175/1520-0442\(1993\)006<2103:CZOTCU>2.0.CO;2](https://doi.org/10.1175/1520-0442(1993)006<2103:CZOTCU>2.0.CO;2)
- García-Ruiz, J.M., López-Moreno, J.I., Vicente-Serrano, S.M., Lasanta-Martínez, T., Beguería, S., 2011. Mediterranean water resources in a global change scenario. *Earth-Science Rev.* 105, 121–139. <https://doi.org/10.1016/j.earscirev.2011.01.006>
- García-Valdecasas Ojeda, M., Gámiz-Fortis, S.R., Castro-Díez, Y., Esteban-Parra, M.J., 2017. Evaluation of WRF capability to detect dry and wet periods in Spain using drought indices. *J. Geophys. Res. Atmos.* 122, 1569–1594. <https://doi.org/10.1002/2016JD025683>
- Gascoin, S., Hagolle, O., Huc, M., Jarlan, L., Dejoux, J.-F., Szczypta, C., Martí, R., Sánchez, R., 2015. A snow cover climatology for the Pyrenees from MODIS snow products. *Hydrol. Earth Syst. Sci.* 19, 2337–2351. <https://doi.org/10.5194/hess-19-2337-2015>
- Gilaberte-Búrdalo, M., López-Martín, F., Pino-Otín, M.R., López-Moreno, J.I., 2014. Impacts of climate change on ski industry. *Environ. Sci. Policy* 44, 51–61. <https://doi.org/10.1016/j.envsci.2014.07.003>
- Gilaberte-Búrdalo, M., López-Moreno, J.I., Morán-Tejeda, E., Jerez, S., Alonso-González, E., López-Martín, F., Pino-Otín, M.R., 2017. Assessment of ski condition reliability in the Spanish and Andorran Pyrenees for the second half of the 20th century. *Appl. Geogr.* 79, 127–142. <https://doi.org/10.1016/j.apgeog.2016.12.013>
- Harder, P., Pomeroy, J.W., 2014. Hydrological model uncertainty due to precipitation-phase partitioning methods. *Hydrol. Process.* 28, 4311–4327. <https://doi.org/10.1002/hyp.10214>
- Harpold, A.A., Brooks, P.D., 2018. Humidity determines snowpack ablation under a warming climate. *Proc. Natl. Acad. Sci. U. S. A.* 115, 1215–1220. <https://doi.org/10.1073/pnas.1716789115>
- Hartigan, J.A., Wong, M.A., 1979. Algorithm AS 136: A K-Means Clustering Algorithm. *Appl. Stat.* 28, 100. <https://doi.org/10.2307/2346830>

Jefferson, A.J., 2011. Seasonal versus transient snow and the elevation dependence of climate sensitivity in maritime mountainous regions. *Geophys. Res. Lett.* 38, n/a-n/a. <https://doi.org/10.1029/2011GL048346>

Jiménez, P.A., González-Rouco, J.F., Montávez, J.P., García-Bustamante, E., Navarro, J., 2009. Climatology of wind patterns in the northeast of the Iberian Peninsula. *Int. J. Climatol.* 29, 501–525. <https://doi.org/10.1002/joc.1705>

Knutti, R., Sedláček, J., 2013. Robustness and uncertainties in the new CMIP5 climate model projections. *Nat. Clim. Chang.* 3, 369–373. <https://doi.org/10.1038/nclimate1716>

Liston, G.E., Elder, K., 2006. A Meteorological Distribution System for High-Resolution Terrestrial Modeling (MicroMet). *J. Hydrometeorol.* 7, 217–234. <https://doi.org/10.1175/JHM486.1>

López-Moreno, J.I., Beniston, M., García-Ruiz, J.M., 2008. Environmental change and water management in the Pyrenees: Facts and future perspectives for Mediterranean mountains. *Glob. Planet. Change* 61. <https://doi.org/10.1016/j.gloplacha.2007.10.004>

López-Moreno, J.I., García-Ruiz, J.M., 2004. Influence of snow accumulation and snowmelt on streamflow in the central Spanish Pyrenees. *Hydrol. Sci. J.* 49.

López-Moreno, J.I., Gascoin, S., Herrero, J., Sproles, E.A., Pons, M., Alonso-González, E., Hanich, L., Boudhar, A., Musselman, K.N., Molotch, N.P., Sickman, J., Pomeroy, J., 2017. Different sensitivities of snowpacks to warming in Mediterranean climate mountain areas. *Environ. Res. Lett.* 12. <https://doi.org/10.1088/1748-9326/aa70cb>

López-Moreno, J.I., Goyette, S., Beniston, M., 2009. Impact of climate change on snowpack in the Pyrenees: Horizontal spatial variability and vertical gradients. *J. Hydrol.* 374, 384–396. <https://doi.org/10.1016/j.jhydrol.2009.06.049>

López-Moreno, J.I., Revuelto, J., Gilaberte, M., Morán-Tejeda, E., Pons, M., Jover, E., Esteban, P., García, C., Pomeroy, J.W., 2013. The effect of slope aspect on the response of snowpack to climate warming in the Pyrenees. *Theor. Appl. Climatol.* 117. <https://doi.org/10.1007/s00704-013-0991-0>

López-Moreno, J.I., Vicente-Serrano, S.M., Morán-Tejeda, E., Lorenzo-Lacruz, J., Kenawy, A., Beniston, M., 2011. Effects of the North Atlantic Oscillation (NAO) on combined temperature and precipitation winter modes in the Mediterranean mountains: Observed relationships and projections

for the 21st century. *Glob. Planet. Change* 77, 62–76.
<https://doi.org/10.1016/j.gloplacha.2011.03.003>

Marsh, C.B., Pomeroy, J.W., Spiteri, R.J., 2012. Implications of mountain shading on calculating energy for snowmelt using unstructured triangular meshes. *Hydrol. Process.* 26, 1767–1778. <https://doi.org/10.1002/hyp.9329>

Marty, C., Schlogl, S., Bavay, M., Lehning, M., 2017. How much can we save? Impact of different emission scenarios on future snow cover in the Alps. *Cryosph.* 11, 517–529. <https://doi.org/10.5194/tc-11-517-2017>

Marzol Jaén, V., Dorta, P., Valladares, P., 1996. La distribución de las precipitaciones en una montaña oceánica: la Cordillera Cantábrica., Clima y Agua. ed, Clima y agua. La gestión de un recurso climático, 1996, ISBN 9788479521721, págs. 49-63. Universidad de La Laguna, La Laguna.

Monjo, R., Gaitán, E., Pórtoles, J., Ribalaygua, J., Torres, L., 2016. Changes in extreme precipitation over Spain using statistical downscaling of CMIP5 projections. *Int. J. Climatol.* 36, 757–769. <https://doi.org/10.1002/joc.4380>

Muñoz-Díaz, D., Rodrigo, F.S., 2004. Spatio-temporal patterns of seasonal rainfall in Spain (1912–2000) using cluster and principal component analysis: Comparison. *Ann. Geophys.* 22, 1435–1448. <https://doi.org/10.5194/angeo-22-1435-2004>

Musselman, K.N., Clark, M.P., Liu, C., Ikeda, K., Rasmussen, R., 2017. Slower snowmelt in a warmer world. *Nat. Clim. Chang.* 7, 214–219. <https://doi.org/10.1038/nclimate3225>

Ortega Villazán, M.T., Morales Rodríguez, C.G., 2015. El clima de la Cordillera Cantábrica castellano-leonesa: diversidad, contrastes y cambios. *Investig. Geográficas* 0, 45–67. <https://doi.org/10.14198/INGEO2015.63.04>

Palacios, D., De Marcos, J., 1998. Geomorphologic hazards in a glaciated granitic massif: Sierra de Gredos, Spain, in: Geomorphological Hazards in High Mountain Areas. Springer, pp. 285–307.

Pierce, D.W., Cayan, D.R., Pierce, D.W., Cayan, D.R., 2013. The Uneven Response of Different Snow Measures to Human-Induced Climate Warming. *J. Clim.* 26, 4148–4167. <https://doi.org/10.1175/JCLI-D-12-00534.1>

Polo, M.J., Herrero, J., Pimentel, R., Pérez-Palazón, M.J., 2019. The Guadaleo Monitoring Network (Sierra Nevada, Spain): 14 years of measurements to understand the complexity of snow dynamics in semiarid regions. *Earth Syst. Sci. Data* 11, 393–407. <https://doi.org/10.5194/essd-11-393-2019>

Pons, M., López-Moreno, J.I., Rosas-Casals, M., Jover, È., 2015. The vulnerability of Pyrenean ski resorts to climate-induced changes in the snowpack. *Clim. Change* 131. <https://doi.org/10.1007/s10584-015-1400-8>

Raleigh, M.S., Livneh, B., Lapo, K., Lundquist, J.D., Raleigh, M.S., Livneh, B., Lapo, K., Lundquist, J.D., 2016. How Does Availability of Meteorological Forcing Data Impact Physically Based Snowpack Simulations? *J. Hydrometeorol.* 17, 99–120. <https://doi.org/10.1175/JHM-D-14-0235.1>

Rasouli, K., Pomeroy, J.W., Janowicz, J.R., Carey, S.K., Williams, T.J., 2014. Hydrological sensitivity of a northern mountain basin to climate change. *Hydrol. Process.* 28, 4191–4208. <https://doi.org/10.1002/hyp.10244>

Rasouli, K., Pomeroy, J.W., Marks, D.G., 2015. Snowpack sensitivity to perturbed climate in a cool mid-latitude mountain catchment. *Hydrol. Process.* 29, 3925–3940. <https://doi.org/10.1002/hyp.10587>

Revuelto, J., Azorin-Molina, C., Alonso-González, E., Sanmiguel-Vallelado, A., Navarro-Serrano, F., Rico, I., Ignacio López-Moreno, J., 2017. Meteorological and snow distribution data in the Izas Experimental Catchment (Spanish Pyrenees) from 2011 to 2017. *Earth Syst. Sci. Data* 9. <https://doi.org/10.5194/essd-9-993-2017>

Sanchez-Lorenzo, A., Calbó, J., Wild, M., 2013. Global and diffuse solar radiation in Spain: Building a homogeneous dataset and assessing their trends. *Glob. Planet. Change* 100, 343–352. <https://doi.org/10.1016/J.GLOPLACHA.2012.11.010>

Sanmiguel-Vallelado, A., Camarero, J.J., Gazol, A., Morán-Tejeda, E., Sangüesa-Barreda, G., Alonso-González, E., Gutiérrez, E., Alla, A.Q., Galván, J.D., López-Moreno, J.I., 2019. Detecting snow-related signals in radial growth of *Pinus uncinata* mountain forests. *Dendrochronologia* 57, 125622. <https://doi.org/10.1016/J.DENDRO.2019.125622>

Sanmiguel-Vallelado, A., Morán-Tejeda, E., Alonso-González, E., López-Moreno, J.I., 2017. Effect of snow on mountain river regimes: an example from the Pyrenees 1–16. <https://doi.org/10.1007/s11707-016-0630-z>

Skamarock, W.C., Klemp, J.B., Dudhia, J., Gill, D.O., Barker, D.M., Dudha, M.G., Huang, X., Wang, W., Powers, Y., 2008. A Description of the Advanced Research WRF Version 3. NCAR Tech. Note. <https://doi.org/10.5065/D68S4MVH>

Slater, A.G., Barrett, A.P., Clark, M.P., Lundquist, J.D., Raleigh, M.S., 2013. Uncertainty in seasonal snow reconstruction: Relative impacts of model forcing and image availability. *Adv. Water Resour.* 55, 165–177. <https://doi.org/10.1016/J.ADVWATRES.2012.07.006>

Sospedra-Alfonso, R., Melton, J.R., Merryfield, W.J., 2015. Effects of temperature and precipitation on snowpack variability in the Central Rocky Mountains as a function of elevation. *Geophys. Res. Lett.* 42. <https://doi.org/10.1002/2015GL063898>

Sproles, E.A., Nolin, A.W., Rittger, K., Painter, T.H., 2013. Climate change impacts on maritime mountain snowpack in the Oregon Cascades. *Hydrol. Earth Syst. Sci.* 17, 2581–2597. <https://doi.org/10.5194/hess-17-2581-2013>

Vicente-Serrano, S.M., Rodríguez-Camino, E., Domínguez-Castro, F., El Kenawy, A., Azorín-Molina, C., 2017. An updated review on recent trends in observational surface atmospheric variables and their extremes over Spain. *Cuad. Investig. Geográfica* 43, 209. <https://doi.org/10.18172/cig.3134>

Capítulo 6: Conclusiones

En la presente tesis doctoral se ha mejorado el conocimiento existente sobre el comportamiento del manto de nieve a escala regional en la península ibérica desde una perspectiva climatológica. Para ello se han estudiado tanto el comportamiento actual y reciente del manto de nieve como su sensibilidad a los cambios climáticos. Este estudio se ha realizado en cuatro fases bien diferenciadas, en las que primeramente se ha generado una base de datos mediante el uso de modelos de base física, con el objetivo de suplir la generalizada falta de información disponible. Después se utilizó esta base de datos para realizar la primera climatología del manto de nieve de la península ibérica estudiando también en una fase posterior cómo el índice de telecomunicación NAO se relaciona con la duración y acumulación del manto de nieve. Finalmente, se ha estudiado la sensibilidad del manto de nieve a los cambios de temperatura, precipitación y radiación en onda corta sobre diferentes puntos representativos de las principales cordilleras de la península ibérica.

La base de datos generada se ha realizado a partir de una simulación del modelo numérico mesoatmosférico WRF forzado por el reanálisis ERA-Interim a una resolución espacial de 0.088°, cubriendo el periodo de tiempo entre 1980 y 2014. La simulación de WRF fue proyectada a diferentes bandas altitudinales cubriendo el rango altitudinal entre los 500 y los 2900 m s.n.m para mejorar la representatividad de las variables meteorológicas sobre terreno complejo. A pesar de las insalvables incertidumbres asociadas al uso de modelos, la base de datos se ha mostrado consistente con las observaciones. Concretamente, la base de datos ha mostrado un error de 6.07% y un R^2 de 0.76 en la estimación de probabilidad de existencia de nieve, cuando se ha comparado con la información proporcionada por el satélite MODIS. También se ha probado capaz de reproducir los patrones de variabilidad inter- e intranual del espesor del manto de nieve y SWE, con valores kappa por encima del 0.6 en prácticamente todos los percentiles de acumulación. De esta manera, la base de datos producida tiene potencial para realizar multitud de estudios relacionados con el manto de nieve, en un contexto de casi no existencia de datos observados, y mucho menos de una duración semejante. La base de datos, así como la información usada para validar, se ha liberado siendo posible su utilización por cualquier interesado, pudiéndose descargar de <https://doi.org/10.5281/zenodo.854619>.

Los productos de nieve generados han permitido desarrollar la primera climatología del manto de nieve a nivel regional de la península ibérica. Los resultados han mostrado la gran variabilidad

espacial y temporal del manto de nieve. Las diferencias entre cordilleras son importantes. El Pirineo y la Cordillera Cantábrica, han mostrado los mantos de nieve más duraderos y de mayor espesor, aunque hay que matizar que la superficie del Pirineo con grandes acumulaciones es muy superior. De hecho, a consecuencia de su gran extensión y posición geográfica entre el Mediterráneo y el Atlántico, el Pirineo muestra la mayor variedad de mantos de nieve de todas las cordilleras de la península ibérica. Sierra Nevada ha mostrado los mantos de nieve menos profundos y efímeros, con un desplazamiento medio en altura de 500 m a.s.l. en duración y magnitud del manto de nieve en comparación con los Pirineos o la Cordillera Cantábrica. Por su parte, el Sistema Ibérico y el Central, han mostrado comportamientos intermedios entre Sierra Nevada y la Cordillera Cantábrica y el Pirineo, siendo mucho más próximos a estas dos últimas cordilleras. Las diferencias mostradas entre cordilleras no se pueden explicar simplemente por el gradiente latitudinal existente en la península ibérica, ya que la continentalidad, los patrones de precipitación y la influencia atlántica y mediterránea juegan un papel crucial para definir el comportamiento del manto de nieve.

Ya que el índice NAO ha probado tener una gran influencia en los patrones de temperatura superficial y precipitación de la península ibérica, hemos estudiado la influencia de éste en el manto de nieve de la península ibérica. Todas las cordilleras han mostrado una gran correlación entre el índice NAO de invierno y el máximo de acumulación anual por un lado y la duración de la temporada de nieve por otro. Gracias a la alta resolución de la base de datos generada, se han podido estudiar en detalle los patrones espaciales de la correlación, probándose que la influencia de la NAO es mucho más acusada en las vertientes expuestas a las advecciones favorecidas por las fases negativas de la NAO (vientos de suroeste y oeste). Sierra Nevada es la única cordillera donde no se han encontrado diferencias entre vertientes. Las condiciones húmedas pero templadas de estas advecciones explican un aumento generalizado de las correlaciones de la NAO con la duración y acumulación de nieve hacia las cotas más altas. Así, la dinámica del manto de nieve en las cotas más altas está más condicionada por el régimen pluviométrico que con el térmico, siendo el primero el más relacionado con la NAO. De la misma manera, se ha observado el papel que juega la longitud geográfica en las correlaciones observadas, demostrando que la influencia de la NAO disminuye por lo general en las zonas más orientales de las cordilleras. Los resultados abren la puerta a una posible predicción a largo plazo del manto de nieve en la península ibérica, además de demostrar la necesidad de series largas de nieve para el estudio de tendencias tanto temporales como espaciales.

En cuanto a la sensibilidad del manto de nieve a la variabilidad climática, hemos observado diferentes respuestas en la península ibérica. La sensibilidad del manto de nieve al calentamiento fue muy acusada, con valores que llegaron en algunos casos al 23% de reducción en la duración y 20% en el máximo acumulado por cada grado centígrado de incremento. Mientras que en otros sectores la sensibilidad se disminuyó al 13% de reducción en la duración y 15% en el máximo acumulado. Las mayores diferencias entre cordilleras están causadas principalmente por la climatología dominante de cada zona, que explica diferentes particiones del balance de energía del manto de nieve. Así, las zonas con condiciones más frías son menos sensibles, al igual que las cotas altas menos sensibles que las bajas. Cuando se simularon cambios en la precipitación se obtuvo una gran variabilidad en los valores de sensibilidad al calentamiento, especialmente en las zonas más cálidas o de menos elevación. Estos valores de sensibilidad al calentamiento son negativos incluso en los escenarios de mayor incremento de precipitación, lo que sugiere para el futuro una reducción generalizada de la duración y magnitud del manto de nieve, aunque se produjeran aumentos importantes de las precipitaciones. La sensibilidad del manto de nieve al incremento de radiación incidente en onda corta fue mucho menor que para los cambios en temperatura. A pesar de ello es importante tenerla en cuenta, ya que potencialmente puede reducir la duración y magnitud del manto de nieve entre un 1% y un 2% por 10 Wm^{-2} , lo que puede suponer un cambio significativo en el medio plazo si las actuales tendencias al incremento continúan. Este efecto se vuelve especialmente relevante si se suma al más que probable incremento térmico proyectado para todas las montañas peninsulares. La sensibilidad de las tasas de fusión fue negativa en prácticamente todas las zonas analizadas, lo que sugiere períodos de fusión más largos y menos intensos, que la bibliografía asocia a una menor producción de escorrentía en las zonas de cabecera.

Los resultados hallados en este trabajo dan pie a diferentes líneas de investigación de cara al futuro en el ámbito de la hidroclimatología de la península ibérica. Una vez estudiado el comportamiento del manto de nieve, y gracias a los datos generados, será posible estudiar en profundidad el efecto de la nieve en la hidrología de la península ibérica, así como prever cómo los cambios esperables en el manto de nieve a consecuencia del cambio climático pueden afectar a los recursos hídricos dependientes de la nieve. Por otro lado, existen multitud de índices de teleconexión aparte del índice NAO que influyen en el clima de la península ibérica. En ensayos previos hemos encontrado que, si bien el índice NAO es el que mejor explica los patrones de duración y máximos de acumulación del manto de nieve, otros índices de teleconexión son buenos indicadores de otros parámetros relacionados con la nieve, como pueden ser los eventos de nevadas extremos o la

concentración de las nevadas a lo largo del invierno, efectos interesantes desde el punto de vista climatológico o la gestión de los riesgos naturales. El interés despertado sobre los productos de nieve generados a partir de modelos atmosféricos y de balance de energía, así como los buenos resultados obtenidos mediante esta metodología, abren un amplio campo de trabajo en este ámbito, que puede aplicarse con fines científicos y operacionales a cualquier región fría del planeta. De esta manera, resultaría de gran interés la mejora de la base de datos mediante nuevas simulaciones climáticas que vayan surgiendo. Los más modernos productos de reanálisis actuales tienen un tiempo de actualización cercano al real, con tan solo unos días de retraso. Contando con suficientes recursos computacionales, este nuevo escenario permitiría la actualización de productos de nieve de alta resolución, así como de otras variables meteorológicas, prácticamente en tiempo real en el medio plazo. Además la mejora en distintas técnicas para la observación del clima y del manto de nieve en zonas remotas puede ayudar a mejorar los productos obtenidos mediante la aplicación de métodos de asimilación. Los productos obtenidos de este modo pueden ayudar a seguir avanzando en el conocimiento del manto de nieve a distintas escalas espaciales y su respuesta a cambios ambientales; además de proporcionar una información muy valiosa a geomorfólogos, hidrológos, ecológicos (estudios de fauna, flora y recursos forestales) y diversos ámbitos de la gestión del territorio.

Conclusions

In the current doctoral thesis, the existing knowledge on the behaviour of the snowpack at regional scale from a climatological perspective in the Iberian Peninsula has been improved. Thus, both the current behaviour of the snowpack and its sensitivity to climate change have been studied. This study has been carried out in four well-differentiated phases. Firstly, a snowpack database has been generated through the use of physically based models, to overcome the generalized lack of available observed snowpack data. Then, this database was used to develop the first snow climatology of the Iberian Peninsula, studying also in a later phase how the NAO index influences the duration and magnitude of the snowpack. Finally, the sensitivity of the snowpack to temperature increase, precipitation variability and short wave radiation rise has been studied over different representative areas of the main mountain ranges of the Iberian Peninsula.

The database generated has been developed from a mesoatmospheric simulation of the numerical model WRF forced by ERA-Interim reanalysis at a spatial resolution of 0.088° , covering the time period between 1980 and 2014. The WRF simulation was reprojected at different altitudinal bands covering the altitudinal range between 500 and 2900 m a.s.l. to improve the representativeness of the meteorological variables over complex terrain. Despite the uncertainties associated with the use of models, the database has been consistent with the observations. Specifically, the database has shown an error of 6.07% and an R^2 of 0.76 in the estimation of the probability of the existence of snow, when compared with the information provided by the MODIS sensors. It has also proved capable of reproducing the inter- and intrannual variability patterns of SD and SWE, with kappa values above 0.6 in most of the accumulation percentiles. Thus, the developed database has potential to conduct a multitude of snowpack studies, considering the generalized lack of observed data. The database, as well as the information used to validate it, has been freely released for use at <https://doi.org/10.5281/zenodo.854619>.

The snowpack database has allowed the development the first regional snowpack climatology of the Iberian Peninsula. The results have shown the great spatial and temporal variability of the snowpack with important differences between ranges. The Pyrenees and the Cantabrian Mountains have shown the longest lasting and thickest snowpack, although it should be noted that the surface of the Pyrenees with large accumulations is much larger. In fact, as a result of its great extension and geographical position between the Mediterranean and the Atlantic, the Pyrenees show the greatest variety of snowpack behaviours of all the mountain ranges of the Iberian Peninsula. Sierra Nevada

has shown the shallowest and most ephemeral snowpack, with an average displacement at altitude of 500 m a.s.l. in duration and magnitude of the snowpack compared to the Pyrenees or the Cantabrian Mountains. The Iberian and Central Systems have shown an intermediate behaviour between Sierra Nevada and the Cantabrian and Pyrenean mountain ranges, being much closer to the latter two. The differences shown between mountain ranges cannot be explained simply by the latitudinal gradient existing in the Iberian Peninsula, since continentality, precipitation patterns and the Atlantic and Mediterranean influence play a crucial role in defining the behaviour of the snowpack.

NAO index has proven to have a great influence on the surface temperature and precipitation patterns of the Iberian Peninsula. Thus, we have studied the influence of the NAO index on the snowpack of the Iberian Peninsula. All mountain ranges have shown high correlations between the winter NAO index and the maximum annual accumulation and duration of the snowpack. Thanks to the high resolution of the database generated, it has been possible to study in detail the spatial patterns of the correlation in detail. It was proved that the influence of the NAO is much more pronounced on the slopes exposed to the advections favoured by the negative phases of the NAO (southwest and west winds). Sierra Nevada is the only mountain range where no differences between slopes have been found. The humid but mild conditions of these advections explain a generalized increase in the correlation of the NAO with the duration and accumulation of snow towards the highest elevations. Thus, the dynamics of the snowpack at higher elevations is more conditioned by the rainfall regime than by the thermal regime, the former being more related to the NAO. Similarly, the role played by geographical longitude in the correlations has been studied, showing that the influence of the NAO generally decreases in the most eastern areas of the mountain ranges. The results provide a good starting point to potentially develop long-term prediction of the snowpack in the Iberian Peninsula. In addition, the results demonstrate the need of long term series of snow data for the study of both temporal and spatial trends.

We have observed different sensitivities of the snowpack to climatological variability over the Iberian Peninsula. The sensitivity of the snowpack to warming was very marked, reaching 23% of reduction in duration and 20% in the accumulated maximum for each °C of increase. While in other sectors the sensitivity was reduced to 13% reduction in duration and 15% in the accumulated maximum. The greatest differences between mountain ranges are caused mainly by the dominant climate of each zone, which explains different partitions of the energy balance of the snowpack. Thus, the areas with colder conditions are less sensitive, as the higher elevations are less sensitive

than the lower ones. When changes in precipitation were simulated, a great variability in the sensitivity values to warming was obtained, especially in the warmer or lower elevation areas. These values of sensitivity to warming are negative even in the scenarios of greatest increase in precipitation. The results suggest a future generalized reduction in the duration and magnitude of the snowpack, even with increases in precipitation up to +20%. The sensitivity of the snowpack to the increase of incident short-wave radiation was much lower than for changes in temperature. Despite this, it is important to take it into account, since it can potentially reduce the duration and magnitude of the snow cover by between 1% and 2% per 10 Wm⁻². Thus, it could represent a significant change in the medium term if the current trends of increase continue. This effect becomes especially relevant if it is added to the more than probable thermal increase projected for all the Iberian mountains. The sensitivity of the melting rates was negative in most of the areas analyses, suggesting longer and less intense melting periods, which the literature associates with a lower production of runoff in the headwaters.

The findings of this work give opportunity to different lines of research for the future in the field of hydroclimatology of the Iberian Peninsula. Once the behaviour of the snowpack has been studied, and thanks to the data generated, it will be possible to study in depth the effect of snow on the hydrology of the Iberian Peninsula, as well as to forecast how the expected changes in the snowpack as a result of climate change may affect snow-dependent water resources. On addition, there are a multitude of teleconnection indices besides the NAO index that influence the climate of the Iberian Peninsula. In previous tests we have found that, although the NAO index is the one that best explains the patterns of duration and maximum accumulation of the snowpack, other teleconnection indices are good indicators of other snow-related parameters. Thus, extreme snowfall events or the concentration of snowfall throughout the winter are related with other indices, having interesting effects from the point of view of climate or natural risk management. The interest shown in the snow products generated by atmospheric and energy balance models, as well as the good results obtained by this methodology, open up a wide field of work in this area, which can be applied for scientific and operational purposes to any cold region of the planet. Thus, it would be of great interest to improve the database by means of new climatic simulations that may arise. The most modern reanalysis products currently available have an update time close to the real one, with only a few days delay. With sufficient computational resources, this new scenario would allow high-resolution snow products and other meteorological variables to be updated in near-real time in the medium term. Furthermore, improvements in different techniques for the observation of

climate and snow cover in remote areas can help to improve the products obtained through the application of assimilation methods. The products obtained in this way can help to further advance the knowledge of the snow cover at different spatial scales and its response to environmental changes; in addition, they provide valuable information to geomorphologists, hydrologists, ecologists (studies of fauna, flora and forest resources) and various areas of land management.

NOTAS: